CENTER FOR INFRASTRUCTURE ENGINEERING STUDIES

Characterization of a New FRP Bar of Reinforcement of Concrete

By

Dr. John Myers

Dr. Antonio Nanni

And

Francesco Micelli

University Transportation Center Program at

The University of Missouri-Rolla

UTC
R49

Disclaimer

The contents of this report reflect the views of the author(s), who are responsible for the facts and the accuracy of information presented herein. This document is disseminated under the sponsorship of the Department of Transportation, University Transportation Centers Program and the Center for Infrastructure Engineering Studies UTC program at the University of Missouri - Rolla, in the interest of information exchange. The U.S. Government and Center for Infrastructure Engineering Studies assumes no liability for the contents or use thereof.

Technical Report Documentation Page

1. Report No.	2. Government Accession No.	3. Recipient's Catalog No.
UTC R49		

4. Title and Subtitle	5. Report Date
Characterization of a New FRP Bar ofr Reinforcement of Concrete	June 2002
	6. Performing Organization Code

7. Author/s	8. Performing Organization Report No.
Dr. John Myers, Dr. Antonio Nanni, and Francesco Micelli	RG000915

9. Performing Organization Name and Address	10. Work Unit No. (TRAIS)
Center for Infrastructure Engineering Studies/UTC program University of Missouri - Rolla 223 Engineering Research Lab Rolla, MO 65409	11. Contract or Grant No. DTRS98-G-0021

12. Sponsoring Organization Name and Address	13. Type of Report and Period Covered
U.S. Department of Transportation Research and Special Programs Administration 400 7th Street, SW Washington, DC 20590-0001	Final
	14. Sponsoring Agency Code

15. Supplementary Notes

16. Abstract

Dow Chemical and its partners are developing a new GFRP bar to be used for concrete reinforcement. The bar needs to be fully characterized in order to be specified as suitable reinforcement for concrete members as per the newly approved ACI 440 design guidelines. The objective of this battery of tests is to provide the first level validation of the product under development. Tests will be conducted on a prototype, 12-mm diameter, smooth, GFRP rod samples.

17. Key Words	18. Distribution Statement
Fiber reinforced polymer bar, non-corrosive reinforcement	No restrictions. This document is available to the public through the National Technical Information Service, Springfield, Virginia 22161.

19. Security Classification (of this report)	20. Security Classification (of this page)	21. No. Of Pages	22. Price
unclassified	unclassified	127	

Form DOT F 1700.7 (8-72)

TABLE OF CONTENTS

_Toc513277289

LIST OF FIGURES

LIST OF TABLES

ABSTRACT

Over the last decade fiber-reinforced polymer (FRP) reinforcement consisting of glass, carbon, or aramid fibers embedded in a resin such as vinyl ester, epoxy, or polyester has emerged as one of the most promising and affordable solutions to the corrosion problems of steel reinforcement in structural concrete. Another application of FRP rods in construction was developed to retrofit and repair reinforced concrete (RC) and masonry structures, using a recently developed technology known as near surface mounted (NSM) rods. The application of FRP rods in new or damaged structures requires the development of design equations that must take into account the mechanical properties and the durability properties of FRP products. The mechanical properties measurement requires special test methods developed for FRP products, since it is known that the mechanical properties are related to the direction and content of fibers. Technical codes and standards were developed in Japan, Canada and U.S.A. in order to assure the structural safety, as it regards the recent applications of these materials in civil engineering. Several concerns are still related to the structural behavior under severe environmental and load conditions for long-time exposures. For the case of glass FRP rods, is the high pH of the pore water solution (pH=12.5-13) created during the hydration of the concrete.

In this study an effective tensile test method is described for a mechanical characterization of FRP rods. Several FRP specimens with different sizes and surface characteristics were tested to validate the proposed procedure. An effort has also been made to develop an experimental protocol to study the effects of accelerated ageing on FRP rods. The physico-mechanical properties of six types of commercial carbon and glass FRP rods were investigated; the rods were subjected to alkaline solution exposure, and environmental agents, including freeze-thaw, high relative humidity, high temperature and ultraviolet (UV) radiations exposure. The mechanical properties were investigated by performing tensile and short beam tests. A further investigation was carried out at a micro-level using SEM microscopy. SEM images of conditioned

specimens were analyzed and presented in this study. The sorption behavior was observed by means of simple gravimetric measurements in order to study the diffusion of the alkaline solution, since the penetration of the aggressive agents, producing micro cracking in the polymeric matrix, brings to fibers damage caused by chemical attack. The experimental data showed the effectiveness of the proposed tensile test method and the influence of aggressive agents on durability of the tested FRP rods. A complete protocol in order to investigate mechanical properties and long-term behavior of FRP rods is presented. Based on experimental results, design recommendations and important aspects related to durability are furnished in order to help manufacturers and designers.

ACKNOWLEDGMENTS

The authors would like to acknowledge the Center for Infrastructure Engineering Studies, University of Missouri Rolla, and Innovation Engineering Department, University of Lecce, (ITALY), that supported this study. The authors acknowledge also Kenny H. Hallison, Material Research Center, and Jeff S. Thomas, the Basic Engineering Department, for their precious collaboration.

1 INTRODUCTION

1.1 Use of FRP Rods in Civil Engineering Structures

Fiber-reinforced polymer (FRP) materials have been used in aerospace, aircraft and naval industries for several years, because of the advantages in high strength/weight ratio. Several technologies were developed for manufacturing FRP materials as laminates, rods, filament wound tanks and many others. FRP materials have a number of advantages when compared to traditional construction materials such as steel and concrete. FRP materials have been utilized in small quantities in the building and construction companies for decades (Chambers, 1965; Hollaway, 1978; Makowsky, 1982). At the moment, numerous successful applications using FRP composites for repair, strengthening and reinforcement of concrete and masonry structures such as bridges, piers, columns, beams, walls, walkways, pipelines etc. have been reported. Nearly 600 articles concerning FRP use in the construction industry published between 1972 and 1998 are available. This expresses a measure of the significant potential that FRP materials showed in the last decades. Japan, Canada and U.S.A. developed design codes for use of FRP in civil engineering applications, but further reviews and experimental data are still needed.

In this research work the use of FRP in construction does not refer to the strengthening and repair techniques using FRP sheets or laminates, but only FRP rods used for substituting steel in new constructions, or for repair with NSM technique.

Typically FRP rods are produced by pultrusion, which is a well known manufacturing method used to produce FRP products with constant cross section.

FRP offers excellent corrosion resistance, as well as the advantages of high stiffness to weight ratio when compared to conventional construction materials. For instance, such ratio for carbon FRP (CFRP) is 10 to 15 times higher than that of steel. Other advantages of FRP include good fatigue properties, damage tolerance, non-magnetic properties, ease of transportation and handling, low energy consumption during fabrication of raw materials, and the potential for real-time monitoring. Although these advantages are important, the tailorability is the biggest advantage of using FRP in structural

applications. Reinforcement can be arranged according to the loading condition so fibers direction can be optimized for the desired performance.

The apparent high cost of FRP compared to conventional materials has been an unfavorable restraint. However, a direct comparison on the unit price basis may not be appropriate. FRP reinforcement in concrete structures should be used as a substitute of steel rebars for that cases in which aggressive environment produce high steel corrosion, or lightweight is an important design factor, or transportation cost increase significantly with the weight of the materials.

In Tables 1 and 2, typical mechanical and thermal expansion properties of steel and FRP reinforcement are illustrated, in order to show which is the potential and the limitations of FRP rods as reinforcement in RC construction.

Several data related to experimental studies and in-situ applications of FRP rods are now available for the use of FRP rods and tendons in reinforced concrete (RC) and prestressed concrete (PC) structures (Chambers, 1965; Hollaway, 1978; Makowsky, 1982; Aiello et al., 2000; Pecce et al., 2000; Ashour, et al. 1993; Balaguru et al., 1993; Michaluk et al., 1998; Benmokrane et al. 1996; Masmoudi et al., 1996; Iyer, 1993; Mufti, et al. 1993; Noritake et al., 1993; Rostasy, 1993; Santoh et al., 1993)

Table 1: Typical tensile properties of reinforcing bars

	Steel	***GFRP***	***CFRP***	***AFRP***
Nominal yield stress MPa (ksi)	276 - 517 (40 – 75)	N.A.	N.A.	N.A.
Tensile strength MPa (ksi)	482 – 689 (70 – 100)	482 - 1585 (70 – 230)	600 - 3688 (87 – 535)	1724 - 2537 (250 – 368)
Elastic modulus $x10^3$ MPa (x 10^3 ksi)	200 (29)	35 – 51 (5.1 – 7.4)	(103 – 579) 15 - 84	(41 – 125) 6.0 – 18.2
Yield strain (%)	1.4 – 2.5	N.A.	N.A.	N.A.
Ultimate strain (%)	6 - 12	1.2 – 3.1	0.5 – 1.9	1.9 – 4.4

*Typical values of fibers content (by volume) = 0.5 to 0.7

Table 2: Typical values of thermal expansion coefficients for reinforcing bars*

Direction	Coefficient of Thermal Expansion (CTE), x 10^6 / F			
	Steel	***GFRP***	***CFRP***	***AFRP***
Longitudinal	6.5	3 to 5	-4 to 0	-3 to 1
Transversal	6.5	11 to 12	41 to 58	33 to 44

*Typical values of fibers content (by volume) = 0.5 to 0.7

In the last year a new technology has also been developed using FRP rods in structural rehabilitation of deficient RC structures. In fact, the use of Near Surface Mounted (NSM) FRP rods is a promising technology for increasing flexural and shear strength of deficient RC and PC members. Advantages of using NSM FRP rods with respect to externally bonded FRP laminates are the possibility of anchoring the rods into adjacent members, and minimal installation time (Alkhrdaji et al., 1999). Furthermore, this technique becomes particularly attractive for flexural strengthening in the negative moment regions of slabs and decks, where external reinforcement would be subjected to mechanical and environmental damage and would require protective cover which could interfere with the presence of floor finishes. The method used in applying the rods is described as follows. A groove is cut in the desired direction into the concrete surface. The groove is then filled halfway with epoxy paste, the FRP rod is placed in the groove and lightly pressed. This forces the paste to flow around the rod and fill completely between the rod and the sides of the groove. The groove is then filled with more paste and the surface is leveled. Experimental studies and few applications were performed by researchers in order to improve the potential of this new technique (De Lorenzis et al., 2000 (A & B); Mayo et al., 1999). Another application of FRP rods is the anchorage of FRP externally bonded sheets in RC members, used for shear strengthening, as it can be seen in Figure 1 (Khalifa et al., 1999).

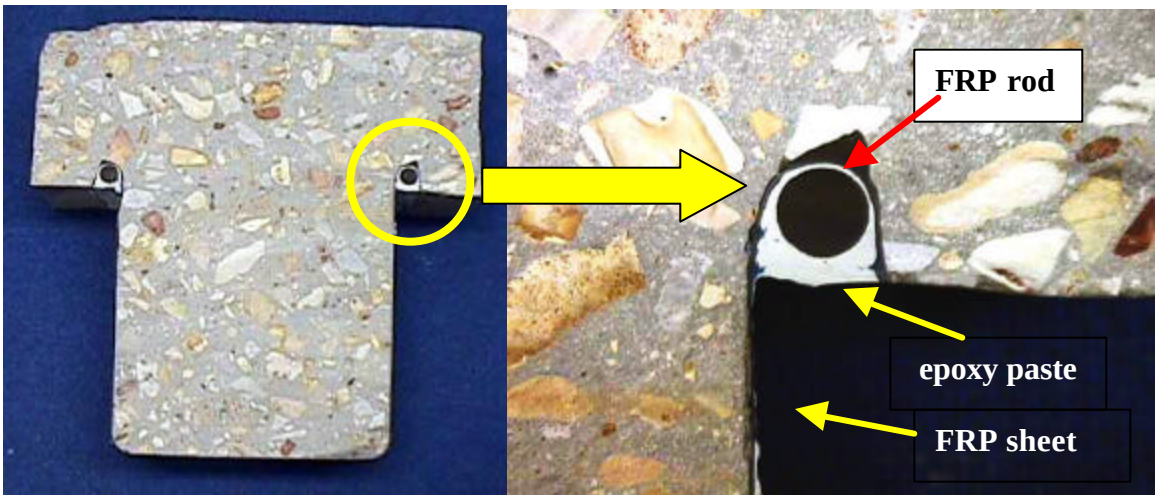

Figure 1: Anchorage system using FRP rods

FRP rods were also used for structural repointing of masonry structures, (Tinazzi et al., 2000; De Lorenzis, 2000 (C)). An example of FRP installation procedure is illustrated in Figure 2. Recent installations of FRP rods were also conducted in Europe for the repair of historical buildings such us churches and ancient monuments (La Tegola, 2000 A & B). In Figure 3 it can be seen how Aramid FRP (AFRP) rods were installed for the structural rehabilitation of a cracked masonry column.

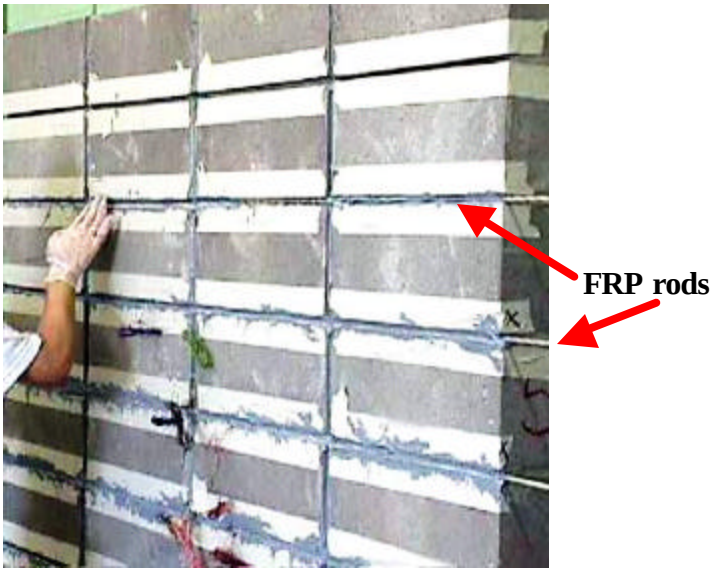

Figure 2: FRP installation for structural repointing in masonry walls

Figure 3: Column confinement with AFRP rods

Several studies were also conducted to investigate the bond properties between FRP rods and concrete (Bakis, et al., 1995; Boothby, et al., 1995; Al-Zahrani, et al., 1996; Uppuluri, et al., 1996; Freimanis, et al., 1998). These studies did not investigate durability and bond behavior, therefore an open field for research on long-term behavior would be the investigation of the interface stresses after long-term service conditions. In fact, although experimental studies and numerical methods helped to model the mechanical behavior at the interface, the analytical approaches do not take in account, at the moment, the possible degradation that could bring to a weakness of the bond. It is easy to understand the importance o such a problem, because it could mean that the mechanisms of stress transfer from concrete to the fibers used in design assumptions are not valid after a long-term environmental exposure time.

Ultimately, a successful replacement of steel reinforcement with FRP requires a change in construction methods and typologies. This is necessary if the justification of FRP reinforcement should not be limited to corrosion resistance or magnetic permeability, since the practice and the configurations that were successful with conventional materials become obsolete when new materials are introduced (Nanni, 1993). A clear example of

the new requirements related to the use FRP could be the analysis of FRP reinforced beams. Failure of FRP reinforcement is undesirable, such failure is sudden, catastrophic, and can release a great amount of stored elastic energy. An over-reinforced section, with crushing concrete failure is preferable to an under-reinforced section with FRP rupture. All the present RC codes avoid crushing concrete, since is axiomatic that steel-controlled failure is ductile.

This example shows how the design approach when using FRP reinforcement departs from the traditional RC design codes. This is only one of the several aspects that should be reviewed in order to furnish new guidelines and not a forced adaptation of traditional equations.

2 DURABILITY AND MECHANICAL TESTS OF FRP REINFORCEMENT

2.1 Durability of FRP Used in Construction

Beyond the cost issues, the most significant technical obstacle preventing the extended use of FRP materials is a lack of long-term and durability performance data comparable to the data available for traditional construction materials. Although there have been numerous studies on creep, stress corrosion, fatigue, environmental fatigue, chemical and physical ageing, and natural weathering of composites, most of these studies are not related to civil engineering applications. The importance of these results is very low if it is noted that composites used for aerospace or naval application are produced in controlled chambers, with high quality control (temperature, pressure, void contents, cure monitoring, fiber content, etc.), while the installation of FRP in construction usually takes place in-situ. Hence, the infrastructure community must be concerned with long-term behavior as well as different materials and service environment. In order to expand the use of FRP in civil structures, relevant durability data must be available in the building codes and standards.

In general durability of a structure and of a material can be defined as *the ability to resist cracking, oxidation, chemical degradation, delamination, wear, and/or the effects of*

foreign object damage for a specific period of time, under the appropriate load conditions and specified environmental conditions.

This concept is realized in design through the application of sound design principles and the principles of damage tolerance whereby levels of performance are guaranteed through relationships between performance levels and damage/degradation accrued over specified periods of time. In this sense, damage tolerance is defined as the ability of a material or a structure to resist failure and continue performing prescribed levels of performance in the presence of flaws, cracks, or other forms of damage for a specified period of time under specified environmental conditions. The overall concept is illustrated schematically in Figure 4.

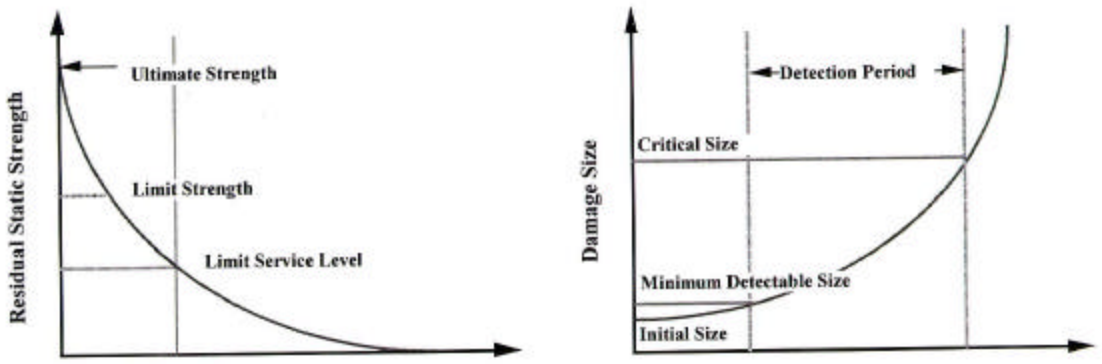

Figure 4: Concepts of durability and damage tolerance to design

The following different damage mechanism are distinguished in order to classify the potential problems related to the long-term behavior of FRP rods used in civil engineering:

- Effects of solutions on mechanical properties
- Creep and stress relaxation
- Fatigue and environmental fatigue damages
- Weathering

All these mechanisms can be considered as a consequence of the attack by external agents including:

- Moisture and aqueous solutions
- Alkaline environment
- Thermal effects (freeze-thaw cycling, high temperatures)
- Fatigue loads
- Ultra-violet (UV) radiation
- Fire

There is strong evidence that the rate of degradation of polymer composites exposed to fluid environment is related to the rate of sorption of the fluid (Bott et al., 1969). Thus, an understanding of the diffusion process as well as factors that influence it is crucial in assessing the state of the material. Theoretical treatment of the diffusion problem can be traced back to the work of previous researchers (Weitsman, 1995; Hartley et al., 1949). It can be briefly summarize that the sorption behavior of a polymer or polymer composite depends on: type of fluid, fluid concentration, temperature, applied stress, damage status, chemical structure of the matrix and fiber/matrix interface. (Liao et al. 1998; Chateauminois et al. 1998).

The effect of moisture or alkaline solutions sorption on GFRP rods and laminates vary with the mentioned variables and they produce a loss in strength and stiffness (Tannous et al., 1999; Karbhari et al., 1998; Fried, 1967). The study of the alkaline attack has particular importance in construction applications. FRP rods are immersed in a cementitious environment; this condition was found to be aggressive for the GFRP, due to the high pH level (pH = 13.5) of the pore water solutions and presence of alkaline ions. The alkaline solutions produce an embrittlement of the glass fibers and a damage at the fiber resin interface level by chemical attack and growth of hydration products. These effects lead to a loss in tensile strength and interlaminar transverse properties (Zhang et al., 1999: Nanni et al., 1998; Bascom et al., 1974; Porter et al. 1997, Schutte, 1994; Devalapura, 1997; Franke et al., 1987, Philips, 1987, Morri et al., 1991).

Different tests were conducted using solutions with high pH, but it has been clearly shown that degradation of fibers is not merely due to the high pH levels, but rather than a combination of hydroxylation products (due to the presence of Na^+ and K^+ ions, presence of moisture and high pH, that acts as a catalyst. Although the use of a polymer matrix as a binder around the glass bundles and individual filaments does proved a level of protection to the fiber from the above mentioned degradation, there is still concern related to the migration of pH solutions and alkali salts through the resin to the fiber surface. In fact, although the ultimate strain of matrix usually exceeds that of the fibers, its fracture toughness is low. Hence, in the stressed FRP reinforcement micro cracks in thin outer matrix skin may arise, thus leading to the loss of the ingress of aggressive fluids as shown in Figure 5.

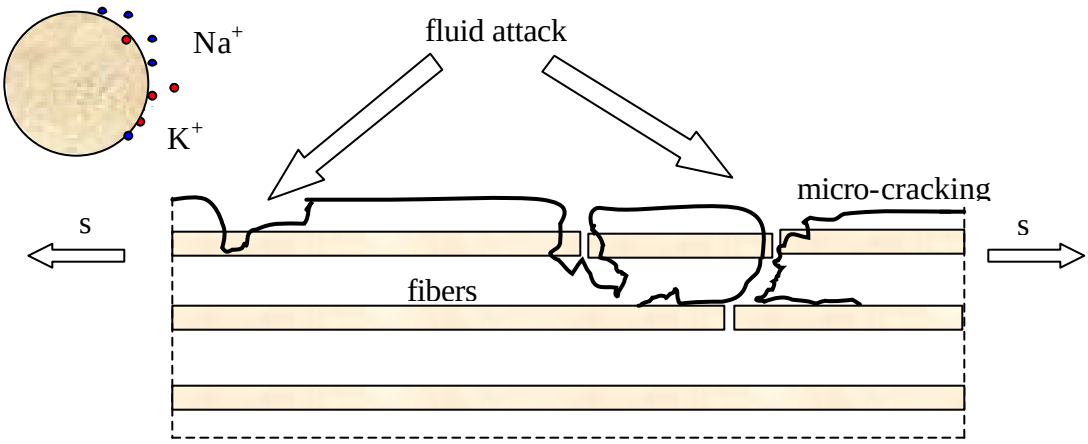

Figure 5: Fluid attack in FRP rods

The study of the real long-term behavior should require a conditioning test program as long as the life of a structure, therefore accelerated test procedures are needed to investigate the durability problems.

In developing accelerated ageing tests, two stages must be considered. First, the potential ageing mechanism should be identified, in order to choose an appropriate means of accelerating them, second, the duration or number of cycles in the accelerated test should be translated into time in natural weathering conditions. The correlation between the

time in accelerated and natural ageing is not a unique function, since it depends on the climatic conditions in different zones, and even within the same zone there may be differences in the microclimate, for instance, the direction in which the structure faces. Establishing a correlation of this kind requires at least some limited data from behavior in exposure sites, which could not be compared with the results of accelerated test. However, even without this information, it is very useful to carry out accelerated tests, since they can provide an indication of whether there is an ageing problem, and severe it might be. A general assessment is provided in ASTM E632 (ASTM, 1982), but it is clear that for a specific ageing programs the protocol should take into account the conditions related to that specific area.

In the last years the ageing process to be considered for accelerate durability test of FRP were classified in three classes: (1) ageing effects associated with the resin, (2)with the fibers, (3) changes at the fiber/matrix interfaces. The environmental ageing that was chosen aimed to study the effects on the strength and stiffness of the rebars, but, since the resin degradation allows a rapid attack of the fibers by external agents, also resin properties should be investigated.

Previous researches (Litherland, et al., 1981; Vijay, et al., 1999; Ganga Rao, et al., 1997), showed how temperature influences the sorption and diffusive properties of alkaline solutions in FRP composites, comparing natural aging and accelerated test results. Therefore it is possible now conducting accelerated test in which the long-term behavior can be simulated with a satisfactory accuracy. The following equation is used to relate the temperature and time used for conditioning with the real conditions:

$$N/C = 0.098 \exp(0.0558T) \qquad \text{Eq. 1}$$

Where:

N = age in natural days

T = conditioning temperature in °F

C = days of accelerated exposure at temperature T

The diagram in Figure 6 represents the relationship in Eq. 1 for T = 60°C (140 ºF).

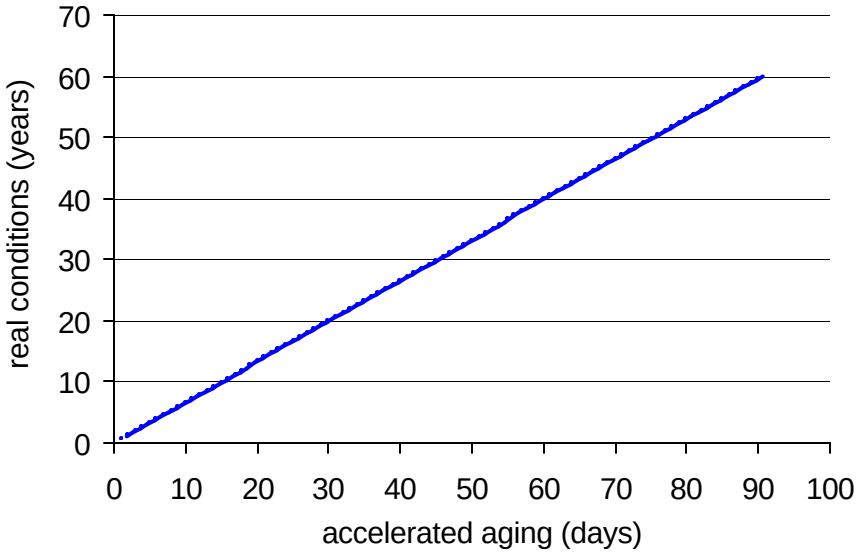

Figure 6: Accelerated aging in alkaline solutions for T = 60 ºC (140 ºF)

Other phenomena effects that must be investigated regarding long-term behavior, are creep and stress relaxation. In fact, since polymers are viscoelastic materials, they exhibit creep and stress relaxation to a great extent (Ferry, 1961, Dillard, 1991). As a result, FRPs are more susceptible to creep than traditional construction materials, especially under the influence of moisture and temperature. Several creep models were developed to study the behavior of polymers and composites. External agents, such as moisture, UV radiation, physical aging, UV exposure, solution penetration, and temperature, play a significant role on creep of FRP. As a consequence of the exposure to the external agents and sustained loads, stress corrosion and stress rupture of the fibers, and/or the matrix can occur (Roberts, 1982; Menges et al., 1984; Van Den Ende et al., 1991; Franke et al., 1992; Jones et al., 1983, Buck, 1998).

Much effort in understanding fatigue damage and failure mechanisms of FRP composites has focused on tensile fatigue, as composites are most efficient in carrying tensile loads. In general, fatigue damage in FRP is progressive and accumulative in nature. It is crucial

for designers to first understand damage initiation and its subsequent role in affecting the long-term behavior. Since the durability effects are of main concern fatigue loads, combined with high humidity and temperature, and aggressive solutions may shorten the fatigue life. Previous studies demonstrated that the fiber/matrix interface region has a controlling effect on the environmental fatigue of FRP composites (Donaldson et al., 1995; Shih et al., 1987, Bevan, 1977). The applied cyclic stresses act as a promoter for solution penetration and fiber damages, due to the cracking of the matrix.

Infrastructure systems are exposed to external agents during their life cycle, so FRP mechanical behavior under natural weathering needs to be understood. Different conditions need to be investigated, including UV radiation, freeze-thaw cycles, high relative humidity, aqueous solution exposure, chemical agents, and combinations of previously described conditions, according to the service condition that are expected.

Thermal effects can cause to micro cracks at the interface between FRP rods and concrete, because of different thermal expansion coefficients, and at high temperature the bond properties decrease strongly (Katz, et al. 1999). Freeze-thaw cycling can accelerate solution penetration, because of cracks growth in the matrix that becomes more rigid and brittle. Freeze-thaw cycles without the presence of high moisture do not significantly affect the mechanical properties of FRP rods as reported in laboratory studies (Homam et al., 2000).

UV exposure leads to surface oxidation due different chemical mechanisms related to the resin type as investigated in previous studies (Chin et al., 1997; Kato et al., 1998). In AFRP composites both fibers and resin are affected by UV light, so that potentially a dangerous decrease in mechanical properties was found in previous studies (Larsson, 1986).

The properties related to fire resistance are a particular aspect of durability. Limited data is available, and only a limited number of tests has been conducted in order to understand the structural safety aspects related to fire behavior of FRP used in construction. Since mechanical properties of the resins are significantly affected by increase of temperature, it is needed to know which the fire effects could be. Another concern is also related to flammability and release of unhealthy compounds due to polymer degradation at high temperature, especially in civil buildings and galleries.

Different materials (fibers and resins) respond differently to external agents and service conditions. As an example in Table 3 a schematic summary is reported, in order to show, the response of FRP laminates as a function of the fiber type.

Table 3: Performance of FRP laminates

Criterion	***Weighting Factor***	***Weighted Rating for Laminates With Various Fibers***		
Range of Weighting Factor	*1 to 3*	Carbon	Aramid	E-Glass
Tensile Strength	*3*	9	9	9
Compressive Strength	*2*	6	0	4
Young's Modulus	*3*	9	6	3
Long-Term Behavior	*3*	9	6	3
Fatigue Behavior	*2*	6	4	2
Bulk Density	*2*	4	6	2
Alkaline Resistance	*2*	6	4	0
Cost	*3*	6	6	9
Total Points		**55**	**41**	**32**
Ranking		**3**	**2**	**1**

Weighting factor: 3 = very important, 2 = important, 1 = not important

Ranking: 3 = very good, 2 = good, 1 = adequate, 0 = inadequate

2.2 Mechanical Characterization of FRP Rods

FRP rods used in civil engineering are unidirectional composites. The direction parallel to the fibers is called the longitudinal direction, in which the mechanical properties are

controlled by the fiber properties. The transversal direction, perpendicular to the fibers, presents lower mechanical properties, controlled by resin and fiber/matrix interface properties. Thus mechanical properties depend on the nature and content of fibers in the longitudinal direction.

It is commonly assumed that the performance of FRP rods in concrete and masonry structures is dictated by the longitudinal properties of these materials; however, in durability studies it is shown that resin properties are also significant as they affect load transfer to the fibers and their chemical and physical protection. Damage and cracking of the resin do not allow the desired stress distribution, and open a preferential way for degradation of fibers. This reflects on longitudinal strength and stiffness.

Micromechanics equations are used to predict properties of unidirectional composites based on raw materials properties and content. However an experimental characterization is necessary for validation and control quality.

The investigation of longitudinal and transverse properties is made by destructive measures, such as tensile test, and short beam test (SBT). Non-destructive techniques can also be used, in accordance with ASTM C1198-96 (ASTM, 1996 A), to measure the longitudinal and transverse modulus.

Different standards were developed for tensile tests of FRP composites (ASTM, 2000; ASTM 1999; EN ISO, 1996 (A & B)), but they refer only to laminates, prepared as rectangular or dumbbell-shaped specimens. At the moment, there is no national or international standard for tensile characterization of FRP rods used in civil engineering. The challenges of composites test methods are the same for both rods and laminates: gripping and system alignment. Inadequate gripping and bending moments cause premature failures, located outside the test length. Previous studies were carried out to support the development of standard and test methods for FRP rods used as concrete reinforcement (Nanni, 1997; Castro et al., 1998; Nanni, et al., 1996; Khin, et al. 1996).

Transversal properties can be detected using SBT according to ASTM D4475 (ASTM, 1996 B). This technique does not provide an absolute measure of interlaminar shear stress (ISS) for design purpose, but it can be used for comparative testing. It is clear that this test could be effective for quality control and durability investigations as it regards the resin properties.

2.3 Tensile Test of FRP Rods

FRP rods are constituted of unidirectional fibers that usually have a percentage in volume between 45 and 60%. The most important mechanical properties that are used in design of RC structures are the tensile properties. It means that a rigorous experimental investigation in order to measure ultimate tensile strength and Young modulus is necessary, for the mechanical characterization of these materials used in construction.

A theoretical prediction of mechanical properties using micro-mechanics equations is accurate only if the quality control of the pultrusion process used for manufacturing is very high. If the fiber content is less than expected, the tensile properties show a dramatic decrease if compared to analytical expectations.

Thus, a tensile characterization of these materials constitutes an output quality control for manufacturers, and an input quality control for designers at the same time.

Since the mechanical properties of FRP rods are controlled by the fibers properties in longitudinal direction, and by resin and interlaminar properties in the transverse direction, a particular protocol must be used in order to face the following problems:

- damages of the rods due to excessive grip force
- fracture out of the test length due to stress concentration and flexural forces (this is caused mainly by a misalignment of the rod)
- inaccurate measurements due to yielding or failure of the anchorages
- slip of the rods out of the anchorages caused by weak friction forces and high tensile stress

The mentioned problems show clearly that traditional methods from gripping metal specimen, shown in Figure 7, are not applicable for FRP rods.

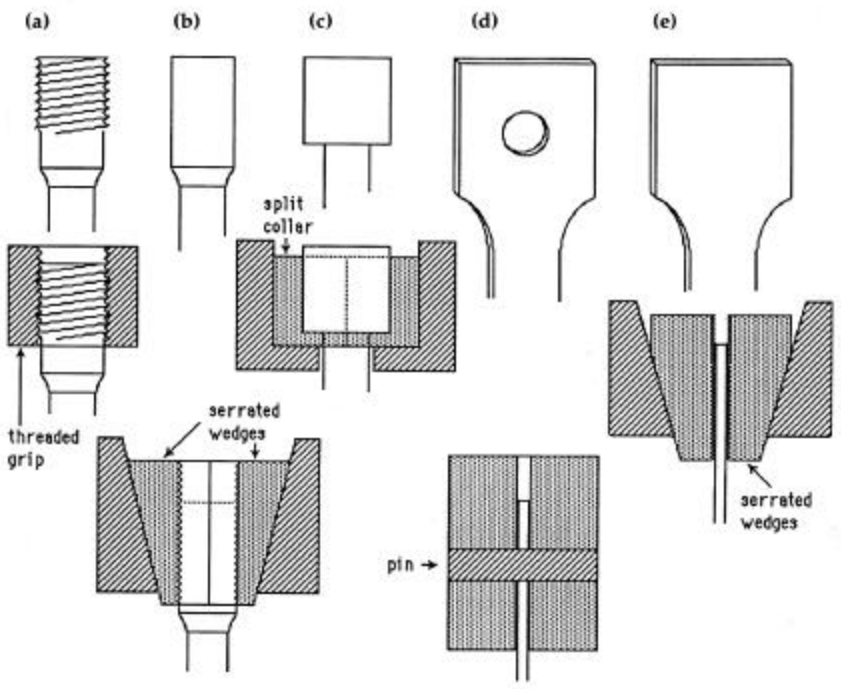

Figure 7: Traditional grip systems used for tensile test

ASTM D 3039, ASTM 638 furnish detailed protocols for testing plastics and composites laminates in form of rectangular laminates, and ASTM D 3916 was developed as a standard for tensile test of GFRP rods. Several studies, contained in a review of Faza and Ganga Rao (1993), showed that the protocol proposed in ASTM 3916 was not easily applicable. Moreover, tensile test problems related to CFRP rods were not faced, since the forces developed for CFRP are higher than AFRP and GFRP. At the moment a widely accepted protocol does not exist, although previous studies investigated the problem.

A variety of gripping systems has been developed to provide anchorage for tensile test of FRP pultruded bars using epoxy systems to bond the rod to the anchorages. Bakis et al. (1996), used a potted grip system showed in Figure 8 (a), for carrying out tensile strength of FRP rebars. The bar ends are rubbed with fine sandpaper and cleaned with acetone in preparation for embedment into conical end anchors. Prior to fill the cone with epoxy, fine silica sand is placed inside the cone to maintain the proper position of the bar. A rubber washer is glued to the small end of the cone to prevent uncured epoxy from

leaking out of the anchors. The embedment length of the bar into the cone is 10 times the bar diameter. The bar is loaded in tension as if to measure pullout strength. This approach eliminates the high lateral compressive force in the grip region.

A similar technique was proposed by Holte et al. (1993) as anchorages for FRP prestressing tendons. In this case the cone was machined to a parabolic profile, (instead of straight) to reduce the interfacial shearing stress where the bar enters the anchor. Tensile tests with the parabolic anchors resulted in failure within the free-length and measured strengths were higher than reported by the manufacturers of the FRP rods.

Figure 8 (b) illustrates another potential gripping system by Erky and Ritzkalla (1993). The ends of the bars are embedded into metal tubes with external threads. A collar or special nut is screwed onto each end of the tube. Load is transferred to the tube using a particular loading system, such as a center load jack, or by modification of the cross heads of an universal testing machine. This system also avoids lateral compressive force on the gripped ends of the FRP rod.

Figure 8 (c) shows the system developed by Rahman et al. (1993), in which epoxy paste is used to embed the rod end into an internal threaded bar. Epoxy resin is used to embed the bar end into the internally threaded tube. The embedment length is ten times the bar diameter. A threaded rod is used to connect the tube to the testing machine loading system.

All the mentioned systems represented in Figure 8 (a, b, c) are similar in the sense that the tensile stress is transmitted to the road by means of shear forces in the epoxy mortar. Sufficient embedment is required since the rods can show pullout failure slipping out from the tubes.

The Figure 8 (d) illustrates the gripping system developed at West Virginia University. A 203 mm-long steel tube, with an internal diameter equal to that of the FRP bar is cut lengthwise into two pieces. The inner surfaces of the split tubes are roughened by sand blasting and coated with an epoxy adhesive. The tubes are then clamped to the FRP rod until the resin is cured. The tensile test is carried out by gripping the tubes in the wedge grips of the testing machine. A minimum length of 1219 mm (47.992 in) has been used, independent of bar diameter. This system differs from the previous ones because

compressive stresses are applied to the ends of the bar, even if the stresses are distributed along the tubes.

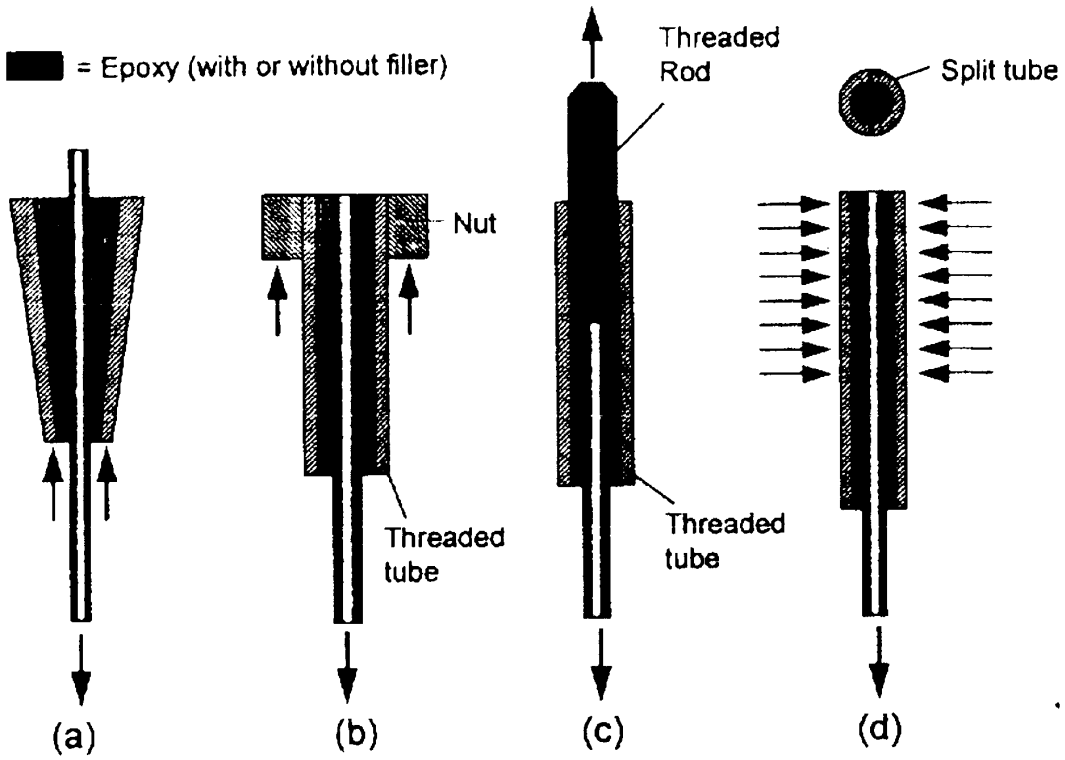

Figure 8: Anchorage systems used for tensile test of FRP rods

An extensive experimental study was carried out by Castro and Carino, (1998), in which the epoxy past was substituted by a cement mortar as shown in Figure 9.

Castro and Carino tested only GFRP rods and investigated the effectiveness of the proposed gripping system, the effects of the length/diameter ratio and different surface shapes of the rods. The new aspect of this method is the use of a cement mortar rather than an epoxy resin or mortar. The loading set-up is similar to other mentioned procedures as showed in Figure 9.

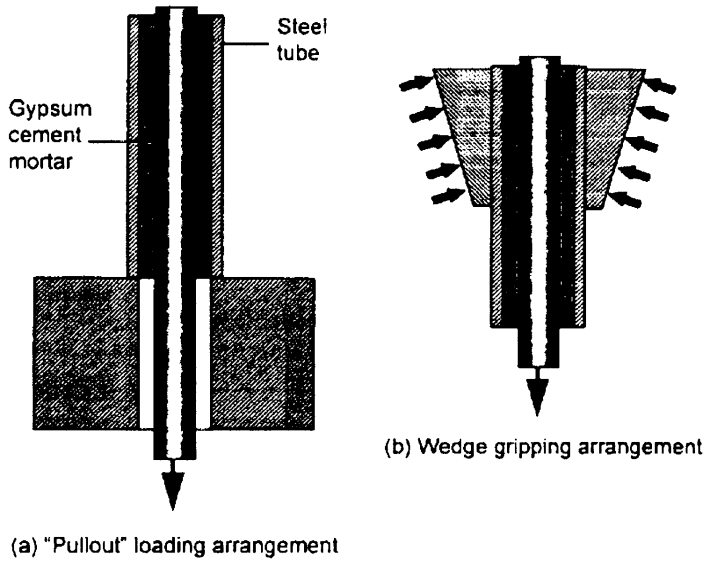

Figure 9: Anchorage developed by Castro and Carino (1998)

Nanni (1995) investigated the use of an alternative to epoxy-based gripping materials, using expansive grouts poured into steel tubes in which the road is pressed by the radial force developed by the expansion of the grout obstructed by the pipe-walls. The anchors were capped at both ends with caps that consisted of 20 mm (0.787 in) long steel plugs. The plugs were threaded an provided with a central hole to allow the correct positioning of the rod.

Double extra heavy (D.H.E. ANSI B36.10) steel pipes were used, with an external diameter of 42.4 mm (1.66 in) and wall thickness of 9.7 mm (0.382 in). The proposed method was found to be effective for an anchorage length at least of 300 mm, in which the slip failure could be observed only when the tensile stress exceeds 2500 MPa (363 ksi).

An optimization of this method has been developed in this research, in terms of costs and time preparation, and it will be shown as different CFRP and GFRP rods can be tested reaching a desired tensile failure in the test-length region with tensile stress that can reach over 2000 MPa (290.3 ksi). The procedure proposed in this study will be shown to be simpler than others and effective in order to characterize different types of FRP rods in terms of materials, cross section shape, and surface properties.

2.4 Scope of the Study

Since a material characterization test has not be developed in technical codes, for FRP rods, the first objective of this work is related to improve a tensile test technique that could be proposed as a standard for tensile characterization of FRP pultruded rods used in civil engineering applications. Different variables are investigated including the geometry of the anchorages, the cross section and the materials of the bars, the loading rate, and the surface characteristics of the bars. The development of the tensile test procedure aims to guarantee the fiber rupture in the test length of the coupon, avoiding all possible factors that could cause a different failure type. The specimen preparation, and loading procedure are the fundamental aspects that contribute to the desired results.

The second objective of the study presented herein regards the durability of FRP rods used in construction. FRP bars used in concrete means that they are exposed to an alkaline environment with aggressive ions for several years. This can cause a loss in mechanical properties, especially for GFRP rods. Twelve different FRP rods were subjected to alkaline exposure for different times, with an accelerated ageing procedure, using high temperature. The mechanical characterization of the rods provided a measure of durability. In addition this study investigates the combination of the effect of temperature cycles, high moisture and UV radiation can affect the long-term behavior of the rods. Since, the effects of the single environmental agents were investigated in previous studies, this study allows to assess the combined effect that is more representative of structural applications.

3 EXPERIMENTAL PROGRAM

This section describes the materials that were used and conditioning procedures. The mechanical test methods are then presented with particular attention to the proposed tensile test method. Finally, the weighting procedure is described.

3.1 FRP Rod Types

Twelve FRP rods were investigated (see table 4) using tensile and short beam tests, six of them were subjected to durability studies. The rods were all manufactured using pultrusion process, and are commercial products used in construction for RC and masonry structures.

Table 4: FRP rod types

Rod (Manufactures)	***Fibers***	***Matrix***	***Section Area mm^2 (in^2)***	***Section***
C1 (M1)	Carbon	Epoxy	53.6 (0.083)	Circular
C2 (M1)	Carbon	Epoxy	50.3 (0.078)	Circular
C3 (M2)	Carbon	Epoxy	49.5 (0.077)	Circular
C4 (M2)	Carbon	Epoxy	31.7 (0.049)	Circular
C5 (M3)	Carbon	Epoxy	71.3 (0.111)	Circular
C6** (M4)	Carbon	Vinylester	61.7 (0.095)	Rectangular
C7** (M4)	Carbon	Epoxy	61.7 (0.095)	Rectangular
G1 (M5)	Glass E	Thermoplastic	113.2 (0.175)	Circular
G2* (M6)	Glass E	Polyester	31.7 (0.049)	Circular
G3 (M3)	Glass E	Vinylester	71.3 (0.111)	Circular
G4 (M3)	Glass E	Vinylester	126.8 (0.197)	Circular
G5 (M3)	Glass E	Vinylester	31.7 (0.049)	Circular

*G2 rods are produced in form of U-shaped product. Straight specimens were cut from U-shaped bars.

**Rectangular section 9.652 x 6.35 mm (0.38 x 0.25 in)

Surface profiles allow to create a more or less strong adherence between concrete and FRP rod, or epoxy past and FRP rod, according to the type of application. This property is very important for performance, as well as design calculations.

The surface conditions are also significant as it concerns the tensile test method, as it will be described later. The different shapes and superficial properties of the investigated rods are show in Figure 10.

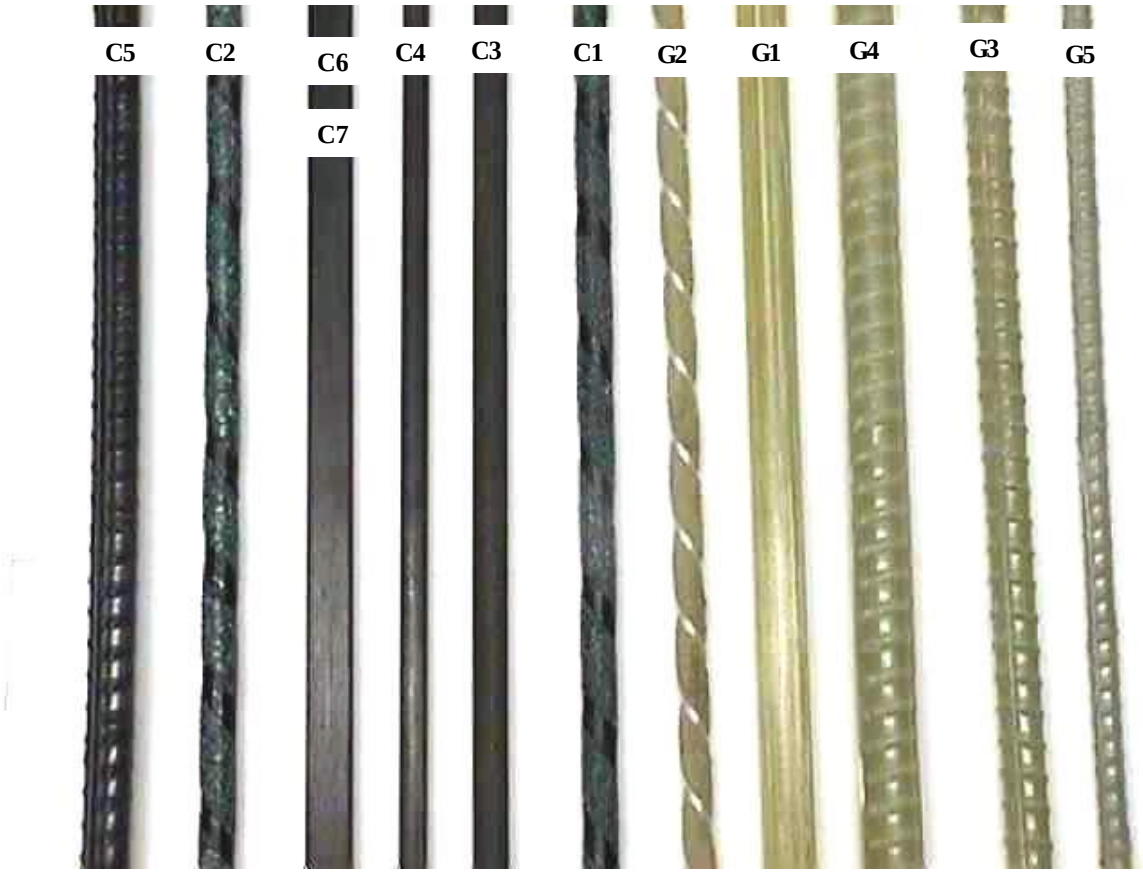

Figure 10: Surface characteristics of tested FRP rods

In Tables 5 and 6 the conditioning regimens and number of tested specimens are shown.

Table 5: Conditioning and tensile test of FRP rods

Specimens	***Control***	***Alkaline Exposure***		***Environmental Cycles***
		21 days @ 60°C (140°F)	42 days @ 60°C (140°F)	
C1 tensile	4	3	3	4
C2 tensile	4	3	3	4
C3 tensile	4	3	3	4
C4 tensile	2	-	-	4
C5 tensile	3	-	-	-
C6 tensile	2	-	-	-
C7 tensile	2	-	-	-
G1 tensile	5	3	3	4
G2 tensile	5	3	3	4
G3 tensile	2	-	-	-
G4 tensile	2	-	-	-
G5 tensile	2	-	-	-
TOTAL	37	15	15	24

Control specimens were kept at temperature of 22°C (72°F) in laboratory environment, avoiding moisture penetration, thermal shocks and mechanical damages due to handling or cutting that could affect the results of the mechanical tests. Totally, 91 tensile tests and 162 short beam tests were performed. In addition electronic microscopy (SEM) was used to observe, at a microscopic level the effects related to the alkaline attack on the resins, fibers, and fiber/matrix interfaces.

Table 6: Conditioning and SBT of FRP rods

Specimens	***Control***	***Alkaline Exposure***			***Environmental Cycles***
		21 days @ 60°C (140°F)	42 days @ 60°C (140°F)	42 days @ 22°C (72°F)	
C1SBT	6	6	6	6	6
C2SBT	6	6	6	6	6
C3 SBT	6	6	6	6	6
C4 SBT	6	-	-	-	6
G1 SBT	6	6	6	6	6
G2 SBT	6	6	6	6	6

3.2 Alkaline Solution Exposure

An attempt has been made in this study to reproduce the alkaline pore water in or from the concrete, rather than a solution with high pH. The solution that was used is the following:

$$0.16\%\ Ca(OH)_2 + 1\%\ Na(OH) + 1.4\%\ K(OH)$$

The values represent the percentages in weight that were solved in distilled water. The pH measurements showed that a pH = 12.6 was the constant values, before and after rods conditioning. The conditioned specimens (C1, C2, C3, G1, and G2 rods) were exposed to the alkaline solution at a temperature T = 140 ºF (T = 60 ºC). Two different exposure times were chosen: 21 days, and 42 days; which correspond to real times of 14 and 28 years in the concrete, respectively. Some SBT specimens were also immersed for 42 days at a temperature of T = 22 ºC (72ºF), just to show the effect of temperature on sorption properties.

All the tensile specimens were exposed for a length of 254 mm (10 in) using the system that is illustrated in Figure 11. SBT specimens were immersed in alkaline solutions,

avoiding the contact of the cross section of the specimens that were isolated with a silicone film.

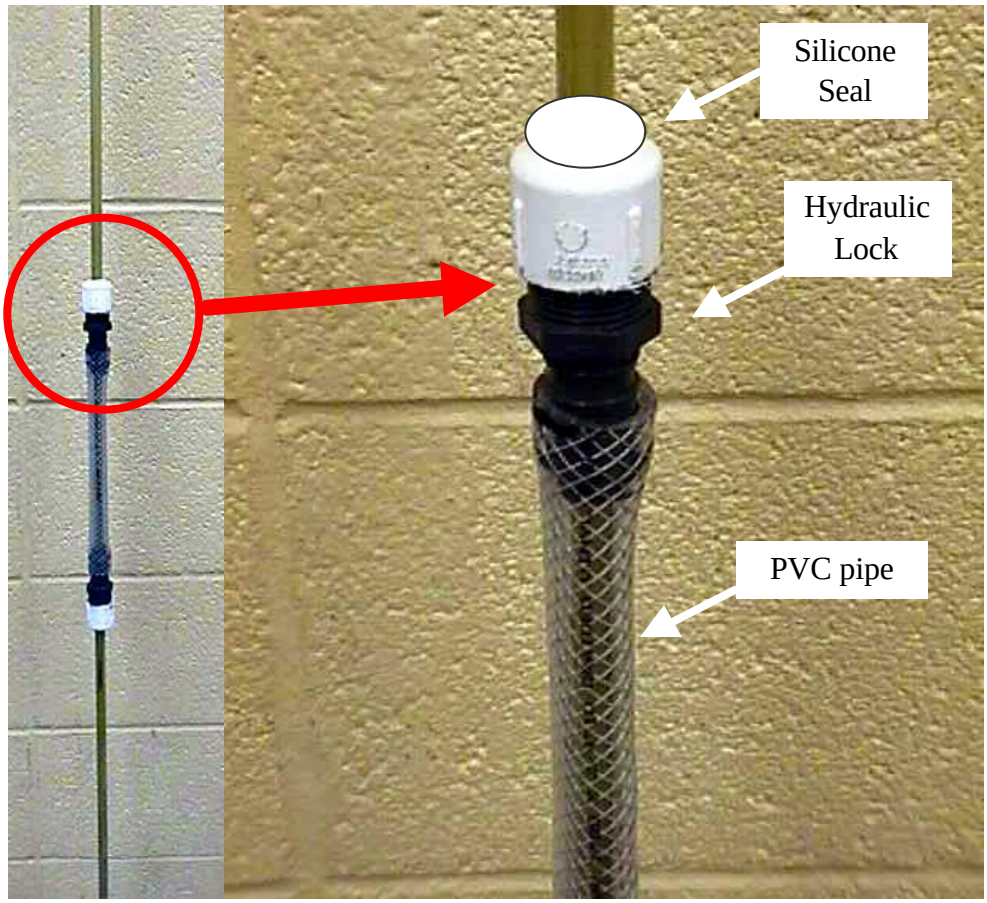

Figure 11: Alkali exposure set-up

The alkaline solution was placed in PVC pipes that were inserted around the tensile specimens. A hydraulic lock and silicone seal were used to avoid leakages of alkaline solution. All the materials were chosen and tested to guarantee performance at high temperature.

A thermal chamber was built to put the rods at 60 ºC (140 ºF) in contact with alkaline solution; the scheme of the thermal chamber is shown in Figure 12.

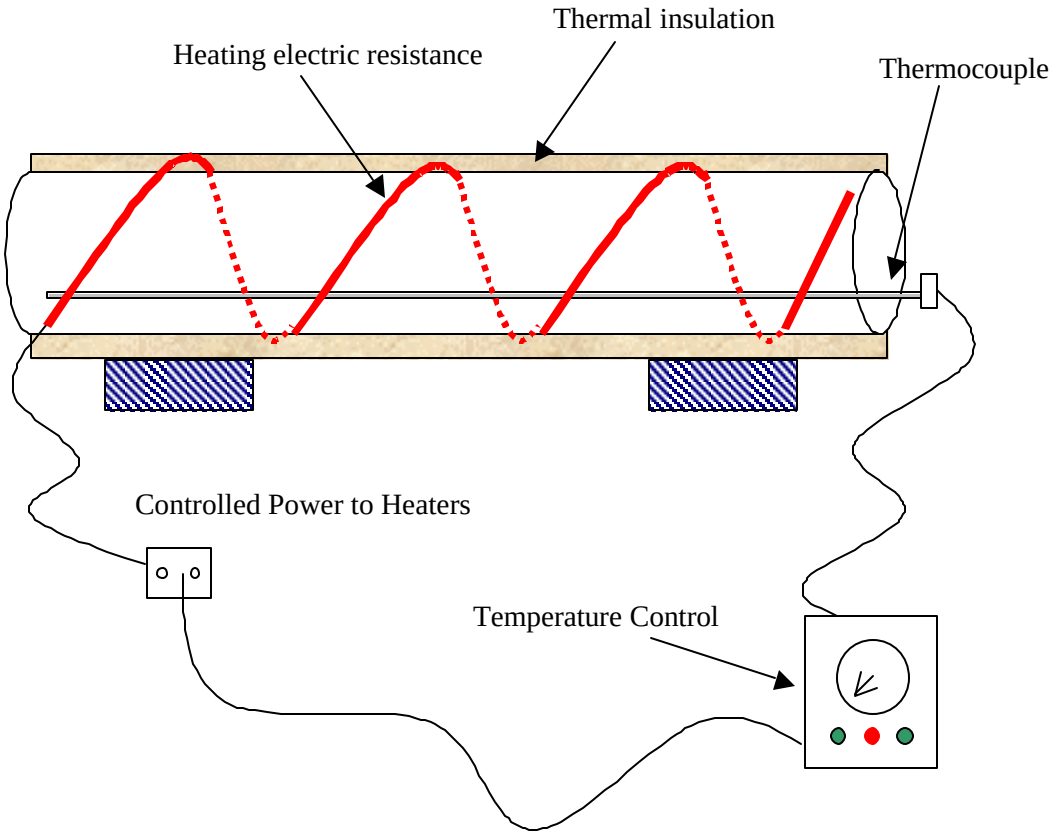

Figure 12: Thermal chamber for high temperature accelerated test

3.3 Environmental Cycles Exposure

The accelerated ageing was performed in an environmental chamber, where the rods were exposed to combined cycles, including freeze-thaw, high temperature, high relative humidity (RH), ultra-violet radiation (UV) exposure.

Different studies demonstrated that environmental exposures to a single agent did not result in a significant loss of mechanical properties, except for wet and dry cycling for some types of materials. At the moment there are not studies that investigated the combined actions, therefore a combination of different agents was chosen.

In Figure 13 a single complete cycle exposure is illustrated.

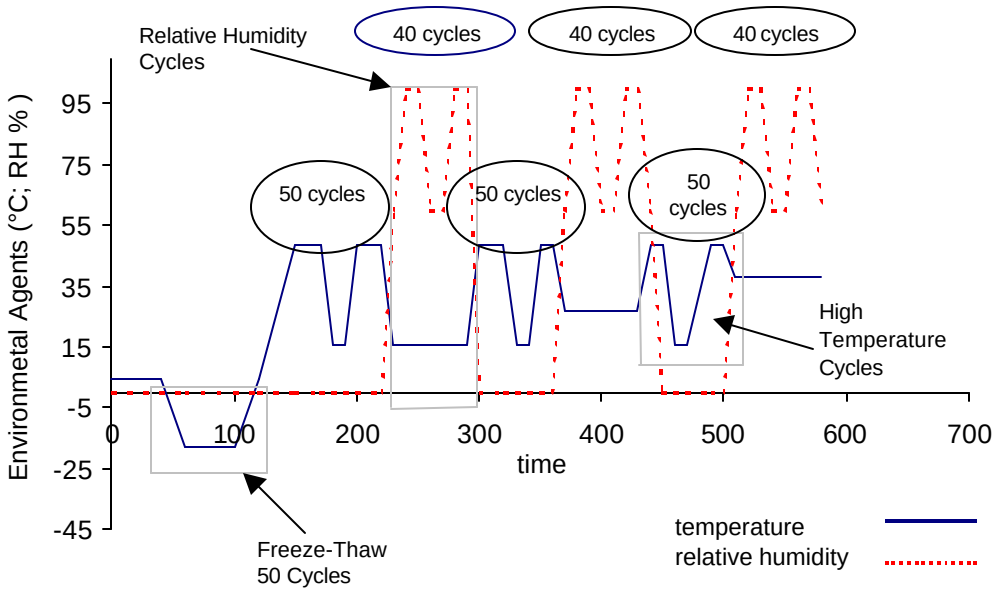

Figure 13: Environmental ageing cycles

High and low temperatures are related to the weather typical of continental Europe and U.S., and the cycling represents the seasonal changes.

First freeze-thaw cycles are considered as a simulation of winter effects. Here the temperature varies from -18 ºC to 4 ºC (0º F to 40º F) in accordance with the ASTM C666-92 freeze-thaw test standard on concrete.

High temperature cycles simulate the summer season effects. Temperature cycle is chosen to vary between 16 ºC and 49 ºC (60 ºF and 120 ºF). The temperature cycles alternate with relative humidity (RH) cycles.

The first RH cycles starts after 50 temperature cycles to simulate rain during summer days. In the first cycle, RH varies between 60% and 100% at a constant temperature of 16 ºC (60 ºF) to simulate the humidity and rain during night times. In the second cycle, RH varies between 60% and 100% at a constant temperature of 27 ºC (80ºF) to simulate humidity and rain during day times. In the third cycle, it is assumed that on bridge decks

as soon as it starts raining, the heat from the concrete bridge deck might escape causing the nearby air temperature to actually rise to a higher level, so RH is varied from 60% to 100% at a constant temperature of 38 ºC (100 ºF).

During all the high temperature and high RH cycles the rods were exposed to UV radiation. The lamps positioned in the chamber exposed the specimens to an irradiance of 6.80 X 10^{-2} W/ cm^2 in a spectral band of 300-800 nm and of 6.10 X 10^{-2} W/ cm^2 in a spectral band of 300-800 nm.

Totally, after each environmental regimen the specimen were exposed to 50 freeze-thaw cycles, 150 temperature and 120 RH cycles, alternating as shown in Figure 9. The rods were exposed to four of the ageing regimens in Figure 9, so the total environmental exposure can be summarized as in Table 7.

Table 7 Total environmental exposure

Cycles	***Temperature Range ºC (ºF)***	***Total Number***	***UV exposure***
Freeze-Thaw	-18 ; 4 (0 ; 40)	200	No
High Temperature	16 ; 49 (60 ;120)	600	Yes
High RH (60% – 100%)	16 (60)	160	Yes
High RH (60% – 100%)	27 (80)	160	Yes
High RH (60% – 100%)	38 (100)	160	Yes

In APPENDIX A the detailed ageing program, and the single environmental cycles that constitute the combined exposure are illustrated. A typical thermal and RH diagram printed by the control system of the environmental chamber is reported in Figure A7.

3.3.1 Tensile test Specimens

Different kinds of tensile test specimens were prepared and tested: different FRP materials, cross section shape, surface roughness, specimen length and anchors dimensions were investigated in order to optimize the tensile characterization of FRP rods.

Since a lot of different products are available, a large range of properties has been investigated in order to propose a procedure that could be used for an extensive class of materials. Even if a surface roughness is required by technical codes, smooth rebars, such as prototypes need to be tested in order to investigate mechanical properties, therefore an effective method should be developed for every kind of surface. In this experimental study the worst cases of smooth surfaces and high stress rebars have been investigated, also for non-circular section, in order to observe the most critical aspects of such characterization. Slip occurrence has been monitored during tests recording load-displacement and load-time curves.

The nominal diameter of the circular-section rods was measured by means of a caliper; four measurements were conducted for each rod. The results showed a good accordance between all specimens of the same type, therefore a mean value of cross section area could be considered without reasonable error. For the rebars that presented a non-uniform diameter because of the presence of a fiber bundle in a spiral pattern, the diameter was computed positioning the caliper in a region without the fiber bundle. The sand coating that was present in some of the investigated rods was considered as part of the nominal diameter, therefore the reported measures are referred to the overall diameter, which is commonly used for engineering purposes.

In Table 8 geometry and other relevant properties of the rods used in this research are reported. Different free test lengths are reported for the same specimen type because different ratios between test length diameter (L/D), and different anchorage length were investigated. Label C is related to Carbon rods, while G is related to glass rods. All the smooth specimens were subjected to light sand blasting. G2 specimens were modified at the free ends in order to increase the gripping forces: an epoxy paste was applied on the surface, and sand particles were bonded before the resin hardening. This procedure allowed to create a rough interface between the rod and the grouted anchors, reducing the possibility to observe a pullout failure instead of a tensile rupture of the fibers.

Table 8: Tensile test specimens properties

Rod	***Surface***	***Free test-length mm (in)***	***Anchorage length mm (in)***	***L/D***
C1	Rough: sand and wound fibers	610 (24)	457 (18)	74
C2	Rough: sand and wound fibers	610 (24) 762 (30) 914 (36)	457 (18) 381 (15) 305 (12)	76 95 114
C3	Smooth: light sand blasting	610 (24) 914 (36)	457 (18) 305 (12)	58 77
C4	Smooth: light sand blasting	457 (18) 610 (24)	381 (15) 305 (12)	72 96
C5	Rough: deformed surface	457 (18)	381 (15)	48
C6*	Smooth: light sand blasting	457 (18)	381 (15)	56*
C7*	Smooth: light sand blasting	457 (18)	381 (15)	56*
G1	Smooth: light sand blasting; Rough: epoxy coated sand	610 (24)	457 (18)	51
G2	Rough: sand and wound fibers	457 (18) 610 (24)	381 (15) 305 (12)	72 96
G3	Rough: deformed surface	457 (18)	381 (15)	48
G4	Rough: deformed surface	457 (18)	381 (15)	36
G5	Rough: deformed surface	457 (18)	381 (15)	72

*rectangular cross-section; the L/D ratio is referred to the mean value between the two dimensions of the cross section. All others are circular cross-section

3.3.2 Specimen Anchorage and Alignment

The anchorage and alignment of the specimen constitutes the most critical path of tensile characterization. The anchorage system consisted of steel tubes filled with expansive grout. The pressure developed by the mortar anchored the rod in the pipe when subjected

to tensile load. The alignment was provided using steel washers and PVC drilled caps at the free end of the pipes. A wood frame built to take the specimens in vertical position during the grout hardening contributed to a perfect alignment of the rods in the center of the pipes.

The composition of the expansive resin used for anchorages is reported in Table 9:

Table 9: Composition of expansive grout

Component	***% by weight***
CaO	77 to 96
SiO_2	2 to 11
Al_2O_3	0.3 to 6
Fe2O3	0.5 to 3
MgO	0 to 2
SO3	0.5 to 5
Organic fillers	1

The full pressure is developed in 72 hours, and it is related to the cavity filled by the grout, as reported in Figure 14. The water to powder ratio should not exceed 0.34, in this application a ratio of 0.29 was used. Different sizes of pipes were used in order to guarantee a sufficient gripping pressure, with compatibility of the yielding strength of the steel. Welded pipes were used as anchorage; the characteristics of the pipes are reported in Table 10. The pipes belongs to the class reported on Table I of the American National Standard for stainless steel pipe (ANSI B36.19 Stainless Steel Pipes), according to ASTM A 312/A 312M (ASTM 2000).

The pressure developed by the grout in the tubes increases with the internal diameter, therefore, even if a higher pressure improves the gripping force on the free end of the rod, yielding strength of the steel should be taken into account. Thus the choose of the wall thickness of the tubes is related to the pressure developed by the grout expansion; but it will be seen that the wall thickness of the tubes is also strongly related to the expected

ultimate strength of the rod, since a tensile force will be applied on the tubes as it will be described.

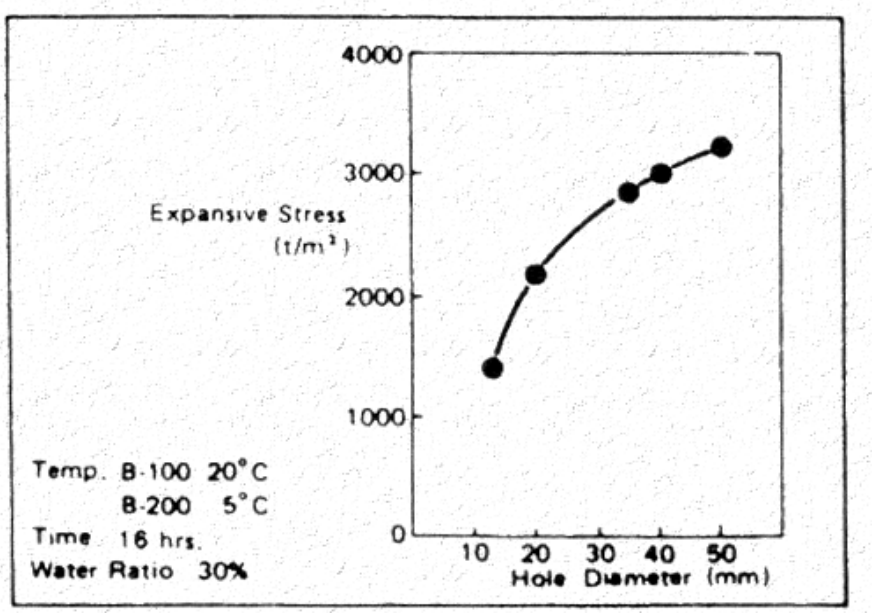

Figure 14: Pressure developed by the grout for different tubes diameter

Table 10: Welded steel tubes used for anchorages

NPS Designator	***Outside diameter mm (in)***	***Nominal wall thickness mm (in)***	***Yielding strength MPa (ksi)***	***Label tubes type***
1 ¼ Schedule 40S	42.16 (1.660)	3.56 (0.140)	205 (30)	I
1 ¼ Schedule 80S	42.16 (1.660)	4.85 (0.191)	205 (30)	II
1 ½ Schedule 80S	48.26 (1.900)	5.08 (0.200)	205 (30)	III

According to the tubes that were used and values furnished in Figure 13, the theoretical values of the stress developed on the walls of the pipes by the grout expansion were computed as follows:

- Tubes type I stress = 119 MPa (17.2 ksi)
- Tubes type II stress = 96 MPa (13.9 ksi)
- Tubes type III stress = 120 MPa (17.4 ksi)

Strain gauges were placed on the external side of the tubes in radial direction during 72 hours of grout hardening. It was seen that after 36 hours the 95% of the final stress was developed, and after 72 hours the following values were found:

- Tubes type I stress = 108 MPa (15.6 ksi)
- Tubes type II stress = 98 MPa (14.2 ksi)
- Tubes type III stress = 123 MPa (17.8 ksi)

It means that the gripping pressure developed on the free-end of the rod was:

- Tubes type I grip pressure = 20 MPa (2.9 ksi)
- Tubes type II grip pressure = 26 MPa (3.7 ksi)
- Tubes type III grip pressure = 29 MPa (4.2 ksi)

A metal washer was welded on one free end of the pipes, the diameter of the washer was chosen sufficiently larger than the diameter of the rod, but with a small tolerance in order to provide the best alignment. When the expansive grout is poured it has a low viscosity, therefore a silicon ring was provided in correspondence of the washer/pipe interface in order to avoid the flow-out of the grout.

When silicon hardened the pipes are ready for inserting the rods: the rod should pass through the washer in the bottom, as shown in Figure 15.

Figure 15: Washer welded for alignment of the rod

The bars were placed in a vertical position using a wood frame built for this purpose. The drilled PVC cap was inserted on the other side of the steel tube making the rod passing through it. To avoid the leaking of the liquid mortar through the small thickness between the rod and the washers on the bottom side silicone was used to close this space.

At this point the tubes were ready to be filled with the expansive grout, and the rods are in perfect alignment because of they pass through the welded washer on the bottom side, through the PVC cap at the other end of the pipe, and through the hole drilled in the wood frame as shown in Figure 16.

After 24 hours that the grout was poured, even if the internal pressure was not fully developed, the solid state of the grout allowed to turn the rods and repeat the same anchorages installation on the other side. The PVC caps of the first side were easily removed and used on the other side; PVC caps inserted on the tubes are shown in Figure 17. A new wood beam on the upper side was easily changed removing the screws in order to insert the steel tube. The diameter of the holes drilled on the wood upper beams was the same as that of the steel tubes.

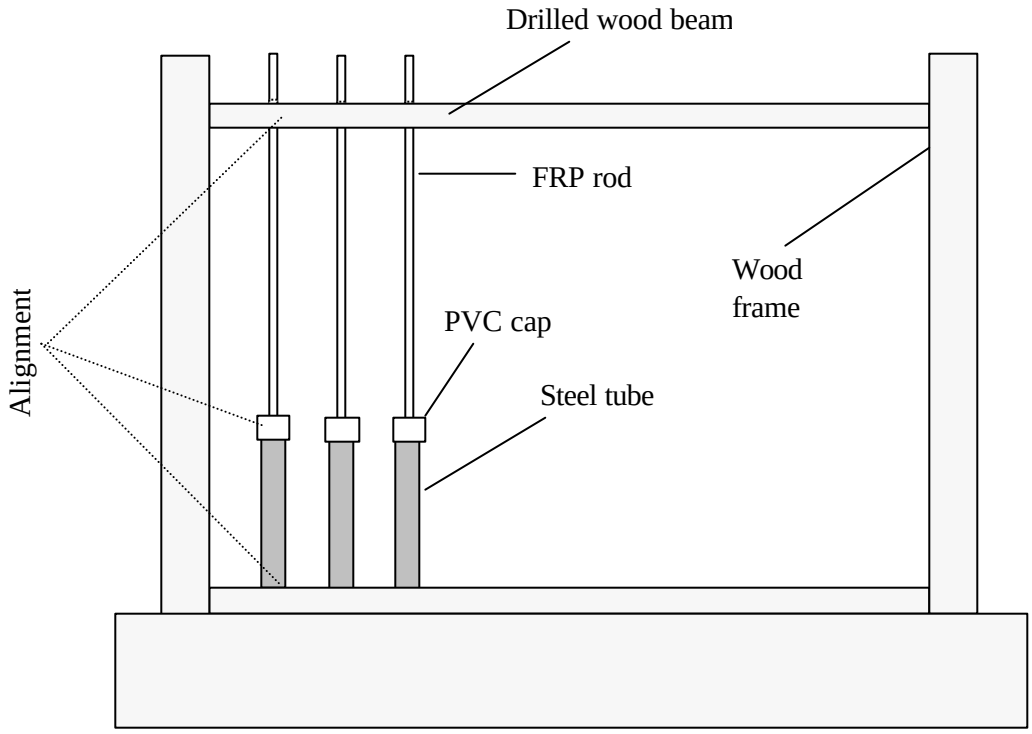

Figure 16: Alignment of the rods

Once the grout hardened the PVC cap was removed from the pipe and was left mobile on the free test length of the specimen. At this point the rods were ready to be tested.

Figure 17: PVC drilled caps used for alignment

In Table 11 different types of pipes used for the investigated rods are reported; the expected load was computed by theoretical formulas of micro-mechanics of FRP composites.

Table 11: Steel tubes used for different expected loads

Rod	***Steel Tube***	***Ultimate expected load kN (kips)***
C1	Type III	120 – 150 (27 - 34)
C2	Types I, II and III	90 – 100 (20 – 22)
C3	Type II	45 – 55 (10 – 12)
C4	Type II	50 – 60 (11 – 13)
C5	Type II	150 – 160 (34 – 36)
C6	Type III	100 – 110 (22 – 25)
C7	Type III	100 – 110 (22 – 25)
G1	Type III	90 – 100 (20 - 22)
G2	Type I	20– 30 (4 - 7)
G3	Type II	60 – 70 (13 - 16)
G4	Type II	90 – 100 (20- 22)
G5	Type I	30 – 40 (7 - 9)

3.3.3 Test Setup and Data Acquisition

Tensile tests were performed using a Tinius-Olsen Universal Testing Machine. The specimen was set-up across the two crossheads of the machine and aligned with the axis of the grips of the machine. The anchor at one end rested on the top crosshead. A 19 mm (¾-in) thick grooved steel plate was inserted between the anchor and the crosshead to distribute the load. Another 19-mm (¾-in) steel plate with the groove was attached at the lower end of the bar for the same purpose. The movable crosshead of the testing machine was positioned so that the plate at the lower end was snug without stressing the bar. In

Figures 18 and 19 the set-up of the rod in the universal machine used for test is illustrated.

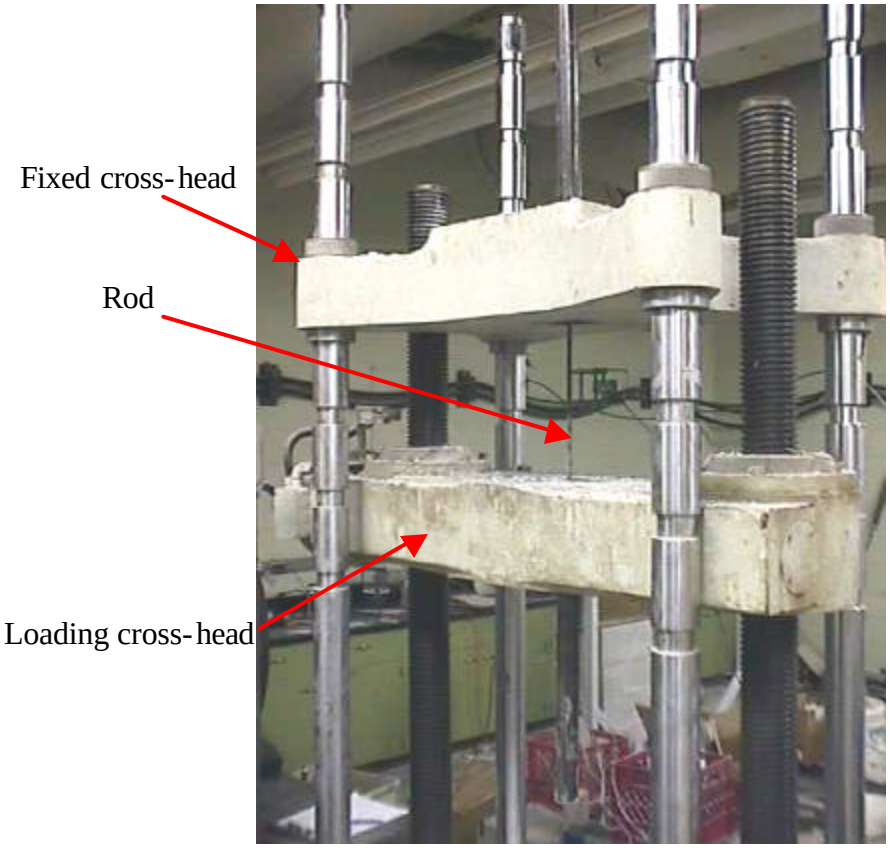

Figure 18: Universal testing machine used for tensile tests

An electronic extensometer with 51 mm (2 in) gage length and 0.025 mm (1/1000 in) accuracy was mounted on the center of specimen test section to measure rod displacement as shown in Figure 20. Strain gauges were also attached in order to measure the strain and compare with the extensometer readings. Load, displacement and strain data were recorded by a data acquisition system, which consists of Data General Conditioner Rack and LABVIEW® acquisition software. The sampling rate was set to 1-Hz. The test was led under displacement control; the loading rate was 22-kN per minute (5-kips per minute).

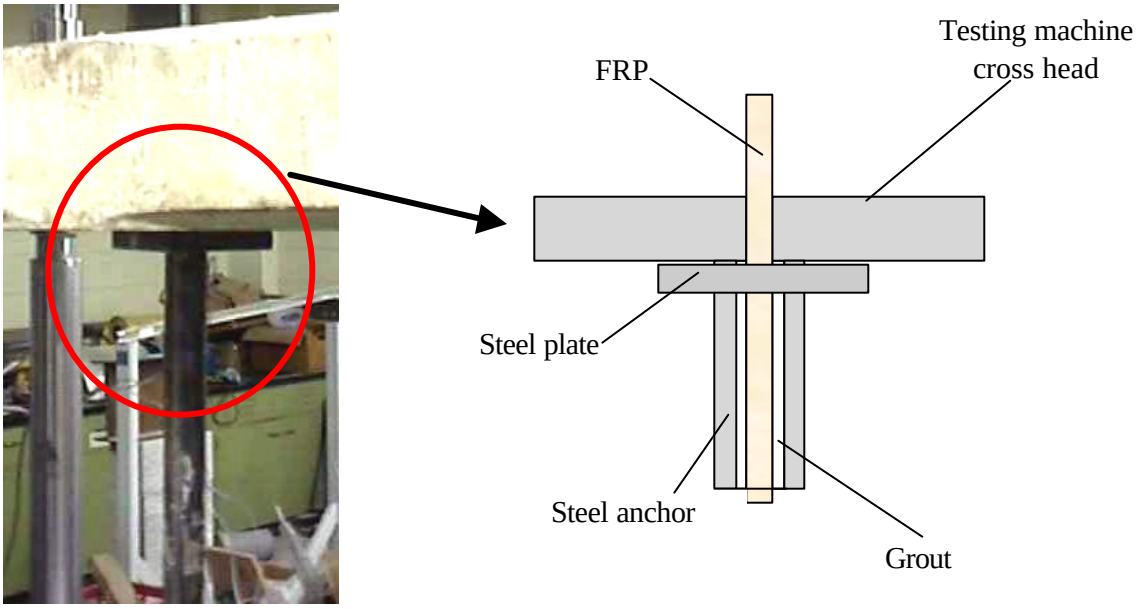

Figure 19: Positioning of the anchorages in the testing machine

Figure 20: Extensometer mounted to the tensile specimen

The following equation was used to calculate the tensile stress of the tested rods:

$$s = \frac{P}{A} \qquad \text{Eq. 2}$$

Where:

s = stress in the FRP rod ;	[MPa] (ksi)
P = Load	[kN] (kips)
A = cross-section area	[mm^2] (in^2)

3.4 Short Beam Test

The measurement of tensile mechanical properties is essential in for the design of FRP reinforcement in a concrete section, but short shear span tests are necessary in order to study the long-term behavior. In fact, if the principal role of the resin is to embed the fibers in order to guarantee a perfect stress transfer from the concrete to the fibers, it has also a protection purpose. Therefore, even if transverse properties are not used in design equation, since they are related to the properties of resin and fiber/matrix interface, cracks in the resin may cause damages in the fibers that are directly exposed to external agents.
Short beam test according to ASTM D4475 was used to investigate the changes in transverse mechanical properties due to accelerated aging. It must be remarked that the interlaminar shear stress measured with the SBT do not furnish values that can be used for design, but only for comparative purposes.

3.4.1 Test Setup and Data Acquisition

The specimens were tested using a Universal Testing Machine INSTRON 4469 with displacement control. The load capacity of the machine was 50 kN (11.25 kips) and the speed range could go from 0.001 to 500 mm/min (from 0.00004 in/min to 20 in/min). The

rate of loading crosshead motion was 1.3 mm/min (0.05 in/min) according to ASTM D4475. The data were recorded automatically by a SATEC TCS 1200 acquisition system. A schematic representation of the short beam test apparatus is illustrated in Figure 21. Different span values were chosen for different type of rods in accordance to the different diameters in order to eliminate flexural effects that could affect the desired horizontal shear failure mode.

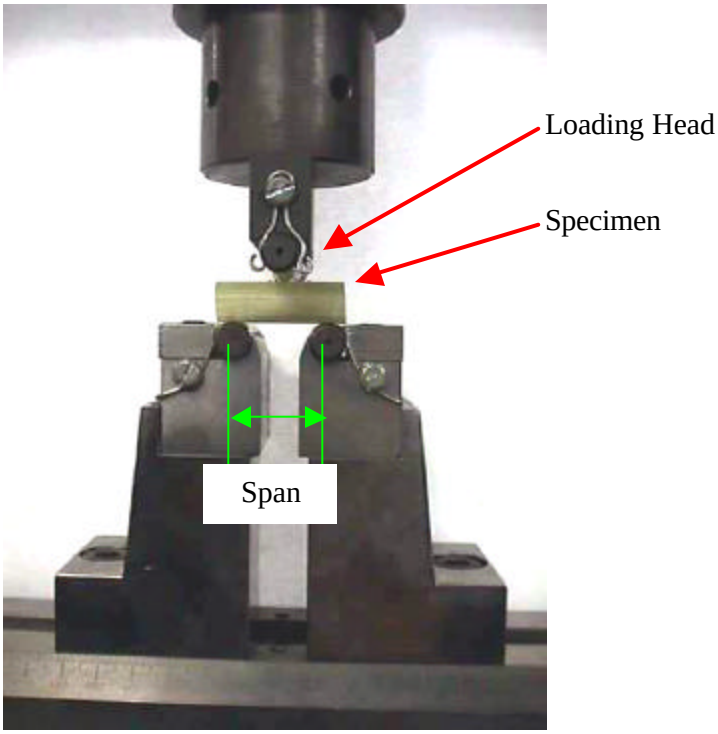

Figure 21: Short beam test set-up

The following equation was used to calculate the value of ISS:

$$S = 0.849\frac{P}{D^2} \qquad \text{Eq. 3}$$

Where:

S = Interlaminar Shear Stress [N/m^2] (psi)

P = Breaking load [N] (lbf)

D = Diameter of the rod [m] (in)

3.5 Gravimetric Measurements

SBT specimens were used for gravimetric measurements; eighteen specimens were weighted for each type of rod every seven days. Six specimens were immersed in alkaline solution and kept at T = 22 ºC (72 ºF) for 42 days; the remaining were immersed in alkaline solution and kept at T = 60 ºC (140 ºF) for 21 and 42 days respectively.

The weight increase investigation represents an important information, in fact absorption properties such as diffusivity of the FRP system can be easily computed once the weight increase is known. Therefore a correlation between absorption properties and ISS should be expected, since fluid penetration generates cracks in the resin and a decrease in transverse mechanical properties.

The fluid content was measured as follows:

$$M_t(\%) = \frac{W - W_d}{W_d} \cdot 100 \qquad \text{Eq. 4}$$

Where:

$M_t(\%)$ = Percentage of fluid content at time t

W_d = weight of the dry specimen at time t=0

W = weight of the moist specimen at time t

If the absorption is linear, as usually happens in FRP systems in the first part of the exposure, the diffusivity *d* can be computed using equation 5 with reference to Figure 22, in which the typical absorption behavior of an FRP system immersed in a fluid is shown:

$$d = \frac{p \cdot R^2}{16}\left(\frac{M_2 - M_1}{M_m}\right)^2 \cdot \left(\frac{1}{\sqrt{t_2} - \sqrt{t_1}}\right)^2 \qquad \text{Eq. 5}$$

Where:

d = diffusivity [mm^2/min] (in^2/min)

R = Radius of the rod [mm] (in)

M_1 = Percentage of fluid content at time t_1

M_2 = Percentage of fluid content at time t_2

M_m = Percentage of fluid content at the end of the linear behavior

t_1 = starting time of observation (min)

t_2 = end time of observation (min)

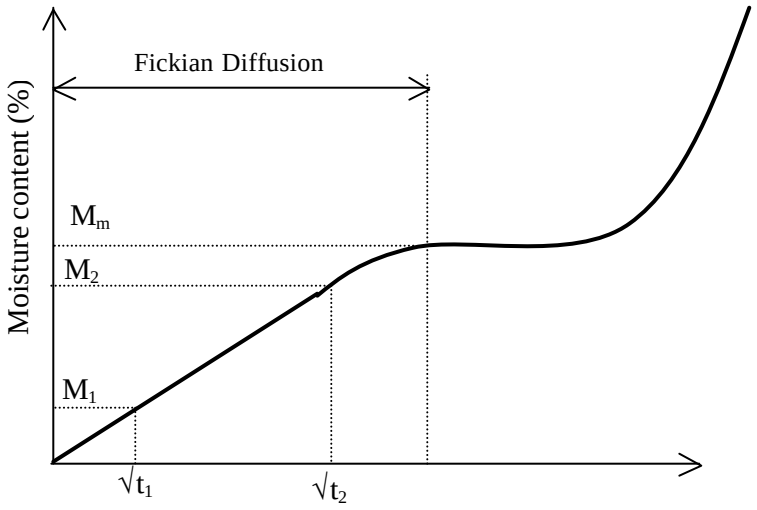

Figure 22: Typical absorption behavior of FRP composites

In correspondence of M_m% the slope of the curve changes dramatically because particular phenomena occur: the fluid penetration after a time t_m causes a macroscopic mechanical degradation of the system. It means that cracking patterns open and allow a fast fluid penetration that is represented by the second curve with increased slope. Therefore after the fickian diffusion region the absorption behavior is controlled by the fluid penetration in the open cracks developed from the surface to the inner part of the sample.

4 TEST RESULTS AND DISCUSSION

The experimental results related to mechanical characterization and absorption properties are presented in the following sections.

4.1 Tensile Properties

Tensile tests showed a perfect elastic behavior until tensile failure occurred, that is the typical brittle behavior of FRP composites with unidirectional fibers.

All tensile specimens failed showing tensile fiber rupture, except for a rectangular specimen C6 that showed a pull out failure due to slippage between the rod and the anchors.

The tensile properties measured after tensile tests are reported in Table 12. It can be observed that all the tests showed small standard deviation of data, confirming values that are typical of FRP rods used in construction, as reported in Table 1.

The mechanical properties related to test 2 of C6 specimens should be intended as values measured before tensile failure, since that after a load of 111 kN (25 kips) was reached the CFRP rod slipped out from the anchorage. It can be attributed to the smooth surface of the rod and to the fact that the gripping pressure developed by the expansive grout inside the steel tube is less effective for rectangular cross section rather than circular. This was the only case in which the specimen did not fail in tension, but, only four CFRP rectangular rods with smooth surface were tested. Thus a further investigation is needed, in order to validate the applicability of the proposed protocol also for non-circular rods, with smooth surface.

Visual observations allowed to remark that tensile failure of GFRP specimens was accompanied by delamination of the fibers, even if the failure was always brittle. CFRP rods showed catastrophic failure, with a violent release of elastic energy that caused expulsion of the anchorages from the machine frame. All the different aspects of the failed specimens can be observed in the pictures reported in Appendix B. All the data expressed in customary units are also reported in APPENDIX B.

Table 12: Tensile test control specimens - SI Units

Rod	*d (mm)*	*Ultimate stress (MPa)*	*Modulus (MPa)*	*Ultimate strain*
G1 test 1	12.00	941	42018	0.0224
G1 test 2		953	42898	0.0222
G1 test 3		951	44547	0.0213
G1 test 4		884	41490	0.0213
G1 test 5		892	41918	0.0213
Mean Values		**924**	**42574**	**0.0217**
Standard deviation		34	1216	0.0006
Variance		4%	3%	3%
G2 test 1	6.35	365	22750	0.0160
G2 test 2		351	33781	0.0104
G2 test 3		393	34470	0.0114
G2 test 4		407	36745	0.0111
G2 test 5		295	22061	0.0134
Mean Values		**362**	**29961**	**0.0124**
Standard deviation		44	6988	0.0023
Variance		12%	23%	18%
G3 test 1	9.53	888	36938	0.0241
G3 test 2		857	37402	0.0229
Mean Values		**873**	**37170**	**0.0235**
Standard deviation		22	328	0.0008
Variance		3%	1%	3%
G4 test 1	12.70	789	35621	0.0222
G4 test 2		789	36614	0.0216
Mean Values		**789**	**36118**	**0.0219**
Standard deviation		0	702	0.0004
Variance		0%	2%	2%
G5 test 1	6.35	1118	35346	0.0316
G5 test 2		996	37434	0.0266
Mean Values		**1057**	**36390**	**0.0291**
Standard deviation		86	1477	0.0036
Variance		8%	4%	12%
C1 test 1	8.26	2566	125165	0.0205
C1 test 2		2410	127300	0.0189
C1 test 3		2212	129003	0.0171
C1 test 4		2415	133729	0.0181
Mean Values		**2401**	**128799**	**0.0187**
Standard deviation		145	3642	0.0014
Variance		6%	3%	8%

C2 test 1	8.00	1900	106780	0.0178
C2 test 2		1878	110422	0.0170
C2 test 3		2251	107628	0.0209
C2 test 4		1946	100200	0.0194
Mean Values		**1994**	**106258**	**0.0188**
Standard deviation		174	4328	0.0017
Variance		9%	4%	9%
C3 test 1	7.94	1010	110856	0.0091
C3 test 2		1015	104113	0.0097
C3 test 3		1012	106870	0.0097
C3 test 4		1015	110993	0.0091
Mean Values		**1013**	**108208**	**0.0094**
Standard deviation		2	3390	0.0004
Variance		0%	3%	4%
C4 test 1	6.35	2034	130085	0.0156
C4 test 2		1852	127953	0.0145
Mean Values		**1943**	**129019**	**0.0151**
Standard deviation		129	1508	0.0008
Variance		7%	1%	5%
C5 test 1	9.53	2126	109215	0.0195
C5 test 2		2182	120018	0.0182
C5 test 3		2151	111959	0.0192
Mean Values		**2153**	**113730**	**0.0190**
Standard deviation		40	7639	0.0009
Variance		2%	7%	5%
C6 test 1	10 x 6	1659	124092	0.0134
C6 test 2*		1803	117198	0.0154
Mean Values		**1731**	**120645**	**0.0144**
Standard deviation		102	4875	0.0014
Variance		6%	4%	10%
C7 test 1	10 x 6	1875	130986	0.0143
C7 test 2		2019	124092	0.0163
Mean Values		**1947**	**127539**	**0.0153**
Standard deviation		102	4875	0.0014
Variance		5%	4%	9%

The mechanical properties measured with extensometer and strain gauges were found to be in satisfactory accordance, as reported in the example in Figure 23 related to a test on C3 rods.

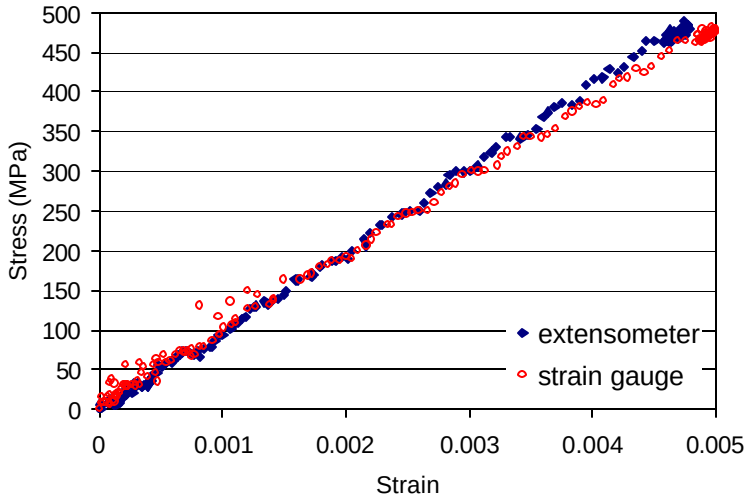

Figure 23: Stress strain curves measured with strain gauge and extensometer

A first comparison between the different mechanical properties can be observed from the following Figures 24 and 25 that illustrate the stress strain curves of the control specimens. It can be observed that all GFRP rods that were tested show similar properties, except for G1 rods that showed lower modulus and lower tensile strength. This is due to a lower fiber content as it will be shown in the following. G1 rods showed the highest stiffness, while G5 had the largest ultimate elongation.

CFRP specimens showed similar properties too, C3 rods presented a lower tensile strength even if they have a comparable stiffness with the other carbon rods.

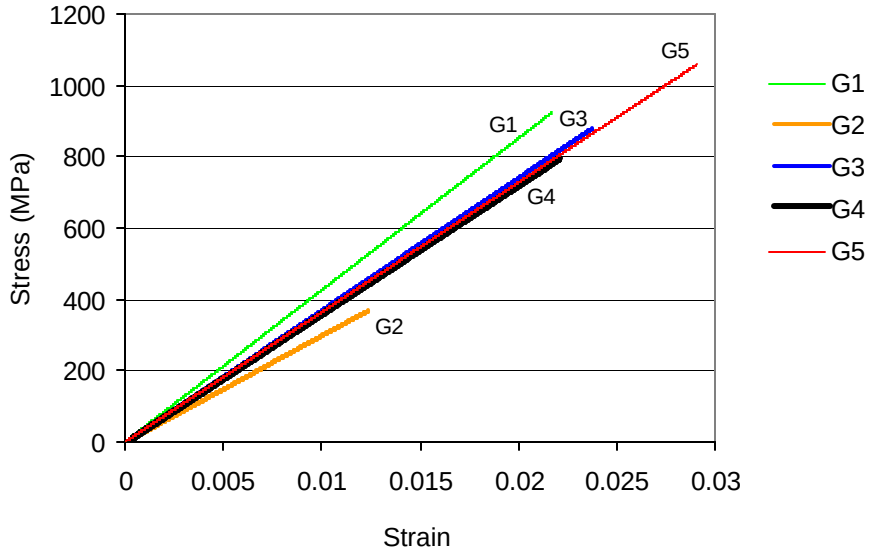

Figure 24: Stress strain curves for control GFRP specimens

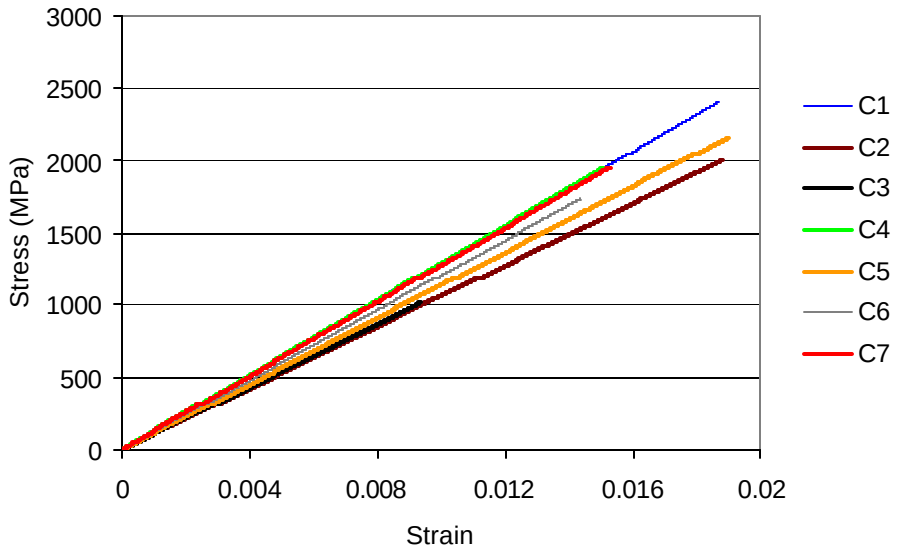

Figure 25: Stress strain curves for control CFRP specimens

Different amount of residual tensile properties were found after the tests of conditioned rods. Test results related to conditioned specimens are reported in Tables 14 - 16.

Table 13: Tensile test after alkali exposure (21 days @ T = 60 °C) – SI Units

rod	***d (mm)***	***Ultimate stress (MPa)***	***Modulus (MPa)***	***Ultimate strain***
G1 test 1	12.00	927	41571	0.0223
G1 test 2		939	38193	0.0246
G1 test 3		907	41709	0.0218
Mean Values		**924**	**40491**	**0.0229**
standard deviation		16	1991	0.0015
Variance		2%	5%	7%
G2 test 1	6.35	220	26197	0.0084
G2 test 2		276	33712	0.0082
G2 test 3		260	33608	0.0077
Mean Values		**252**	**31172**	**0.0081**
standard deviation		29	4309	0.0004
Variance		11%	14%	4%
C1 test 1	8.26	2490	121865	0.0204
C1 test 2		2204	127760	0.0172
C1 test 3		2455	128704	0.0191
Mean Values		**2383**	**126110**	**0.0189**
standard deviation		156	3706	0.0016
Variance		7%	3%	8%
C3 test 1	7.94	1045	119749	0.0087
C3 test 2		988	108029	0.0091
C3 test 3		1015	108925	0.0093
Mean Values		**1016**	**112234**	**0.0091**
standard deviation		28	6523	0.0003
Variance		3%	6%	3%

Table 14: Tensile test after alkali exposure (42 days @ T = 60 °C) – SI Units

rod	*d (mm)*	*Ultimate stress (MPa)*	*Modulus (MPa)*	*Ultimate strain*
G1 test 1	12.00	903	39709	0.0228
G1 test 2		941	43639	0.0216
G1 test 3		941	39503	0.0238
Mean Values		**928**	**40950**	**0.0227**
standard deviation		22	2331	0.0011
Variance		2%	6%	5%
G2 test 1	6.35	170	25784	0.0066
G2 test 2		251	33091	0.0076
G2 test 3		224	32402	0.0069
Mean Values		**215**	**30426**	**0.0070**
standard deviation		41	4035	0.0005
Variance		19%	13%	7%
C1 test 1	8.26	2188	127677	0.0171
C1 test 2		2054	129194	0.0159
C1 test 3		2386	125030	0.0191
Mean Values		**2209**	**127300**	**0.0174**
standard deviation		167	2107	0.0016
Variance		8%	2%	9%
C3 test 1	7.94	1028	123403	0.0083
C3 test 2		1001	111407	0.0090
C3 test 3		1015	114027	0.0089
Mean Values		**1015**	**116279**	**0.0087**
standard deviation		13	6307	0.0004
Variance		1%	5%	4%

Figures 26 and 27 illustrate the data of Table 16, in which residual mechanical properties are reported after testing of the conditioned specimens. These data allow to know important information on the long-term mechanical behavior of the tested FRP rods that will be discussed in the next chapter in order to provide an useful contribute for improving future design guidelines.

Table 15: Tensile test after environmental exposure – SI Units

rod	*d (mm)*	*Ultimate stress (MPa)*	*Modulus (MPa)*	*Ultimate strain*
G1 test 1	12.00	896	39985	0.0224
G1 test 2		897	41709	0.0215
G1 test 3		982	39916	0.0246
G1 test 4		856	39296	0.0218
Mean Values		**908**	**40226**	**0.0226**
standard deviation		53	1036	0.0014
Variance		6%	3%	6%
G2 test 1	6.35	309	24749	0.0125
G2 test 2		421	27576	0.0153
G2 test 3		309	27576	0.0112
G2 test 4		316	29851	0.0106
Mean Values		**338**	**27438**	**0.0124**
standard deviation		55	2089	0.0021
Variance		16%	8%	17%
C1 test 1	8.26	2490	125030	0.0199
C1 test 2		2490	126326	0.0197
C1 test 3		2443	123699	0.0197
C1 test 4		2295	128146	0.0179
Mean Values		**2430**	**125800**	**0.0193**
standard deviation		92	1896	0.0009
Variance		4%	2%	5%
C2 test 1	8.00	2085	117288	0.0178
C2 test 2		1891	110993	0.0170
C2 test 3		1763	105340	0.0167
C2 test 4		1864	107388	0.0174
Mean Values		**1901**	**110252**	**0.0172**
standard deviation		135	5240	0.0004
Variance		7%	5%	3%
C3 test 1	7.94	997	105478	0.0952
C3 test 2		1032	100652	0.1034
C3 test 3		979	100652	0.0980
Mean Values		**1003**	**102261**	**0.0989**
standard deviation		27	2786	0.0042
Variance		3%	3%	4%
C4 test 2	6.35	2245	109394	0.0205
C4 test 3		1964	117887	0.0167
C4 test 4		1999	120645	0.0166
Mean Values		**2069**	**115975**	**0.0179**
standard deviation		153	5864	0.0023
Variance		7%	5%	13%

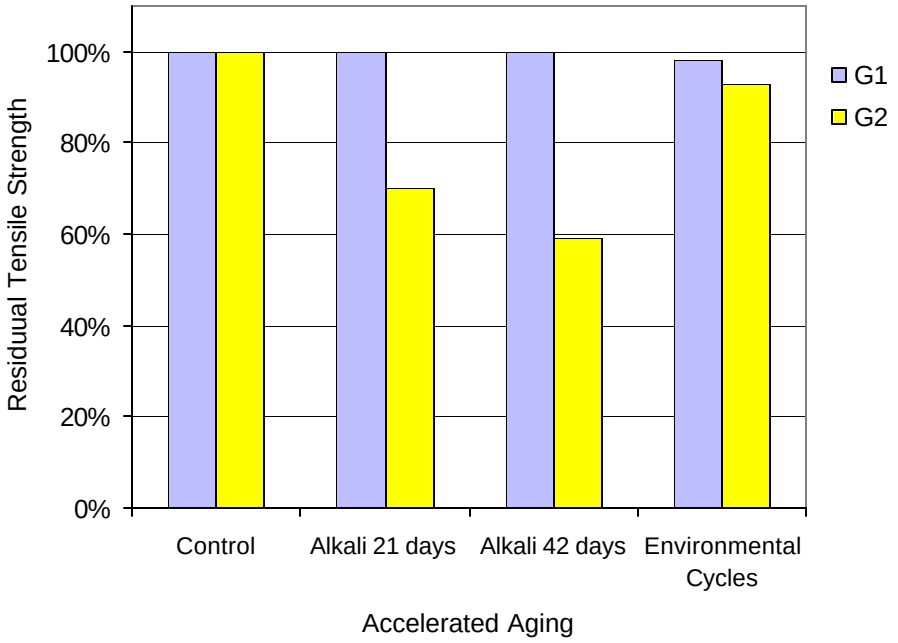

Figure 26: Residual tensile strength for GFRP specimens

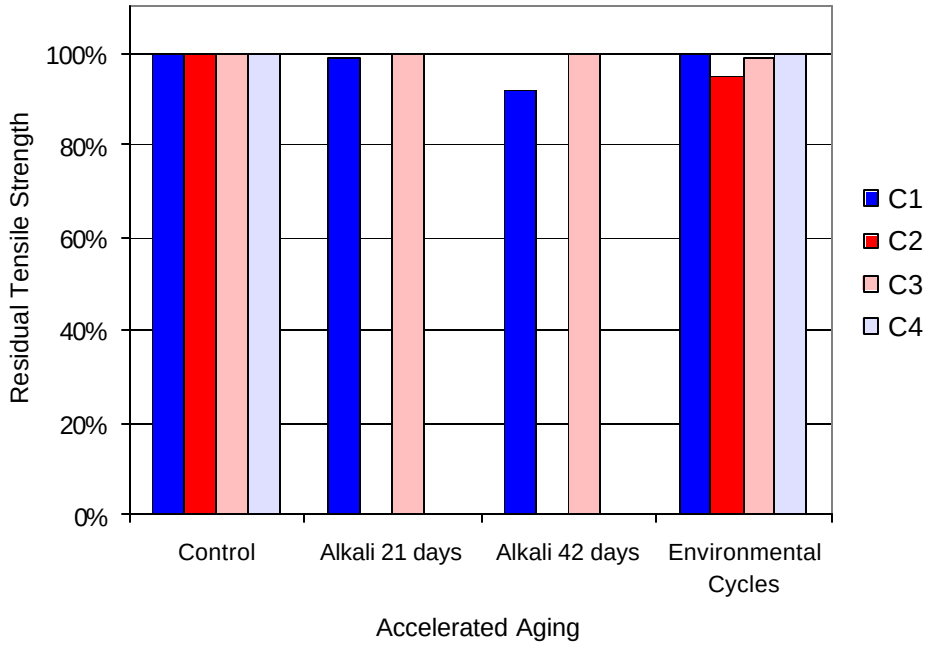

Figure 27: Residual tensile strength for CFRP specimens

Alkaline solution exposure dramatically affected G2 rods, while G1 rods did not show a decrease in mechanical longitudinal properties. Environmental cycles did not reduce the tensile strength of the GFRP specimens. The stiffness value did not show significant variations after conditioning.

CFRP specimens had a good retention of mechanical properties after both conditioning exposures, C1 rods presented a 8% reduction after 42 days in alkaline solution that could be adduced to a resin degradation more than fiber damages, as it will be discussed later. The resin degradation may change the stress distribution to the fibers in the cross section, therefore a premature failure could be expected.

Table 16: Residual Tensile Strength

Rods	***Control***	***Alkali 21 days (T = 60 °C)***	***Alkali 42 days (T = 60 °C)***	***Environmental Cycles***
G1	100%	100%	100%	98%
G2	100%	70%	59%	93%
C1	100%	99%	92%	100%
C2	100%	NA	NA	95%
C3	100%	100%	100%	99%
C4	100%	NA	NA	100%

4.2 Interlaminar Shear Stress

As it was said before transverse properties are mostly related to resin quality, and they furnish a measure of the potential penetration of external agents that could damage the fibers and affect the longitudinal mechanical properties.

Typical load-displacement curves of short shear span beam test for the tested rods are reported in the following Figures 28 – 35.

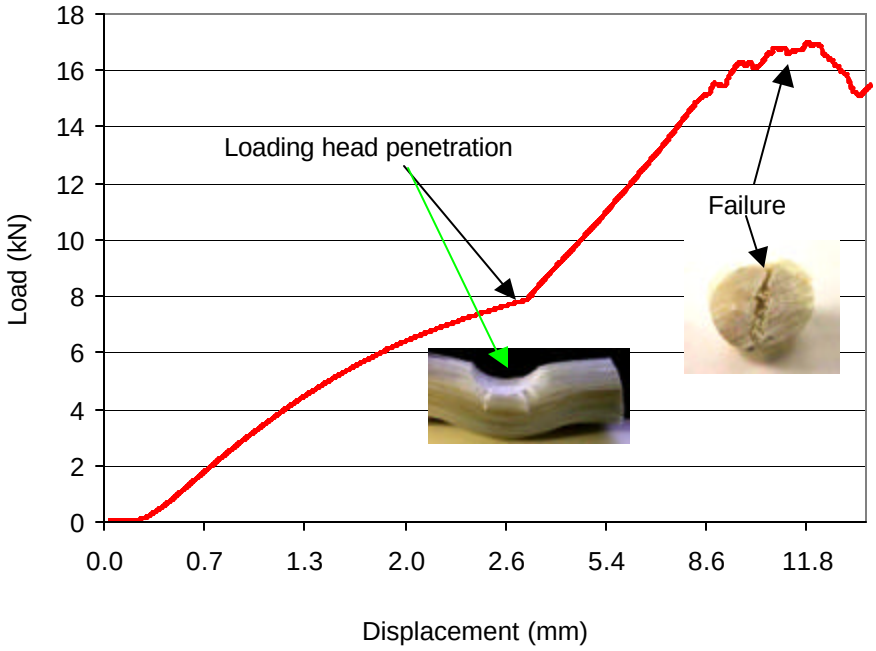

Figure 28: Load displacement curve for G1 rods after ASTM D4475

G1 rods presented a behavior illustrated in Figure 28, that is due to the thermoplastic matrix. In the first part of the test the penetration of the loading head generated the first slope curve, then, after the penetration stopped the specimen reached the shear failure with an increase apparent stiffness. G1 control specimens showed a principal vertical plane of failure, even if other cracks were developed in horizontal direction and were evident after testing. Conditioned specimens had a combined horizontal and vertical shear failure due to extensive cracking developed also along the horizontal plane as illustrated in Figure 29.

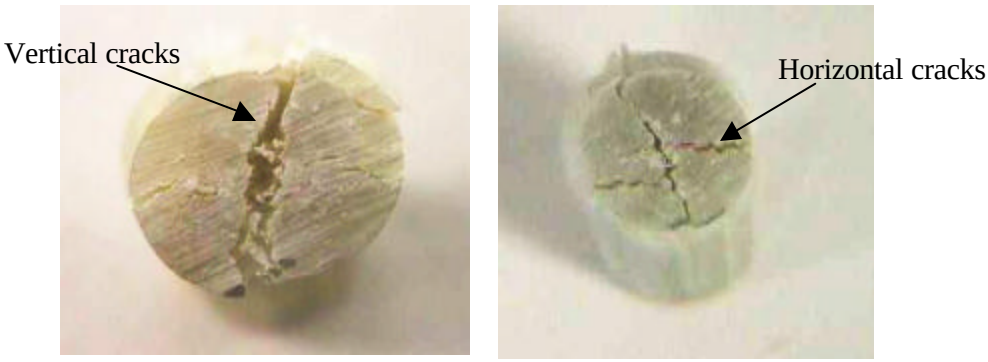

Figure 29: G1 Rods after ASTM D4475

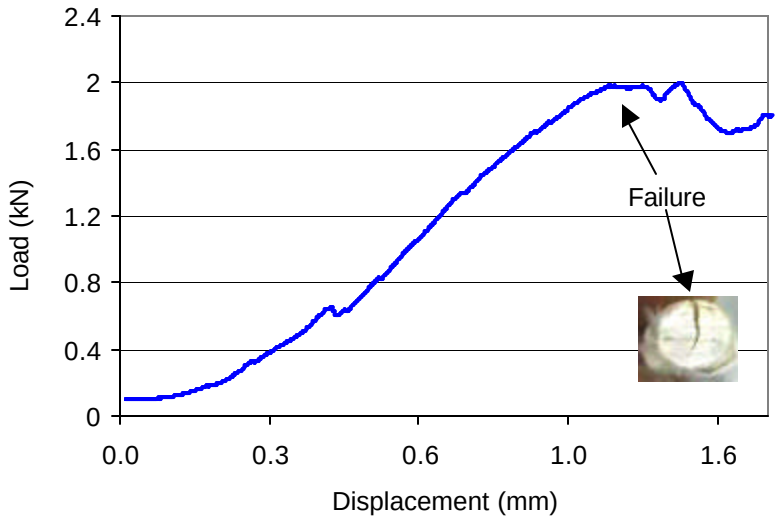

Figure 30: Load displacement curve for G2 rods after ASTM D4475

Control specimens showed a typical load-displacement curve, with vertical failure shear plane due to the ultimate strength of the polyester resin. In figure 31 it can be seen that conditioned specimens after 42 days at 60°C presented extensive micro-cracking due to

fluid penetration. Therefore the failure resulted in a complete splitting of the cross section along different planes, even if the vertical one was the most evident.

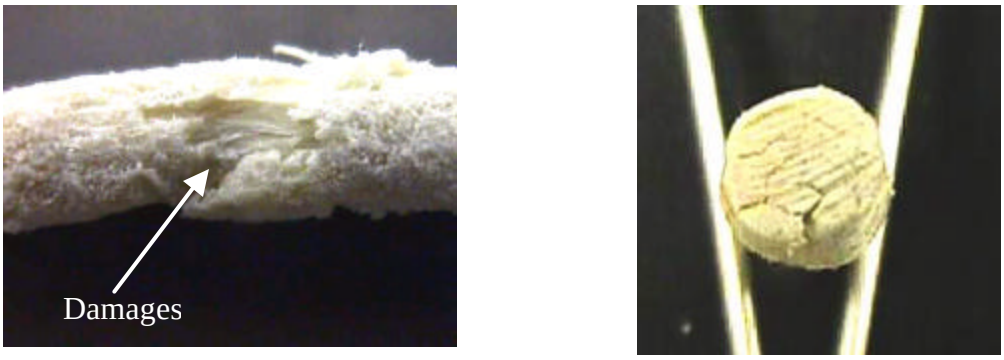

Figure 31: G2 conditioned specimens before ASTM D4475

Figures 32 – 35 illustrate the typical behavior of epoxy CFRP specimens C1, C2, C3 and C4. All the CFRP rods C1, C2 and C4 show an almost linear behavior until the brittle failure occurs. The first part of the curves is due to the penetration of the loading head in the external coating of the rods. All short shear span test on C3 specimens evidenced a change of stiffness at a load of about 2 kN. The loading head did not penetrate into the cross section of the rods, therefore this change of transverse stiffness could be attributed to a redistribution of stress inside the specimen due to the stress developed in the resin.

A vertical failure shear plane was clearly evidenced after testing as expected for epoxy CFRP rods, without the presence of other evident cracking phenomena, either for control specimens, or for conditioned ones.

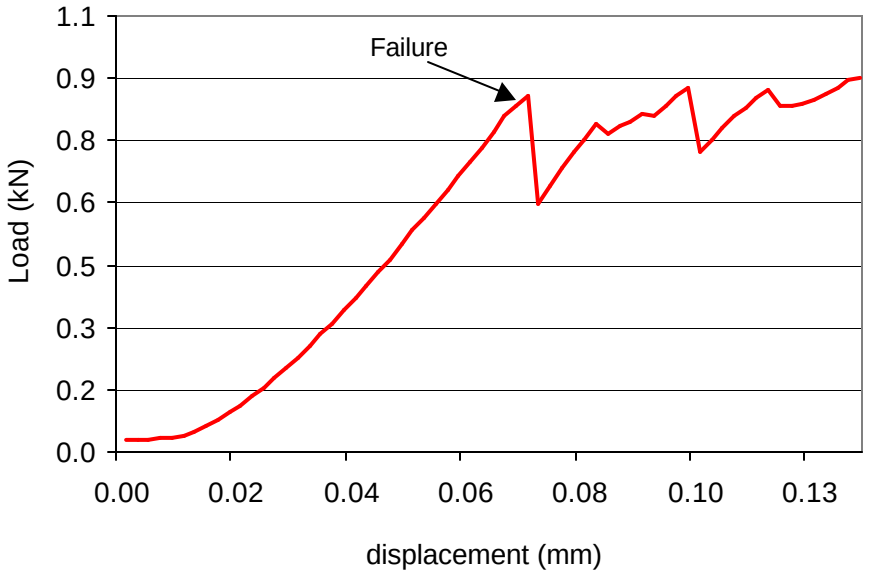

Figure 32: Load displacement curve for C1 rods after ASTM D4475

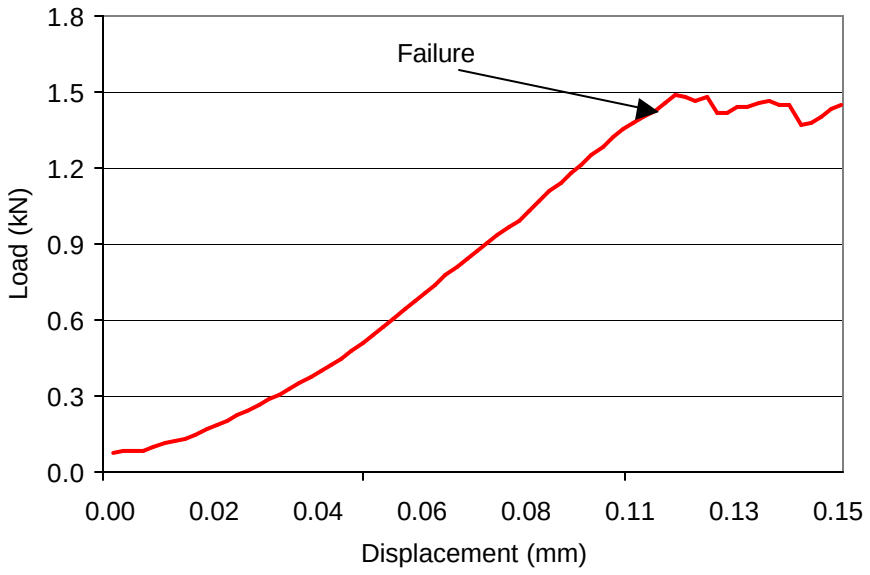

Figure 33: Load displacement curve for C2 rods after ASTM D4475

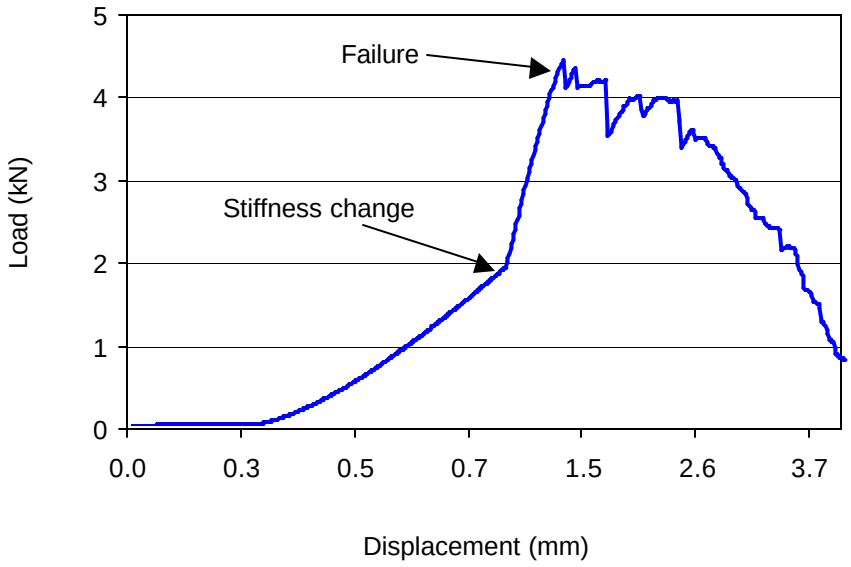

Figure 34: Load displacement curve for C3 rods after ASTM D4475

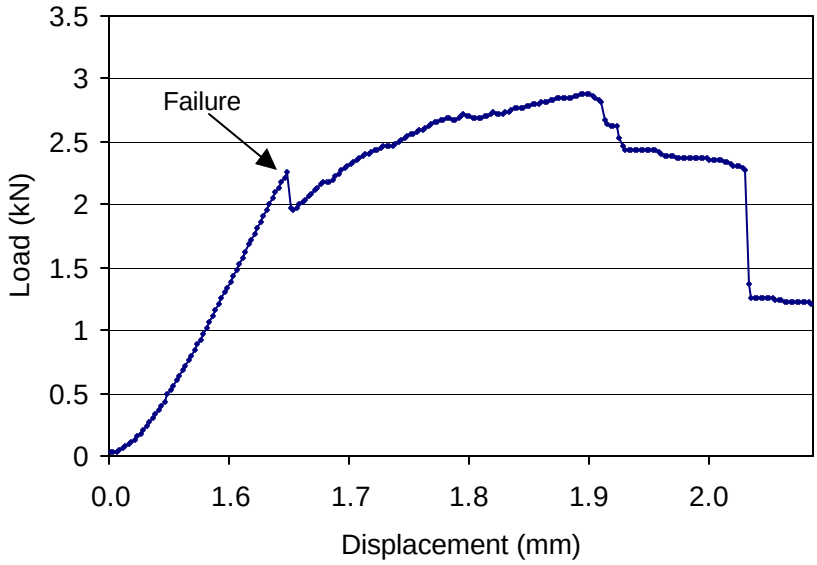

Figure 35: Load displacement curve for C4 rods after ASTM D4475

All these curves were shown in order to understand the experimental behavior of the tested specimens. In the following Tables 17 – 21 all data related to short shear span tests are reported for control and exposed specimens.

Table 17: Short shear span test unconditioned rods - SI Units

G1	***Load (kN)***	***ISS(MPa)***	***Span (mm)***	***Span/D***	***Plane of failure***
TEST 1	16.911	99.706	26	2.2	Vertical / Horizontal
TEST 2	14.554	85.807			
TEST 3	17.374	102.434			
TEST 4	18.744	110.511			
TEST 5	16.564	97.661			
TEST 6	17.881	105.423			
Mean values	**17.005**	**100.257**			
Standard deviation	1.424	8.395			
Variance	8%	8%			
G2	***Load (kN)***	***ISS(MPa)***	***Span (mm)***	***Span/D***	***Plane of failure***
TEST 1	2.309	48.606	19	3.0	Vertical
TEST 2	2.295	48.325			
TEST 3	1.913	40.271			
TEST 4	2.331	49.075			
TEST 5	1.979	41.676			
Mean values	**2.165**	**45.591**			
Standard deviation	0.202	4.252			
Variance	9%	9%			
C1	***Load (kN)***	***ISS(MPa)***	***Span (mm)***	***Span/D***	***Plane of failure***
TEST 1	0.857	10.679	29	3.0	Vertical
TEST 2	0.936	11.660			
TEST 3	1.241	15.461			
TEST 4	0.836	10.413			
TEST 5	0.986	12.289			
Mean values	**0.971**	**12.100**			
Standard deviation	0.162	2.024			
Variance	17%	17%			
C2	***Load (kN)***	***ISS(MPa)***	***Span (mm)***	***Span/D***	***Plane of failure***
TEST 1	1.152	15.282	29	3.6	Vertical
TEST 2	1.312	17.407			
TEST 3	1.428	18.941			

TEST 4	1.957	25.962			
TEST 5	1.521	20.180			
Mean values	**1.474**	**19.554**			
Standard deviation	0.303	4.022			
Variance	21%	21%			
C3	***Load (kN)***	***ISS(MPa)***	***Span (mm)***	***Span/D***	***Plane of failure***
TEST 1	3.195	39.814	24	3.0	Vertical
TEST 2	4.252	52.982			
TEST 3	4.146	51.652			
TEST 4	4.048	50.433			
TEST 5	4.417	55.033			
Mean values	**4.012**	**49.983**			
Standard deviation	0.476	5.935			
Variance	12%	12%			
C4	***Load (kN)***	***ISS(MPa)***	***Span (mm)***	***Span/D***	***Plane of failure***
TEST 1	2.260	47.576	19	3.0	Vertical
TEST 2	2.331	49.075			
TEST 3	2.251	47.389			
TEST 4	2.664	56.099			
TEST 5	2.540	53.476			
Mean values	**2.409**	**50.723**			
Standard deviation	0.184	3.880			
Variance	8%	8%			

Table 18: Short shear span test after alkali exposure (42 days @ T = 22 °C) – SI Units

G1	***Load (kN)***	***ISS(MPa)***	***Span (mm)***	***Span/D***	***Plane of failure***
TEST 1	17.307	102.040	26	2.2	Vertical / Horizontal
TEST 2	15.604	91.996			
TEST 3	17.027	100.388			
TEST 4	17.788	104.872			
TEST 5	16.684	98.369			
TEST 6	17.730	104.532			
Mean values	**17.023**	**100.366**			
Standard deviation	0.812	4.786			
Variance	5%	5%			
G2	***Load (kN)***	***ISS(MPa)***	***Span (mm)***	***Span/D***	***Plane of failure***
TEST 1	2.024	42.612	19	3	Vertical
TEST 2	2.277	47.951			
TEST 3	2.268	47.763			
TEST 4	1.601	33.715			

TEST 5	1.824	38.398			
TEST 6	2.260	47.576			
Mean values	**2.042**	**43.003**			
Standard deviation	0.282	5.927			
Variance	14%	14%			

C1	***Load (kN)***	***ISS(MPa)***	***Span (mm)***	***Span/D***	***Plane of failure***
TEST 1	1.023	12.746			
TEST 2	1.116	13.910			
TEST 3	1.027	12.801			
TEST 4	1.450	18.066	29	3.6	Vertical
TEST 5	1.508	18.786			
TEST 6	1.090	13.577			
Mean values	**1.202**	**14.981**			
Standard deviation	0.218	2.715			
Variance	18%	18%			

C2	***Load (kN)***	***ISS(MPa)***	***Span (mm)***	***Span/D***	***Plane of failure***
TEST 1	1.401	18.587			
TEST 2	1.414	18.764			
TEST 3	1.601	21.242			
TEST 4	1.570	20.829	29	3	Vertical
TEST 5	1.566	20.770			
TEST 6	1.552	20.593			
Mean values	**1.518**	**20.131**			
Standard deviation	0.087	1.149			
Variance	6%	6%			

C3	***Load (kN)***	***ISS(MPa)***	***Span (mm)***	***Span/D***	***Plane of failure***
TEST 1	4.444	115.244			
TEST 2	4.639	120.320			
TEST 3	4.234	109.822			
TEST 4	4.795	124.357	24	3	Vertical
TEST 5	4.417	114.552			
TEST 6	4.315	111.898			
Mean values	**4.474**	**116.032**			
Standard deviation	0.208	5.407			
Variance	5%	5%			

Alkaline exposure at 22°C was used in order to show the effects of high temperature on accelerate ageing. It can be seen that after 42 days of alkali exposure at room

temperature transverse mechanical properties were not affected for both GFRP and CFRP rods.

Table 19: Short shear span test after alkali exposure (21 days @ T = 60 °C) – SI Units

G1	***Load (kN)***	***ISS(MPa)***	***Span (mm)***	***Span/D***	***Plane of failure***
TEST 1	14.509	85.545	26	2.2	Vertical / Horizontal
TEST 2	13.931	82.136			
TEST 3	13.344	78.674			
TEST 4	11.943	70.413			
TEST 5	12.650	74.583			
TEST 6	13.042	76.891			
Mean values	**13.237**	**78.040**			
Standard deviation	0.913	5.384			
Variance	7%	7%			
G2	***Load (kN)***	***ISS(MPa)***	***Span (mm)***	***Span/D***	***Plane of failure***
TEST 1	0.418	8.803	19	3	Vertical
TEST 2	0.427	8.991			
TEST 3	0.240	5.057			
TEST 4	0.374	7.867			
TEST 5	0.391	8.242			
TEST 6	0.334	7.024			
Mean values	**0.364**	**7.664**			
Standard deviation	0.069	1.459			
Variance	19%	19%			

C1	***Load (kN)***	***ISS(MPa)***	***Span (mm)***	***Span/D***	***Plane of failure***
TEST 1	1.148	14.297	29	3.6	Vertical
TEST 2	0.738	9.199			
TEST 3	0.716	8.922			
TEST 4	0.667	8.312			
TEST 5	0.552	6.872			
TEST 6	0.672	8.368			
Mean values	**0.749**	**9.328**			
Standard deviation	0.206	2.564			
Variance	27%	27%			

C2	***Load (kN)***	***ISS(MPa)***	***Span (mm)***	***Span/D***	***Plane of failure***
TEST 1	1.535	20.357	29	3	Vertical
TEST 2	1.165	15.459			
TEST 3	1.161	15.400			
TEST 4	1.210	16.049			

TEST 5	1.139	15.105			
TEST 6	0.934	12.391			
Mean values	**1.191**	**15.794**			
Standard deviation	0.194	2.577			
Variance	16%	16%			

C3	***Load (kN)***	***ISS(MPa)***	***Span (mm)***	***Span/D***	***Plane of failure***
TEST 1	3.581	92.864			
TEST 2	4.786	124.126			
TEST 3	4.355	112.937			
TEST 4	3.870	100.362	24	3	Vertical
TEST 5	3.581	92.864			
TEST 6	3.581	92.864			
Mean values	**3.959**	**102.670**			
Standard deviation	0.506	13.112			
Variance	13%	13%			

Table 20: Short shear span test after alkali exposure (42 days @ T = 60 °C) – SI Units

G1	***Load (kN)***	***ISS(MPa)***	***Span (mm)***	***Span/D***	***Plane of failure***
TEST 1	12.018	70.859			
TEST 2	10.239	60.369			
TEST 3	12.228	72.092			
TEST 4	11.116	65.535	26	2.2	Vertical / Horizontal
TEST 5	11.356	66.952			
TEST 6	11.387	67.135			
Mean values	**11.391**	**67.161**			
Standard deviatio n	0.707	4.167			
Variance	6%	6%			
G2	***Load (kN)***	***ISS(MPa)***	***Span (mm)***	***Span/D***	***Plane of failure***
TEST 1	0.178	3.746			
TEST 2	0.294	6.181			
TEST 3	0.165	3.465	19	3	Vertical
TEST 4	0.214	4.495			
TEST 5	0.160	3.372			
Mean values	**0.202**	**4.252**			
Standard deviation	0.055	1.165			
Variance	27%	27%			

C1	***Load (kN)***	***ISS(MPa)***	***Span (mm)***	***Span/D***	***Plane of failure***
TEST 1	0.658	8.202	29	3.6	Vertical
TEST 2	0.689	8.590			
TEST 3	0.712	8.867			

TEST 4	0.578	7.204			
TEST 5	0.534	6.650			
TEST 6	0.525	6.539			
Mean values	**0.616**	**7.675**			
Standard deviation	0.081	1.010			
Variance	13%	13%			

C2	***Load (kN)***	***ISS(MPa)***	***Span (mm)***	***Span/D***	***Plane of failure***
TEST 1	0.770	10.208			
TEST 2	0.983	13.040			
TEST 3	0.996	13.217			
TEST 4	1.005	13.335	29	3	Vertical
TEST 5	0.974	12.922			
TEST 6	0.987	13.099			
Mean values	**0.953**	**12.637**			
Standard deviation	0.090	1.199			
Variance	9%	9%			

C3	***Load (kN)***	***ISS(MPa)***	***Span (mm)***	***Span/D***	***Plane of failure***
TEST 1	3.421	88.711			
TEST 2	3.750	97.248			
TEST 3	3.127	81.097			
TEST 4	3.034	78.675	24	3	Vertical
TEST 5	4.359	113.052			
TEST 6	2.948	76.464			
Mean values	**3.440**	**89.208**			
Standard deviation	0.538	13.947			
Variance	16%	16%			

Table 21: Short shear span test after environmental exposure – SI Units

G1	***Load (kN)***	***ISS(MPa)***	***Span (mm)***	***Span/D***	***Plane of failure***
TEST 1	18.948	111.717			
TEST 2	17.369	102.407			
TEST 3	16.569	97.687			
TEST 4	16.155	95.248	26	2.2	Horizontal / Vertical
TEST 5	17.361	102.355			
TEST 6	17.045	100.493			
Mean values	**17.241**	**101.651**			
Standard deviation	0.961	5.665			
Variance	6%	6%			

G2	***Load (kN)***	***ISS(MPa)***	***Span (mm)***	***Span/D***	***Plane of failure***
TEST 1	2.144	45.141	19	3	Vertical

TEST 2	2.228	46.921			
TEST 3	2.224	46.827			
TEST 4	2.046	43.081			
TEST 5	2.331	49.075			
TEST 6	2.135	44.954			
Mean values	**2.185**	**46.000**			
Standard deviation	0.098	2.066			
Variance	4%	4%			

C1	***Load (kN)***	***ISS(MPa)***	***Span (mm)***	***Span/D***	***Plane of failure***
TEST 1	0.939	11.693			
TEST 2	0.845	10.529			
TEST 3	1.183	14.741			
TEST 4	1.023	12.746	29	3.6	Vertical
TEST 5	1.050	13.078			
TEST 6	1.041	12.967			
Mean values	**1.013**	**12.626**			
Standard deviation	0.114	1.420			
Variance	11%	11%			

C2	***Load (kN)***	***ISS(MPa)***	***Span (mm)***	***Span/D***	***Plane of failure***
TEST 1	1.543	20.475			
TEST 2	1.668	22.127			
TEST 3	1.330	17.643			
TEST 4	1.263	16.758	29	3	Vertical
TEST 5	1.268	16.817			
TEST 6	1.699	22.540			
Mean values	**1.462**	**19.393**			
Standard deviation	0.200	2.653			
Variance	14%	14%			

C3	***Load (kN)***	***ISS(MPa)***	***Span (mm)***	***Span/D***	***Plane of failure***
TEST 1	3.274	84.904			
TEST 2	4.052	105.092			
TEST 3	3.954	102.554	24	3	Vertical
TEST 4	4.008	103.939			
TEST 5	4.181	108.438			
Mean values	**3.894**	**100.985**			
Standard deviation	0.357	9.249			
Variance	9%	9%			

C4	***Load (kN)***	***ISS(MPa)***	***Span (mm)***	***Span/D***	***Plane of failure***
TEST 1	2.180	45.890	19	3	Vertical
TEST 2	2.553	53.757			
TEST 3	2.500	52.633			

TEST 4	2.233	47.014			
TEST 5	2.433	51.229			
Mean values	**2.380**	**50.105**			
Standard deviation	0.165	3.475			
Variance	7%	7%			

In APPENDIX C experimental results related to short shear span tests are reported in customary units.

Since ASTM D4475 does not allow to measure design values for transverse properties, but it is only a test protocol in order to compare interlaminar shear stress of FRP rods, in Figures 36 and 37 a comparison between control and exposed specimens highlights the most important information furnished by these tests. All data related to residual transverse properties are also reported in Table 22.

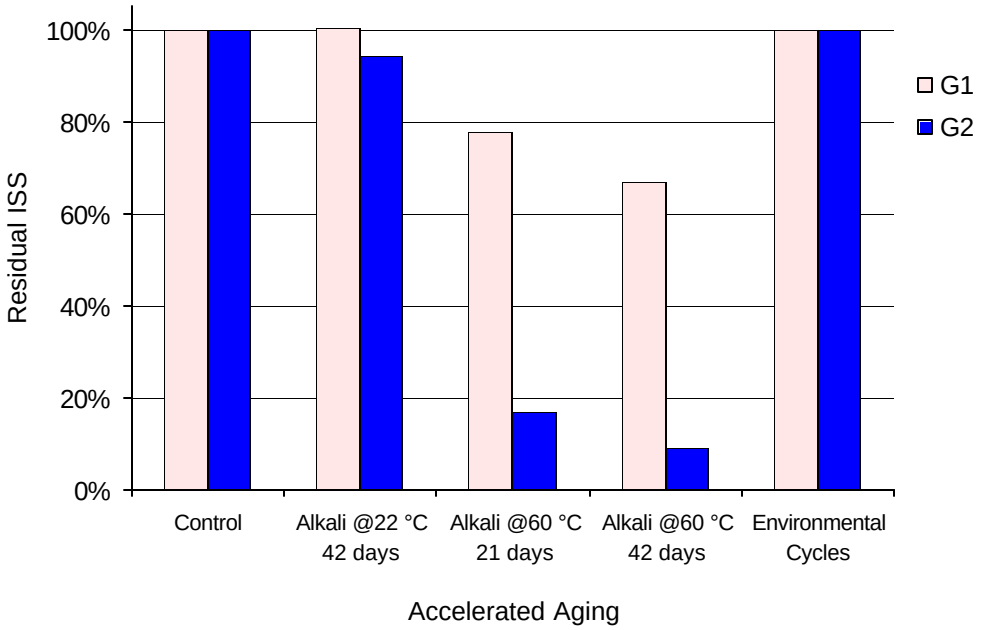

Figure 36: Residual ISS of GFRP specimens

A significant decrease in transverse properties was observed for GFRP specimens. Polyester G2 rods lost totally their interlaminar shear strength after immersion in alkali

solution at 60°C for 42 days. A progressive decrease in ISS was measured for longer exposure times. Environmental cycles did not affect resin properties, and the effect of higher temperature for alkali exposure regimen is highlighted since the ISS was totally retained for specimens conditioned at room temperature.

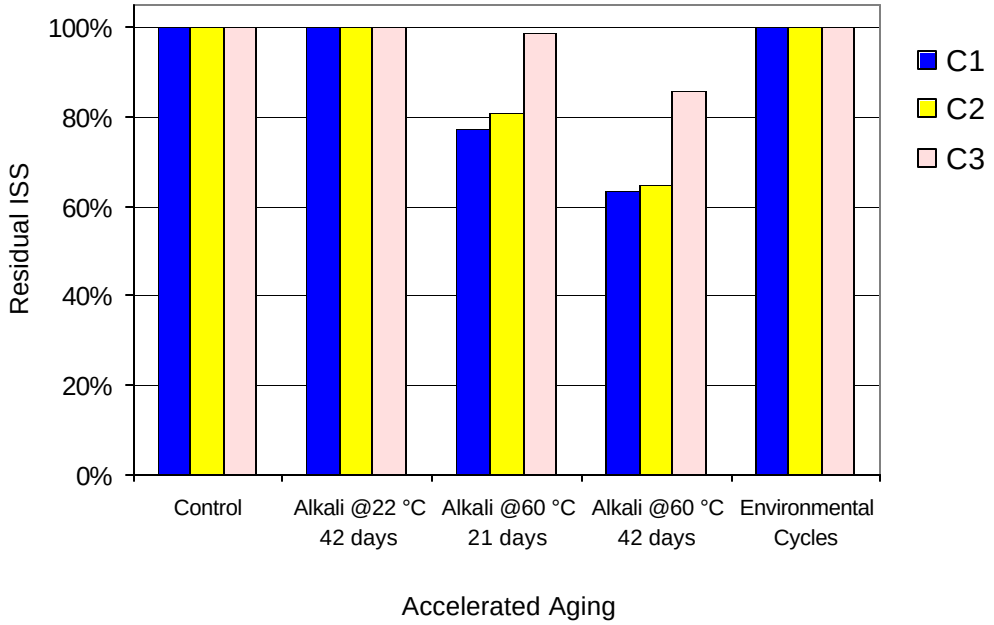

Figure 37: Residual ISS of CFRP specimens

CFRP specimens were also affected by alkali exposure, while environmental aging did not attack the resin properties. C1 and C2 rods, having the same epoxy matrix, showed a similar behavior; C3 specimens showed the highest retain in residual ISS after immersion. The effect of temperature is evident also in this case, since the same exposure time at room temperature did not affect the resin mechanical properties.

Table 22: Residual interlaminar shear strength

Rods	***Control***	***Alkali @ 22 °C 42 days***	***Alkali @ 60 °C 21 days***	***Alkali @ 60 °C 42 days***	***Environmental Cycles***
G1	100%	100%	78%	67%	100%
G2	100%	94%	17%	9%	100%
C1	100%	100%	77%	63%	100%
C2	100%	100%	81%	65%	100%
C3	100%	100%	99%	86%	100%
C4	100%	n.a.	n.a.	n.a.	100%

4.3 Absorption Properties

The absorption properties were measured by weighting the rods and recording the weight increase. In Figures 38 the results of weight increase for GFRP specimens are reported, while in Figure 39 the absorption behavior of CFRP rods is illustrated.

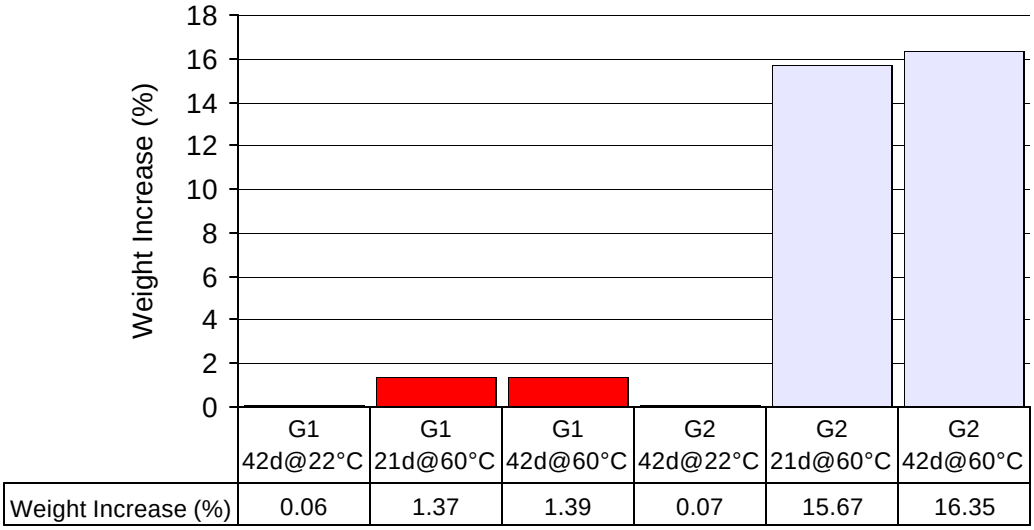

Figure 38: Weight increase in GFRP rods after conditioning

A large difference in weight increase emerged from gravimetric tests of G1 and G2 rods. G2 rods showed a high fluid penetration that led to a weight increase of 16% after 42

days of exposure at 60 °C. It can be observed that there are not significant differences of weight after 21 and 42 days of accelerated exposure in alkali solution. This data show that a saturation value was reached after the first period of 21 days, and further exposure in alkaline solution revealed that an equilibrium status was established between the specimens and the conditioning solution.

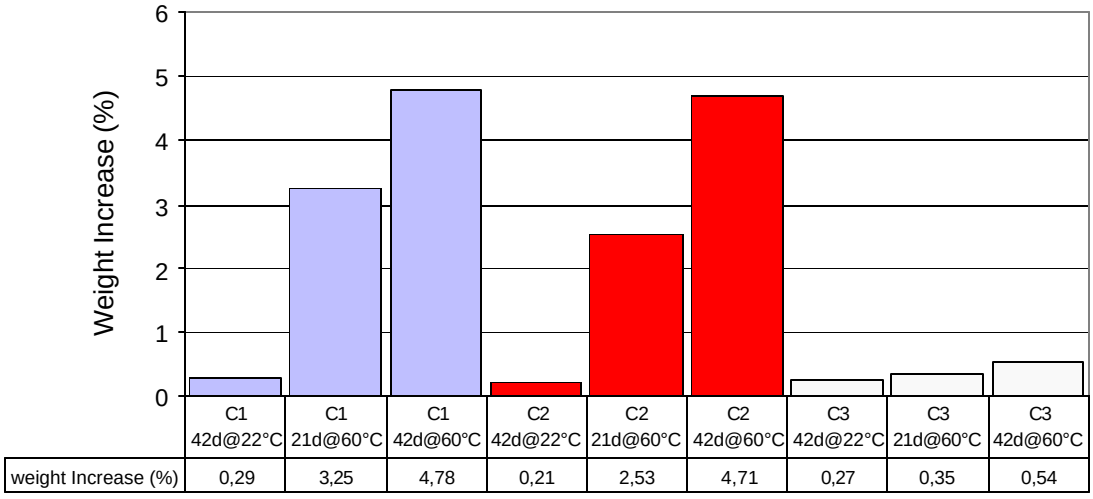

Figure 39: Weight increase in CFRP rods after conditioning

Different absorption behavior was measured for different epoxy- CFRP systems as can be observed in figure 39. C3 rods presented a lower weight increase, while fluid penetration in C1 and C2 specimens increased the weight by 4.78% and 4.71% respectively.

In order to understand the absorption behavior the diagrams of the weight increase can be plotted with the square root of time as is illustrated in the following Figure 40. In Figure 40 the diagram was drawn using data related to the absorption behavior of specimens exposed to alkaline solution at 60 °C for 42 days.

The first part of the diagram is linear for all the specimens, the slope of the curve is related to the diffusivity of the solution into the resin. It can be seen that polyester resin showed a higher fluid absorption, while the epoxy resin in C3 rods presented the lowest diffusivity. After this region that could be modeled using Fick's law, the diffusion

mechanism changed, and the different resin systems showed a different behavior. The last region, in fact, is controlled by the presence of micro-cracks in the resin that allow a higher or less amount of fluid penetration, that is proportional to the second slope of the curves. G1, G2 and C3 rods presented a constant value of weight increase which means that an equilibrium value for mass exchange was established, while C1 and C2 rods continued to increase their weight until the end of the exposure time.

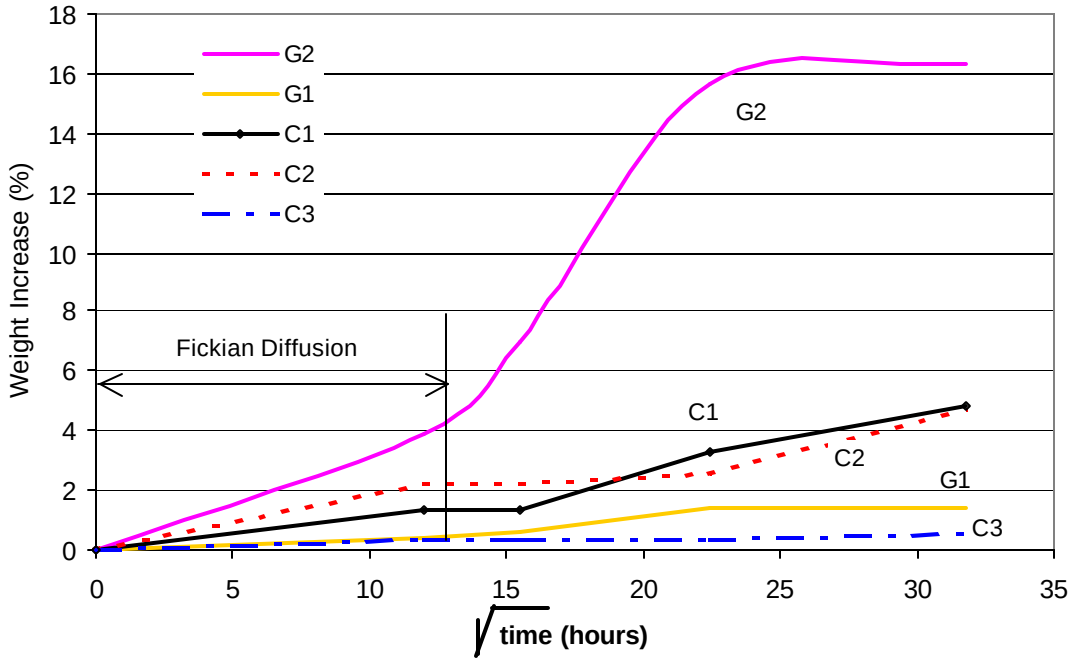

Figure 40: Absorption behavior in alkaline solution

These results showed how different resins, (also for different epoxy based), can have an absorption behavior that can change in correspondence of different diffusive properties. These properties highlighted the performance of the resin after exposure, and are related to residual mechanical properties measured in mechanical tests

4.4 Electronic Microscopy SEM Images

Electronic microscopy observations were used to understand macroscopic phenomena by micro-structural investigations. Alkali conditioned specimens were cut in longitudinal and transverse direction and embedded in an epoxy resin to prepare them for SEM investigations.

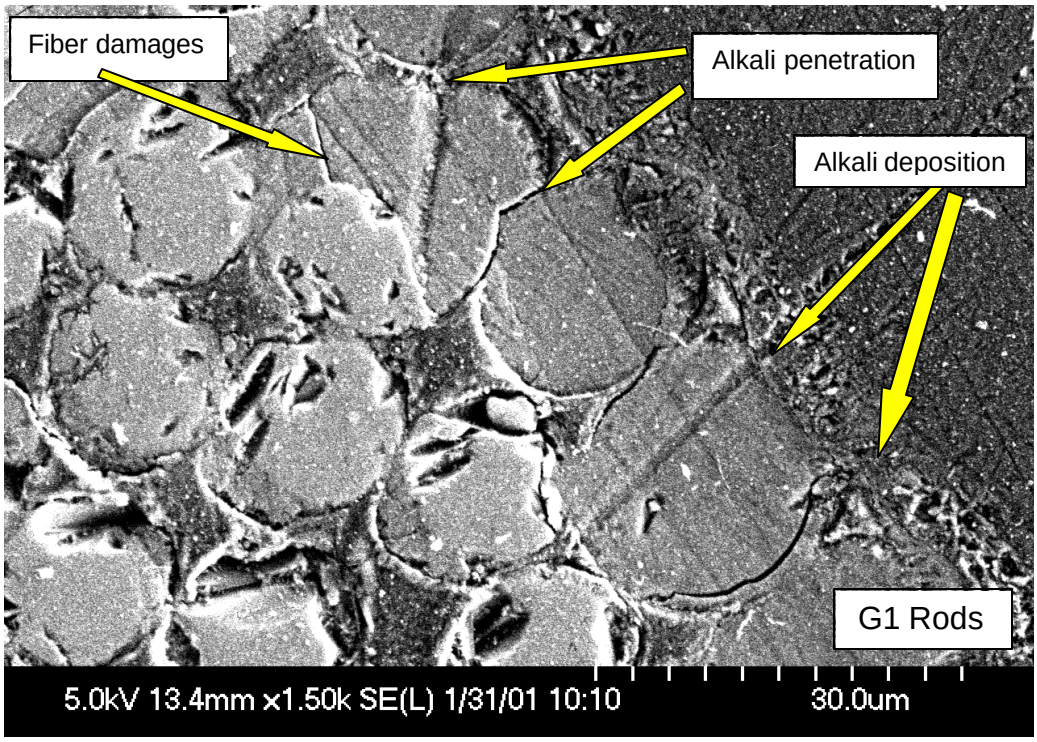

Figure 41: SEM transverse section of G1 specimens

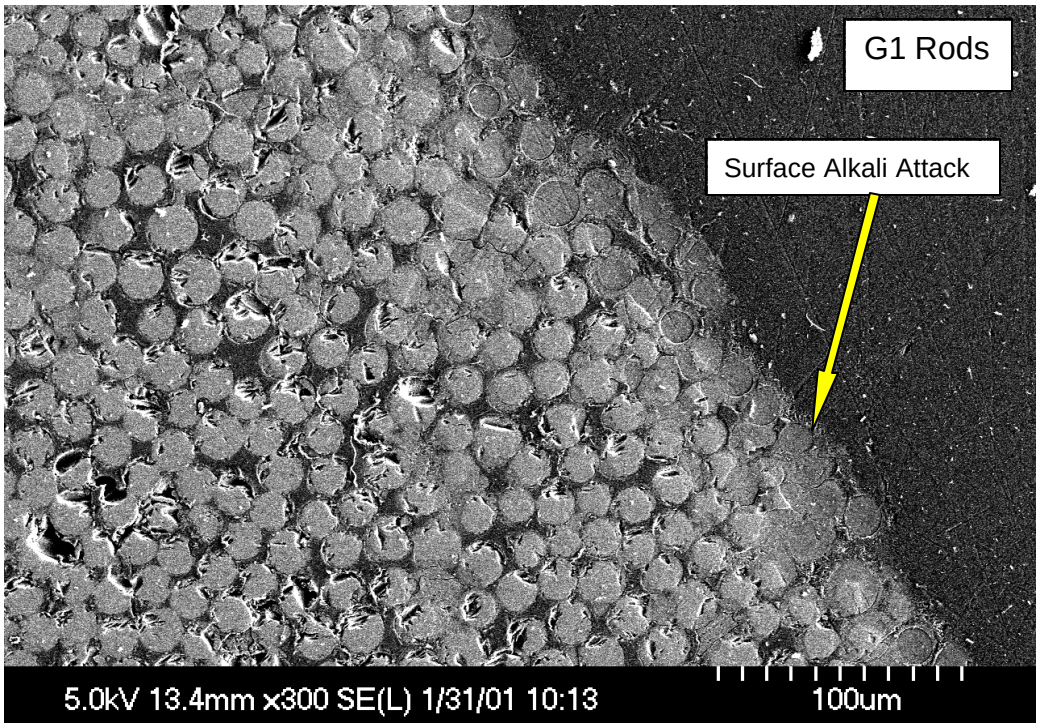

Figure 42: SEM transverse section of G1 specimens

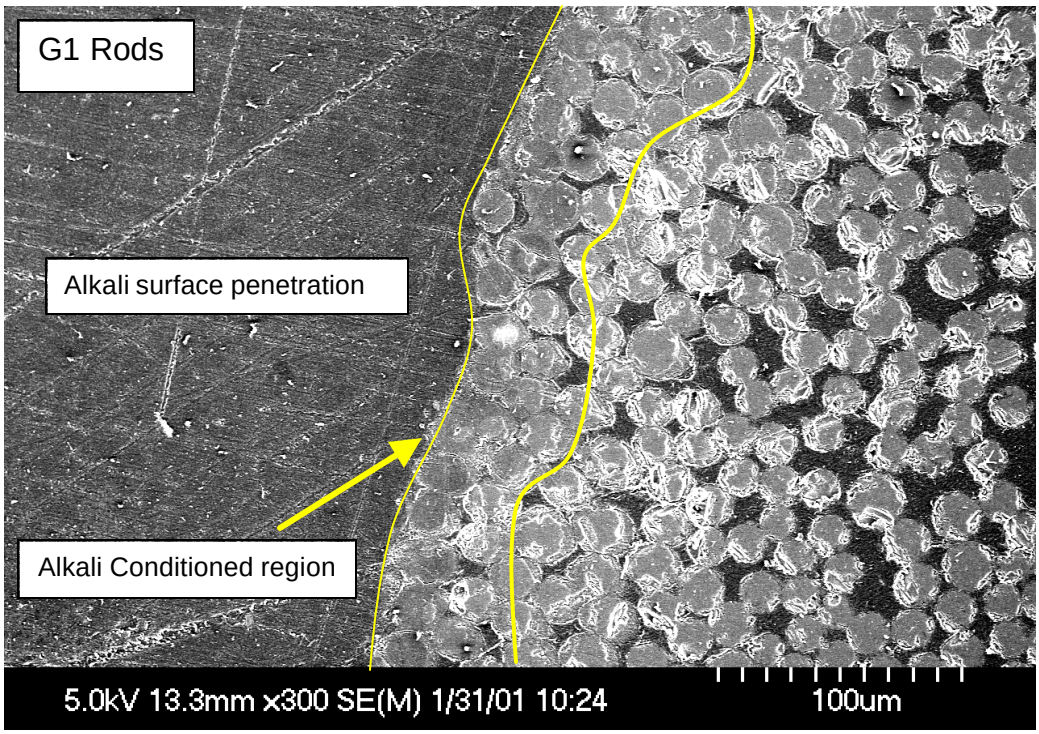

Figure 43: SEM transverse section of G1 specimens

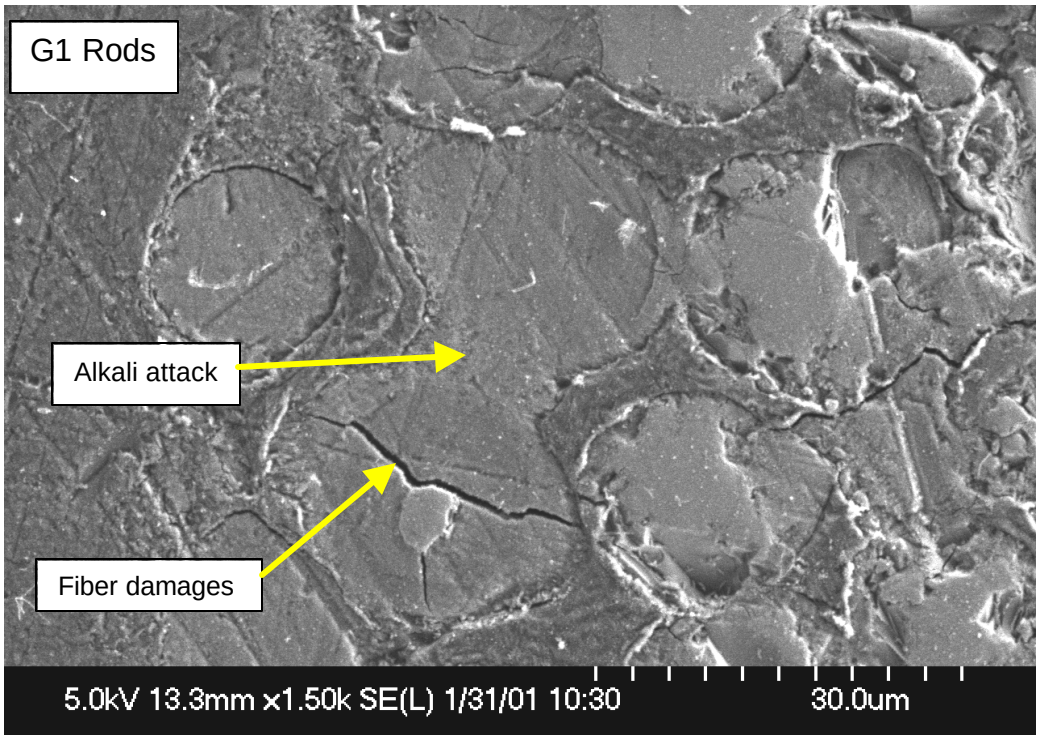

Figure 44: SEM transverse section of G1 specimens

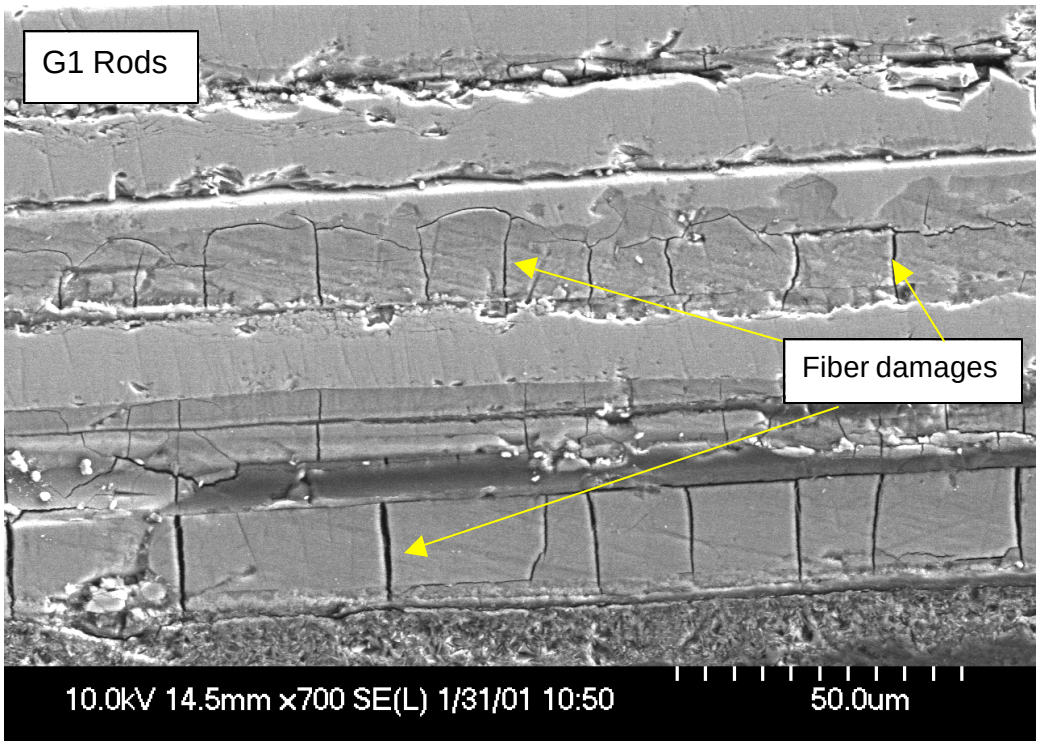

Figure 45: SEM longitudinal section of G1 specimens

Figure 46: SEM longitudinal section of G1 specimens

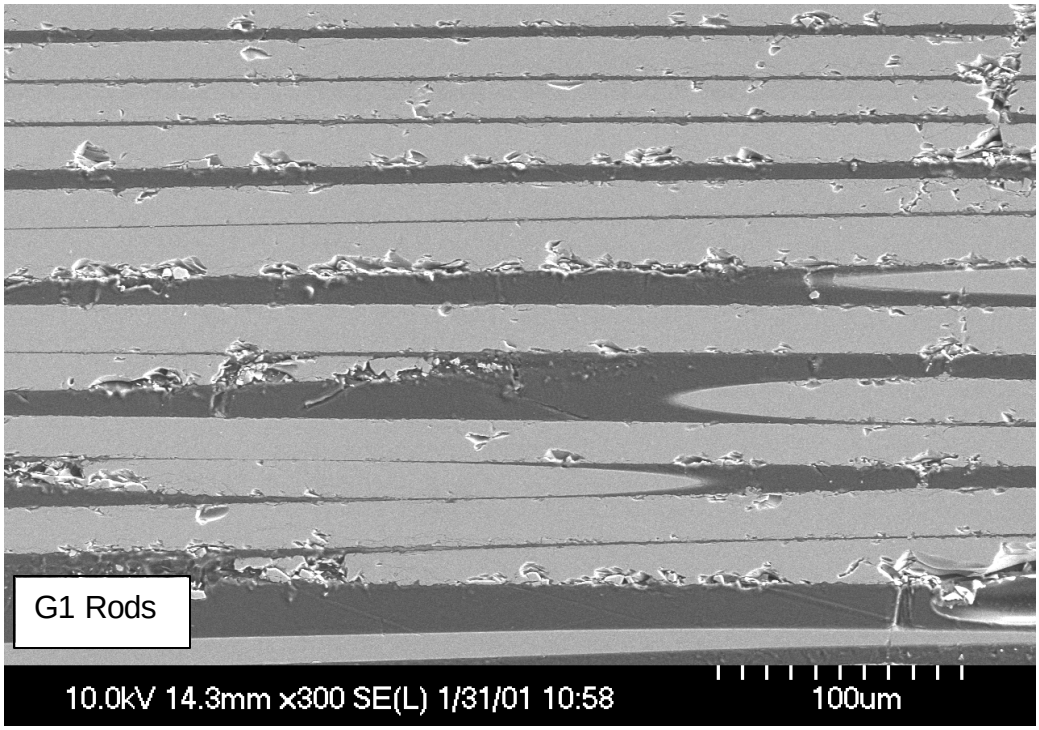

Figure 47: SEM longitudinal section of G1 specimens

Figures 41 and 42 highlighted a high amount of fibers in the cross section, and the alkali conditioned region seems to be limited to the external layers of the rod. Damages of the fibers due to alkali penetration are shown and indicated in Figures 43 and 44, other damages due to cut of the specimens are evident but they should be distinguished from those generated by chemical attack.

Longitudinal cuts evidenced the same information as can be observed in Figures 44 and 45 that are related to the external layer of the rod that were affected by alkali ions, while in Figure 46 the longitudinal cut in the inner region of the rod showed undamaged fibers.

Figure from 47 to 49 illustrate the effects of alkali penetration in G2 specimens. In Figures 47 and 48 damages of resin and fibers in transverse cross section are shown; in Figure 50 the extensive cracking, visible also without microscopy, due to fluid penetration is evident in the longitudinal cross-section.

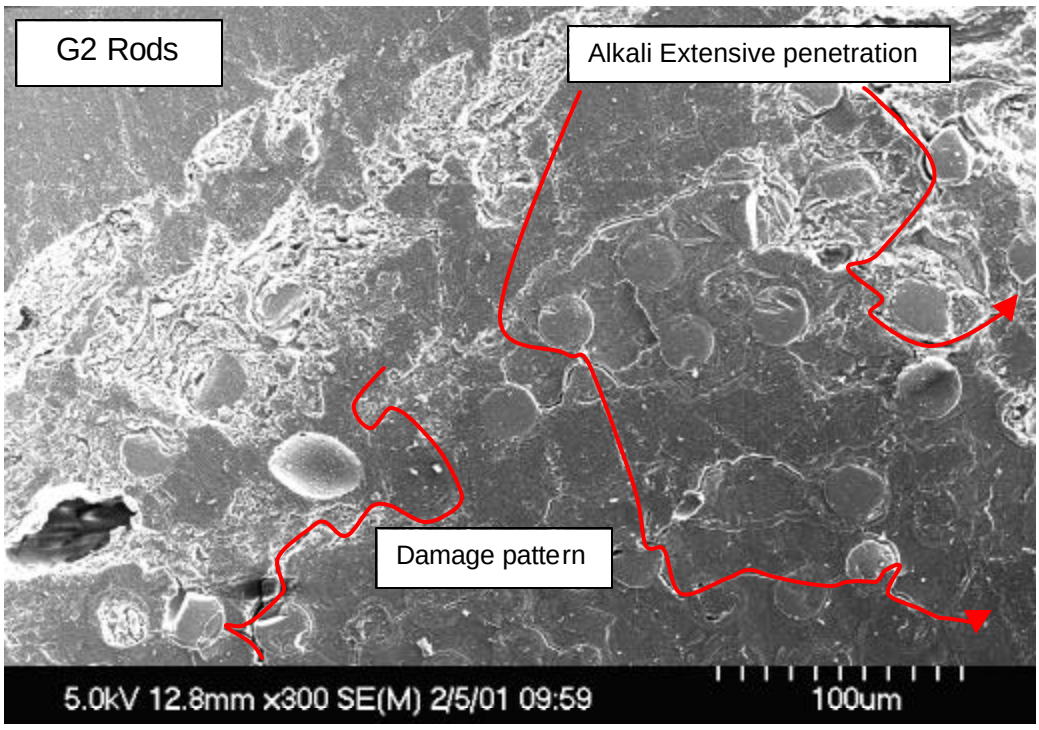

Figure 48: SEM transverse section of G2 specimens

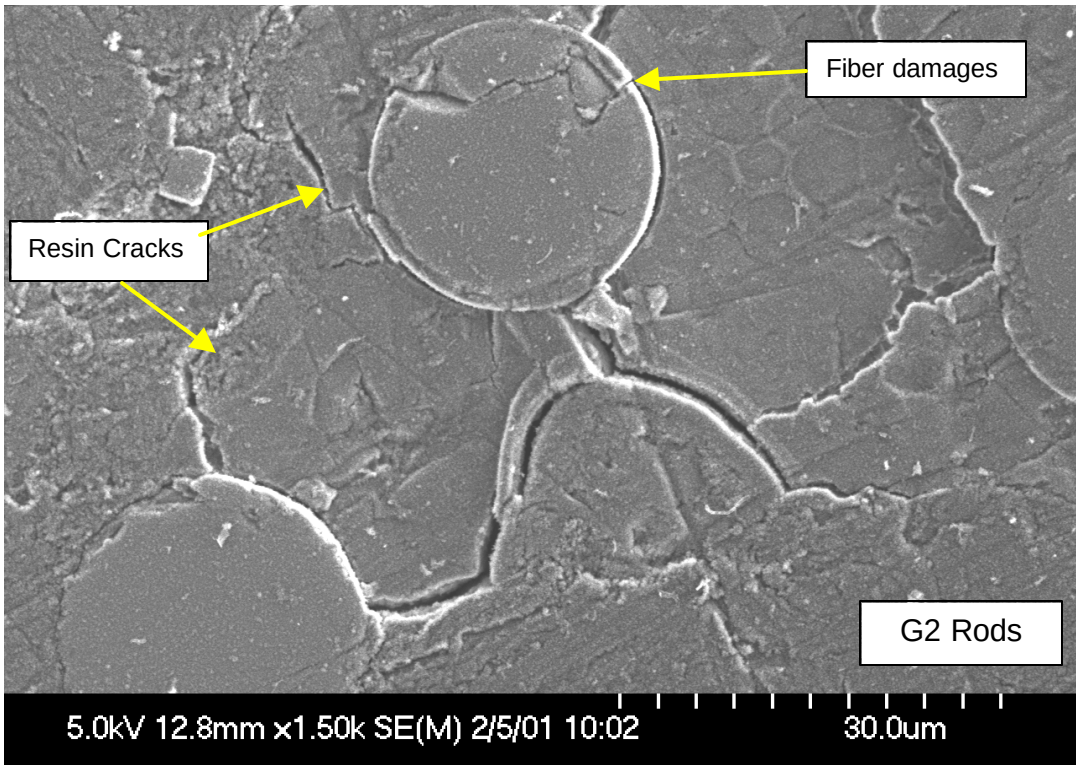

Figure 49: SEM transverse section of G2 specimens

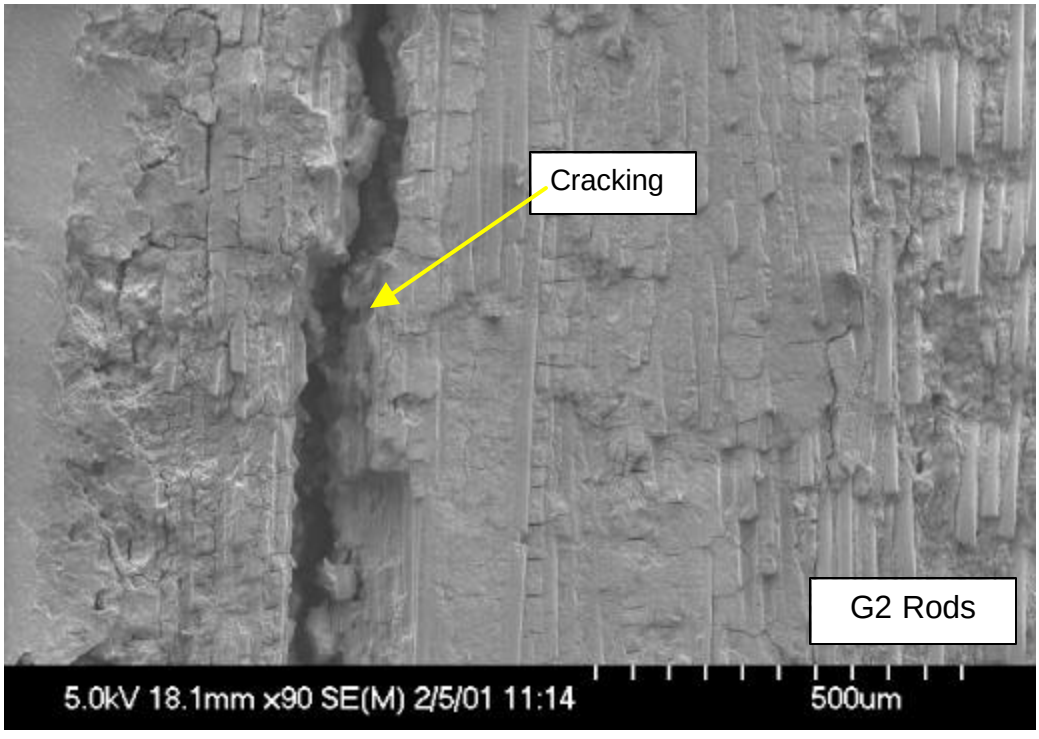

Figure 50: SEM longitudinal section of G2 specimens

SEM images of G2 rods showed a low glass fiber content in the cross section, and an extensive cracking of the resin that seemed to be very weak against alkali penetration that damaged the fibers, once the cracks developed through the fiber/matrix interface.

Even if carbon fibers are not affected by alkali penetration, as demonstrated in several studies on composite materials, SEM images were investigated also for C1 and C3 rods. Thus observations on CFRP specimens allowed to know fiber content in the cross section and resin damages after fluid immersion.

Figures 50 and 51 are related to C1 rods that are made with an epoxy matrix. In Figure 50 a visible crack in the fiber matrix interface is visible in the cross section of C1 specimen, while Figure 51 illustrates the longitudinal cross section.

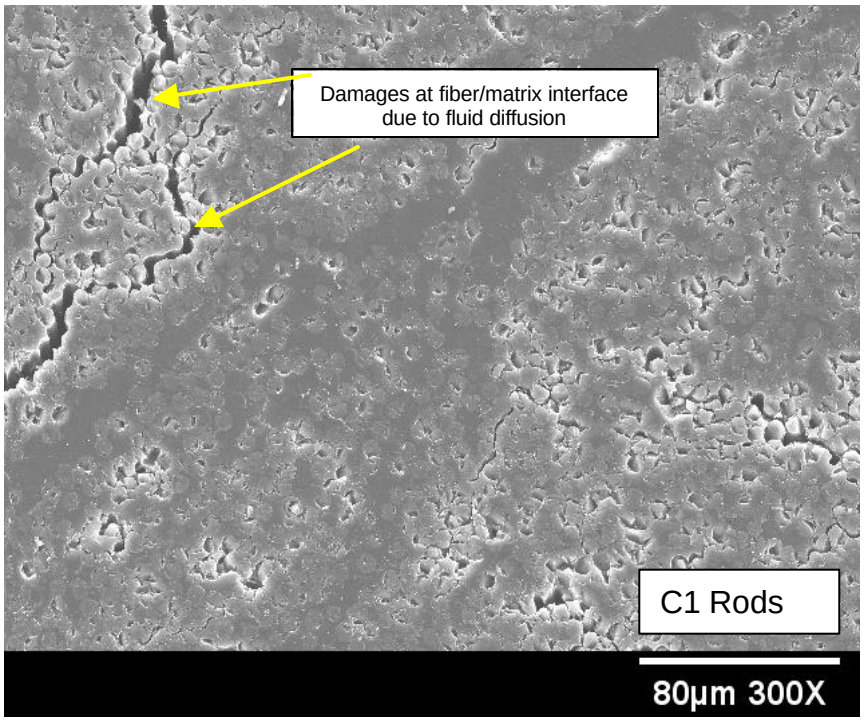

Figure 51: SEM transverse section of C1 specimens

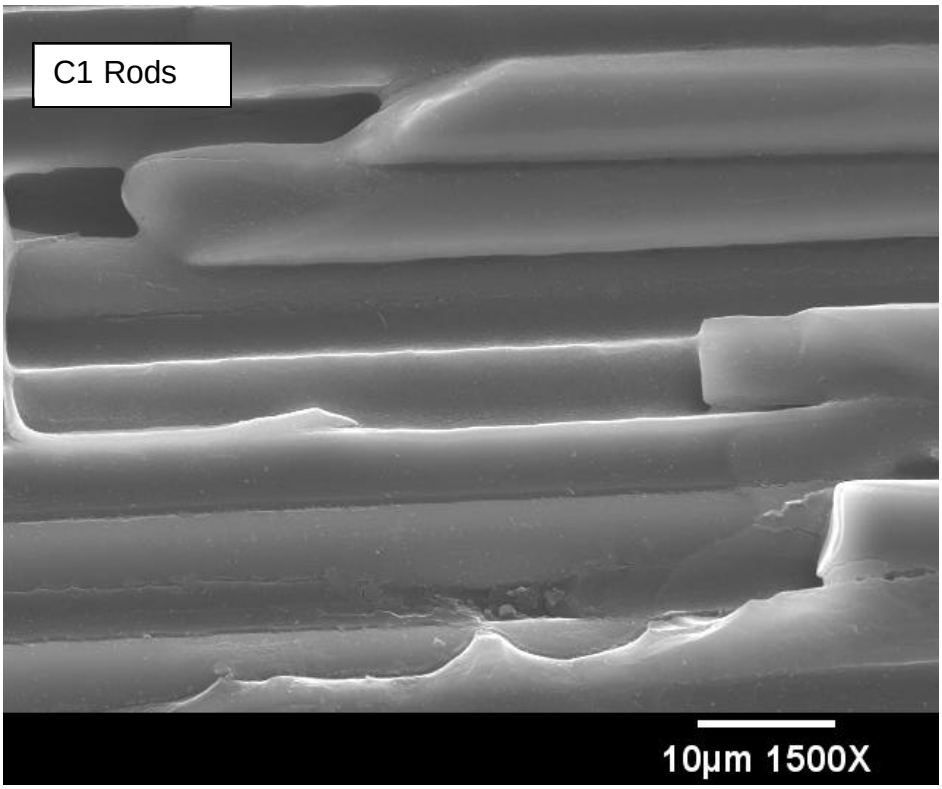

Figure 52: SEM longitudinal section of C1 specimens

A serious damage can be observed at the fiber/resin interface in Figure 50, it can be attributed to the penetration of fluid in the superficial layers of the rod, while Figure 51 highlights that fibers were not affected by the presence of alkali agents, even if the resin was damaged.

The following Figures 52 and 53 are related to the C3 specimens that showed the lowest moisture residual content after immersion and the highest ISS after short shear span test.

Damages that appear in correspondence of the carbon fibers are due only to cutting and are not concerned with alkali penetration that was very low, since the resin created an almost perfect coating of the fibers.

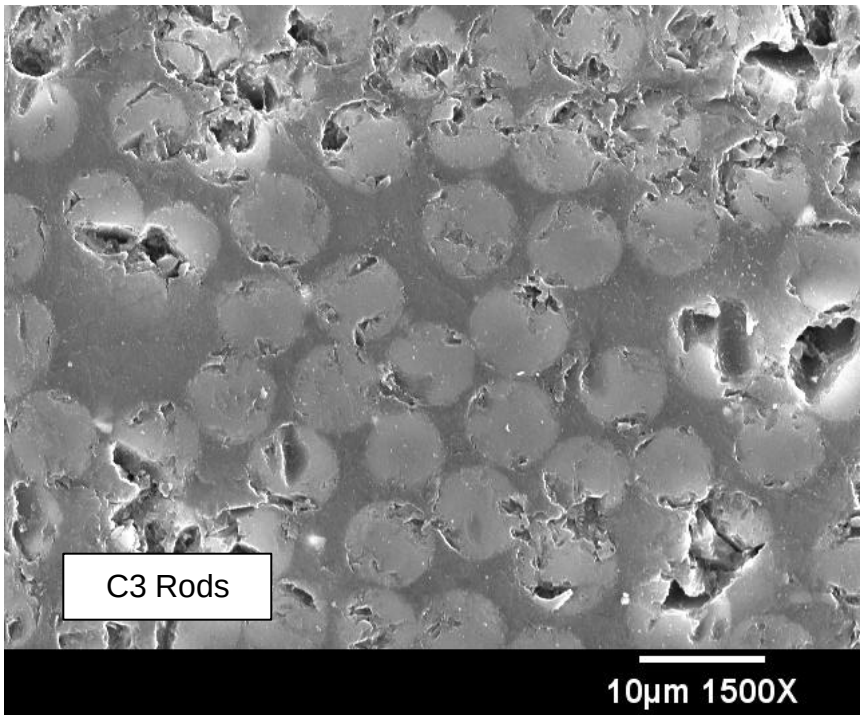

Figure 53: SEM longitudinal section of C3 specimens

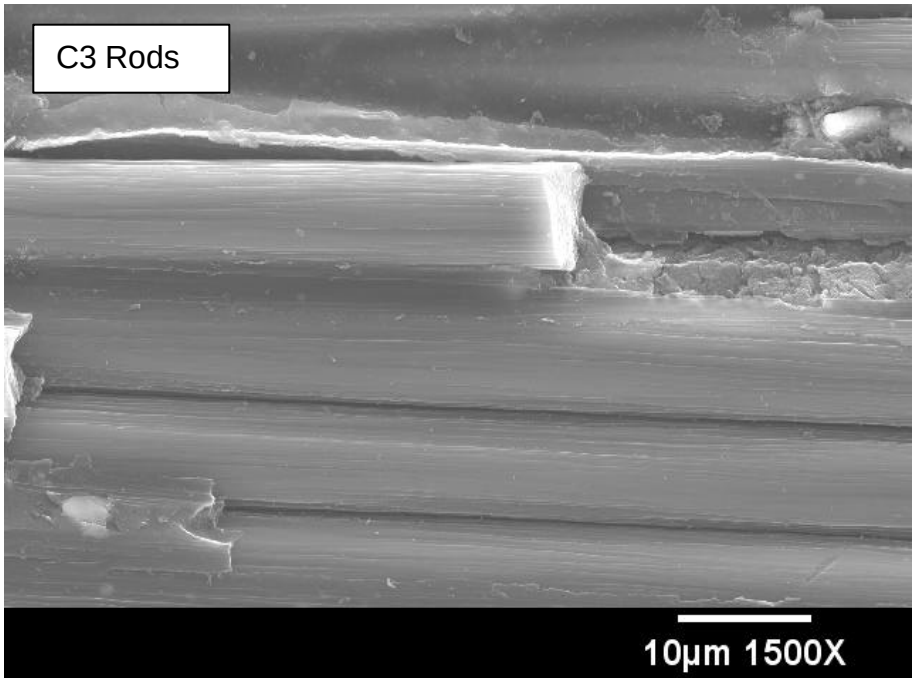

Figure 54: SEM transverse section of C3 specimens

Figure 52 shows that no cracks are visible in the resin, therefore in Figure 53 the fibers appear without any damage or defect due to a possible aggressive fluid penetration.
The SEM images related to CFRP highlighted important information on the CFRP system, in fact, even if carbon fibers are not affected by alkaline environment, the weakness of the resin or resin interface could open a way for aggressive agents that could be different from alkali ions, for example as it may happen in an acid environment.

4.5 Discussion of Results

A discussion of results will be provided herein, taking into account all the results from different physical and mechanical tests. This allows to evidence the synergies between physical and mechanical measurements, and to draw important remarks that focus on the design aspects for the use of FRP reinforcement in reinforced concrete structures.
Different mechanical properties were found for the different products investigated. The SEM investigations helped to understand the fiber content, that furnished important information about the tensile properties.
Longitudinal and transverse mechanical properties were carefully measured and consistency was found in collecting data to be used for material characterization and durability studies.
The combined environmental factors did not affect the durability of CFRP and GFRP rods, in fact no weight increase was found after high humidity combined cycles, and residual mechanical properties of fibers and resins were not affected by the accelerated conditioning. There are less concerns related to the long-term safety, regarding a possible environmental attack represented by low temperature and high temperature cycles combined with high humidity exposure periods. In almost all field applications the rods are embedded in concrete, and for some applications, they are embedded in an epoxy paste. The information derived from these tests can be considered conservative, since the rods were directly exposed to the agents in an environmental chamber.
Different behaviors were found after the immersion in alkaline solution. In terms of absorption behavior, a high diffusion of solution was recorded in the polyester matrix, while the thermoplastic system was affected only in the external layers. This can be clearly deduced from gravimetric tests and SEM investigation. Mechanical test

confirmed this phenomenon, in fact the transverse properties of G2 rods decreased to very low values, while G1 rods only decreased 30%. Since glass fibers suffer the alkali ions attack, tensile properties of G2 specimens showed a significant reduction. SEM images could detect from a microscopic point of view damages and their location in the structure of the composite materials. Mechanical test traduced the effects of the external agents in a decrease of strength and stiffness. Carbon fiber rods did not show significant change in tensile mechanical properties, as confirmed by SEM images that detected the undamaged fibers. Although the ultimate strength did not vary, weight measurements and SEM images highlighted damages in the epoxy systems used in C1 and C2 rods. Short shear span test measured the mechanical effects of the solution penetration.

Test results show that fiber content and properties control the mechanical strength used in design, but the choice of the resin affects the durability of the rod.

The tested polyester matrix showed unsatisfactory performance and the use of this resin should be avoided, especially in a concrete environment.

The tested epoxy systems showed different performance, this is related to the chemical nature of the epoxy based chains that constitute the resins.

G1 and C3 rods showed the lower absorption after exposure, that could be attributed to a low diffusivity of the resins.

Bond measurements should be conducted in order to assure that the superficial attack would not damage the interfacial adhesion with concrete.

5 CONCLUSIONS

A set of conclusions is drawn herein, in order to furnish information and recommendations that could help in the characterization and development of FRP reinforcement for concrete structures.

An improvement of long term behavior of FRP reinforcement may result from efforts by researchers and manufacturers in selecting appropriate materials.

5.1 Test Protocol for Characterization and Durability Investigation of FRP Rods

An experimental method was used for characterization of FRP rods and for investigations of durability effects due to environmental exposure and alkaline exposure. A combination of physical and mechanical tests is proposed. Electronic microscopy was also used to observe the effects of the degradation phenomena.

The following conclusions are reported in order to help future researchers and engineers for conducting characterization and durability studies:

- Grouted anchors with alignment devices allowed to perform tensile tests that showed fiber rupture for different cross section geometry and surface conditions. Expansive grout may substitute epoxy resin to develop a gripping force for tensile test. Particular benefits of the proposed protocol can be summarized:
  - No damages due to gripping force
  - Perfect tensile stress developed during the test
  - Easy preparation of the specimens
- Ratio between test length and diameter of rebars did not affect tensile test results.
- Recommended anchorage lengths and steel pipes geometry are reported in Table 23.
- Environmental combined agents were used to simulate external conditions in an environmental chamber and alkaline accelerated exposure was used to simulate cementitious environment in which the rods are embedded during the service life. A pH of 12.6 was chosen and K^+ and Na^+ were introduced because their chemical attack generates glass fiber damages.
- Short shear span test according to ASTM D4475 is recommended in order to study resin properties.
- Gravimetric measures are recommended after any solution immersion, since the weight increase furnishes, without any other information, a measure of potential degradation of the system.

Table 23: Recommendations for tensile test of FRP rods

Rod	*Diameter mm (in)*	***Steel tubes***		***Expected ultimate load kN (kips)***	***Anchorage lenth mm (in)***
		Min. Outside diameter mm (in)	*Min. Wall thickness mm (in)*		
CFRP	4 (0.16)	42 (1.65)	3.5 (0.14)	15 – 45 (3 – 10)	250 (10)
CFRP	6 (0.24)	42 (1.65)	4.8 (0.19)	45 – 80 (10 – 18)	300 (12)
CFRP	8 (0.31)	42 (1.65)	4.8 (0.19)	80 – 140 (18 – 31)	350 (14)
CFRP	10 (0.39)	48 (1.88)	5.0 (0.2)	140 – 180 (18 – 40)	450 (18)
GFRP	6 (0.24)	42 (1.65)	3.5 (0.14)	20 – 40 (4 – 9)	250 (10)
GFRP	8 (0.31)	42 (1.65)	4.8 (0.19)	40 – 60 (9 – 13)	300 (12)
GFRP	10 (0.39)	42 (1.65)	4.8 (0.19)	60 – 90 (13 - 20)	300 (12)
GFRP	12 (0.47)	42 (1.65)	4.8 (0.19)	90 – 120 (20 – 27)	350 (14)
GFRP	14 (0.55)	48 (1.88)	5.0 (0.20)	120 – 165 (27 - 37)	400 (16)

- Electronic microscopy would be recommended when it is necessary to know the damage mechanisms caused by aggressive agents. Fiber, matrix, and interfacial defects could be well detected after accelerated ageing.
- Analysis of the results deriving from the proposed protocol would allow to understand not only the amount of decrease in engineering properties, but also the factors and mechanisms that caused this macroscopic degradation.

5.2 Long-term Behavior of Tested Rods

Different results showed how different resin contribute to increase the durability of FRP rebars, especially for GFRP specimens, since glass fiber are more sensitive to external agents. The following conclusions can be drawn to describe the performance of the tested rods subjected to accelerated aging:

- G1 Rods:
  - high strength and high elastic modulus
  - good durability after environmental cycles
  - good durability after alkali exposure
  - low decrease in resin properties and damages in the external layers due to fluid absorption
  - bond test should be performed after alkali exposure to ensure that adherence properties were not significantly influenced

- G2 Rods:
  - low strength and low elastic modulus
  - low elongation at the ultimate load
  - good durability after environmental cycles
  - resin damages caused alkali penetration that affected tensile properties
  - transverse properties decreased to very low values after alkali exposure
  - polyester resin should be avoided and substituted with vinyl ester or epoxy

- C1 and C2 Rods:
  - high strength and high elastic modulus
  - good durability after environmental cycles
  - good durability of longitudinal properties after alkali exposure
  - resin damages caused alkali penetration that affected tensile properties
  - transverse properties decreased to very low values after alkali exposure
  - epoxy resin used as matrix should be improved to assure perfect coating of the fibers

- bond test should be performed after alkali exposure to ensure that adherence properties were not significantly influenced

- C3 Rods:
  - low strength and high elastic modulus
  - low elongation at the ultimate load
  - good durability after environmental cycles
  - good durability after alkali exposure
  - perfect coating furnished by the epoxy matrix after alkali exposure

5.3 Durability and Structural Safety: Design Recommendations

Although design guidelines were drawn in different countries, including USA, Japan, Canada and UK, recommendations and coefficients that could take into account the long-term behavior of FRP reinforcement were not well defined. Several studies were conduced and provisions for mechanical and durability characterization were furnished.
Provisional values can be provided using also the results of this experimental studies. In particular it was observed that GFRP presents higher sensitivity to external agents, including alkaline cementitious environment, while CFRP can be used with less concerns as was also demonstrated in previous researches.
With reference to ACI 440H (ACI provisions), an environmental knock-down factor C_e can be used to compute the FRP design strength from experimental results, and recommendations should be furnished also regarding resin degradation:

- $C_e = 0.90$ can be used for CFRP reinforcement
- $C_e = 0.70$ can be used for GFRP reinforcement
- Residual tensile strength should not be less than 75% after experimental accelerated aging according to the proposed protocol
- Residual transverse properties should not be less than 65 % after experimental accelerated aging according to the proposed protocol

- Weight increase should not be more than 2.5 % for CFRP rods and not more than 2% for GFRP rods after accelerated fluid immersion
- Extreme environmental conditions or specific environments should be investigated using a coefficient of reduction of 0.8 for all the acceptance criteria mentioned above.

Therefore design reduction coefficients should be accompanied also by acceptance criteria that is expressed by the proposed specifications, in order to guarantee a long-term quality that should help to increase the confidence of designers and contractors for using of FRP reinforcement in civil structures.

5.4 Recommendations for Future Works

The first limitation of the experimental work presented herein is the absence stress during the accelerated aging of the rods. Other aspects should be investigated, and further recommendations should be provided in order to establish quality specifications that will help to draw common design guidelines.
Therefore the following recommendations for future work are provided:

- Tensile stress comparable to service loads should be applied during further durability test to see the effect of the applied load.
- Combined effects of fluid penetration (alkali, acid etc.) and environmental agents could provide more information on durability in aggressive environments
- Resin properties should be investigated for all the products that are candidate to substitute steel reinforcement in construction, since a degradation of the resin accelerate fiber damages.
- Creep experimental investigations are needed, especially for prestressing tendons, in order to establish coefficients for prestressed FRP rods.
- Further tests are needed in order to validate this method for rectangular CFRP rods with smooth surface.
- The same conditioning regimen should be provided using water or other solution (marine water, acid solutions etc.) in order to study the effects of accelerated

diffusion mechanisms that cause fluid penetration. This is essential for marine structures or other members immersed in a solution or subjected to aggressive vapors during their service life.

REFERENCES

ACI, (2000), "Guide for the Design and Construction of Concrete Reinforced with FRP bars", American Concrete Institute Committee 440.

Aiello M. A. and Ombres L., (2000), "Load-Deflection Analysis of FRP Reinforced Concrete Flexural Members", *J. Comp.Constr.*, ASCE, Vol. 4, No. 4, pp. 164-171.

Alkhrdaji, T.; Nanni, A.; Chen, G.; and Barker, M. (1999), "Upgrading the transportation Infrastructure: Solid RC Decks Strengthened with FRP", *Concrete International*, ACI, Vol. 21, No. 10, October, pp. 37-41.

Al-Zahrani, M. M., Nanni, A., Al-Dulaijan, S. U., and Bakis, C. E., (1996), "Bond of Fiber Reinforced Plastic (FRP) Rods to Concrete," *Proc. 51st Ann. Conf. of the Composites Institute, Soc. Plastics Engineers*, New York, 1996, pp. 3A.1-3A8.

Ashour, S. A. and Wafa, F. F, (1993), "Flexural Behavior Of High-Strength Fiber Reinforced Concrete Beams" *ACI Struct. J.*, Vol. 90, No. 3, pp 279-287.

ASTM (2000), American Society for Testing and Materials, ASTM A 312/A 312M "Standard specification for seamless and welded austenitic stainless steel pipes", October 2000.

ASTM, (1982), American Society for Testing Materials E 632 "Standard Practice for Developing Accelerated Tests to Aid Prediction of the Service Life of Building Components and Materials".

ASTM, (1994), American Society for Testing Materials D 3916 "Standard Test Method for Tensile Properties of Pultruded Glass-Fiber-Reinforced Plastic Rod".

ASTM, (1996 A), American Society for Testing and Materials, ASTM C1198 "Standard Test Method for Dynamic Young's Modulus, Shear Modulus, and Poisson's Ratio for Advanced Ceramics by Sonic Resonance", August 1996.

ASTM, (1996 B), American Society for Testing and Materials, ASTM D 4475 "Standard Test Method for Apparent Horizontal Shear Strength of Pultruted Reinforced Plastic Rods By The Short Beam Method", November 1996.

ASTM, (1999), American Society for Testing and Materials, ASTM 638 "Standard Test Method for Tensile Properties of Plastics", November 1999.

ASTM, (2000), American Society for Testing and Materials, ASTM D3039/D 3039 "Standard Test Method for Tensile Properties of Polymer Matrix Composite Materials", April 2000.

Bakis, C. E., Nanni, A., Boothby, T. E. Huang, H., Al-Zaharani, M. M., and Al-Dulaijan, S. U., (1995), "Measurement of Bond of FRP Composite Reinforcement in Concrete Structures," *Proc. 10th Intl. Conf. on Composite Materials*, Vol. 6, A. Poursatip and K. Street, Eds., Woodhead Publishing, Ltd., 1995, pp. 635-642.

Bakis, C.E., Nanni, A., and Terosky, J.A., (1996), "Smart Pseudo-Ductile, Reinforcing Rods for Concrete: Manufacture and Test", *Proc. 1st Int. Conf. On Composites in Infrastructures, ICCI 96*, Tucson, Arizona, pp. 95-108.

Balaguru, P. N. and Dipsia, M. G., (1993), "Properties Of Fiber Reinforced High-Strenght Semi lightweight Concrete" *ACI Mat. J.*, Vol. 90, No. 5, pp 399-405.

Bascom, W.D., (1974) "The Surface Chemistry of Moisture-Induced Composite Failure", *Interfaces in Polymer Matrix Composites*, Ed. Plueddemann E.P., Academic Press, New York, 1974, pp. 79-108.

Benmokrane, B., and Masmoudi, R. (1996), "FRP C-Bar as Reinforcing Rod for Concrete Structures", *Proc. Of Advanced Composite Materials in Bridges and Structure 2nd International Conference*, Ed. M.M.El-Badry, Montreal, Quebec, Canada, August 11-14, 1996, pp.181-188.

Bevan, L.G., (1977), "Axial and Short Beam Shear Fatigue Properties of CFRP Laminates", *Composites*, October 1977, pp. 227-232.

Boothby, T.E., Nanni, A., Bakis, C.E., and Huang, H., (1995),"Bond of FRP Rods Embedded in Concrete," Engineering Mechanics, *Proc. 10th Conf., Vol. 1, S. Sture, ed., American Soc. Civil Engineers*, New York, 1995, pp. 114-117.

Bott, T.R., and Barker, A.J., (1969), "The behavior of Model Composites in Contact with Different Environments", *Transactions of the Institute of Chemical Engineers*, Vol. 47, 1969, pp. T188-T193.

Buck, S.E., Lischer D.W., Nemat-Nasser, S. (1998), "The Durability of E Glass/Vinyl Ester Composite Materials Subjected to Environmental Conditioning and Sustained Loading ", *Journal of Composite Materials*, Vol. 32, No. 9/1998.

Castro, P.F., and Carino, N.J., (1998), “Tensile and Non-Destructive Testing of FRP bars”, *J. Comp. Constr.*, Vol. 2, No. 1, February 1998, pp. 17-27

Chambers, R.E. (1965), “Strutural Fiber Glass-Reinforced Palstics for Building Applications”, *Plastics in Buildings*, I. Skeist Ed., Reinhold Publishing Co., New York, 1965, pp.72-118.

Chateauminois, A., Chabert, B., Soulier, J. P., and Vincent, L., (1993), " Effects of Hygrothermal Aging on the Durability of Glass/Epoxy Composites. Physico-Chemical Analysis and Damage Mapping in Static Fatigue," *Proceedings of the 9th International Conference on Composite Materials* (ICCM/9), pp. 593-600.

Chin J.W., Aouadi K., and Nguyen T., (1997), “Effects of Environmental Exposure on Fiber-Reinforced Plastic (FRP) Materials Used in Construction”, *Journal of Composites and Technology Research*, Vol. 19, No. 4, pp. 205-213.

De Lorenzis (B), L., A. Nanni, and A. La Tegola, (2000), “Flexural and Shear Strengthening of Reinforced Concrete Structures with Near Surface Mounted FRP Rods,” *Proc., 3 rd Inter. Conf. on Advanced Composite Materials in Bridges and Structures,* Humar and A.G. Razaqpur J., Editors Ottawa, Canada, 15-18 Aug. 2000, pp. 521-528.

De Lorenzis, L.(A), A. Nanni, and A. La Tegola, (2000), "Strengthening of Reinforced Concrete Structures with Near Surface Mounted FRP Rods", *Proc. International Meeting on Composite Materials, PLAST 2000, Advancing with Composites 2000*, Ed. I. Crivelli-Visconti, Milan, Italy, May 9-11, 2000, pp. 419-426.

De Lorenzis, L., D. Tinazzi, A. Nanni, A., “Near Surface Mounted FRP Rods for Masonry Strengthening: Bond and Flexural Testing,” Symposium, “*Meccanica delle Strutture in Muratura Rinforzate con FRP Materials*”, Ed. Ceriolo L., Venezia, Italy, December 7-8, 2000, pp.7-18.

Devalapura, R.K., Gauchel, J.V., Greenwood, M.E., Hankin, A., and Humphrey, T. (1997), “Long-Term Durability of GFRP Composites in Alkaline Environments”, *Proc. 3rd Non-Metallic (FRP) Reinforcement for Concrete Structures, International Symposium*, Sapporo, Japan, October 14-16th 1997, Sapporo Japan, Vol.2, pp.83-90.

Dillard, D. A., (1991), "Viscoelastic Behavior of Laminated Composite Materials," in *Fatigue of Composite Materials*, K. L. Reifsnider, Ed., Elsevier, 1991.

Donaldson, S.L., and Kim, R.Y.,(1995) ,“Life Prediction of Glass/Vynilester and Glass Polyester Composites Under Fatigue Loading”, *Proc. Of the 10th International Conference on Composite Materials*, Vol. 1, Canada, August 1995, pp. 577-584

EN ISO/F-DIS 527-4, (1996 A), "Plastics - Determination of tensile properties. Part 4 - Test conditions for isotropic and orthotropic fibre-reinforced plastic composites", 1996.

EN ISO/F-DIS 527-5 (1996 B), "Plastics - Determination of tensile properties. Part 5 - Test conditions for unidirectional fibre-reinforced plastic composites", 1996.

Erki, M.A., and Ritzkalla, S.H., (1993), “Anchorages for FRP Reinforcement”, *Concrete Int*., Vol. 15, No. 6, pp. 54-59.

Faza, S., and Ganga Rao, H. (1993), “Glass FRP Reinforcing Bars for Concrete”, Fiber-Reinforced Plastics (FRP) Reinforcement for Concrete Structures – Properties and Applications, A. Nanni Ed., Elsevier Pub. Co. Inc., NY, pp. 167-188.

Ferry, J.D., (1961), “Viscoelastic Properties of Polymers”, John Wiley & Sons, Inc., New York, 1961.

Franke, L. and Meyer, H. J., (1992), "Predicting the Tensile Strength and Creep-Rupture Behaviour of Pultruded Glass-Reinforced Polymer Rods," *Journal of Materials Science*, Vol. 27, pp. 4899-4980.

Franke, L. and Meyer, H. J., (1992), "Predicting the Tensile Strength and Creep-Rupture Behaviour of Pultruded Glass-Reinforced Polymer Rods," *Journal of Materials Science*, Vol. 27, pp. 4899-4980.

Franke, L. and Overback, E., (1987), “Loss in strength and damage to glass fibers in alkaline solutions and cement extracts”, *Dur. Build. Mat*., No.5, 1987, pp.73-79.

Freimanis, A. J., Bakis, C. E., Nanni, A., and Gremel, D., "A Comparison of Pull-Out and Tensile Behaviors of FRP Reinforcement for Concrete," *Proc. 2nd International Conference on Composites in Infrastructure*, Vol. II, H. Saadatmanesh and M. R. Ehsani, Eds., 5-7 Jan. 1998, University of Arizona, Tucson, AZ, pp. 52-65.

Fried N., (1967), “Degradation of Composite Materials: The Effect of Water on Glass Reinforced Plastics”, *Proc. 5th Symposium on Naval Structural Mechanics*, Philadelphia, USA, 1967, pp. 813-837.

Ganga Rao, H.V.S., and, Vijay P.V., (1997), "Aging of Structural Composites Under Varying Environmental Conditions", *Proc. 3rd Non-Metallic (FRP) Reinforcement for Concrete Structures, International Symposium*, Sapporo, Japan, October 14-16th 1997, Sapporo Japan, Vol.2, pp.91-98.

Hartley, G.S., and Crank, J, (1949), "Some Fundamental Definitions and Concepts in Diffusion Processes", *Transactions of the Faraday Society*, Vol.45, 1949, pp.801-818.

Hollaway, L., (1978), "Glass Reinforced Plastics in Construction: Engineering Aspects" John Wiley & Sons, New York, 1978.

Holte, L.E., Dolam, C. W., and Schmidt, RJ. (1993), "Glass FRP Reinforcing Bars for Concrete", Fiber-Reinforced Plastics (FRP) Reinforcement for Concrete Structures – Properties and Applications, A. Nanni Ed., Elsevier Pub. Co. Inc., NY, pp. 167-188.

Homam S. M., and Sheikh S. A., "Durability of Fiber Reinforced Polymers Used in Concrete Structures", *Proc. 3rd International Conference on Advanced Materials in Bridges and Structures*, Ottawa, Canada, August 15-18th 2000, pp. 751-758

Iyer, S.L., (1993), "Advanced composite demonstration bridge deck" *Proceedings of the International Symposium on Fiber-Reinforced-Plastic Reinforcement for Concrete Structures*, Ed. by Antonio Nanni and Charles W. Dolan, Vancouver, Canada, Mar 28-31, 1993, American Concrete Institute, Detroit, MI, 1993, pp. 831-852. (ACI SP-138)

Jones, F.R., Rock J.W., Wheatley, A.R., (1983), "Stress Corrosion Cracking and its Implications for the Long-Term Durability of E-Glass Fiber Composites", *Composites*, Vol. 14, No. 3, July 1983, pp. 262-269.

Karbhari V.M., Zhao L., Murphy K., and Kabalnova L., (1998), "Environmental Durability of Glass Fiber reinforced Composites – Short Term Effects", *Proc. 1st Conference on Durability of FRP Composites for Construction (CDCC'98)*, Sherbrooke (Canada), August 5-7th 1998, pp.513-524.

Kato Y., Mishimura T., and Uomoto T., (1998), "The Effect of Ultraviolet Rays to FRP Rods", *Proc. 1st Conference on Durability of FRP Composites for Construction (CDCC'98)*, Sherbrooke (Canada), August 5-7th 1998, pp. 487-497.

Katz, A., Berman, N., and Bank, L.C., (1999), "Effect of High Temperature on Bond Strength of FRP Rebars", *J. Comp. Constr.*, Vol. 3, No. 2, pp. 73-81.

Khalifa, A., T. Alkhrdaji, A. Nanni and S. Lansburg, "Anchorage of Surface Mounted FRP Reinforcement," *Concrete International*, ACI, Vol. 21, No.10, Oct. 1999, pp. 49-54.

Khin, M., Harada, T., Tokumitsu, T., and Idemitsu, T., (1996), "The Anchorage Mechanism for FRP Tendons Using Highly Expansive Materials", *Proc. 2nd Int. Conf. on Adv. Comp. Mat. in Bridges and Struct.*, El-Badry M.M. Ed., CSCE, Montreal, Canada, 959-964.

La Tegola A., La Tegola A., De Lorenzis L., and Micelli F., (2000), "Applications of FRP materials for repair of masonry structures", *Proceedings of the Technology Transfer Seminar Advanced FRP Materials for Civil Structures*, October 19th, 2000 Bologna, Italy.

La Tegola A., De Lorenzis L., and Micelli F., (2000) "Confinamento di pilastri in muratura mediante barre e nastri in FRP", *Proc. Symposium, Meccanica delle Strutture in Muratura Rinforzate con FRP Materials,* Ed. Ceriolo L., Venezia, Italy, December 7-8, 2000, pp. 41-52.

Larsson, F. (1986), "The effect of ultraviolet light on mechanical properties of Kevlar 49 composites", *J. Reinf. Plas. Comp.*, No.5, 1986, pp. 19-22.

Liao, K., Schlthseisz, C.R., Hunston, D.L., and Brinson, C.L. (1998) "Long-Term Durability of FRP-Matrix Composite Materials for Infrastructure Applications: A Review", *J. Adv. Mat.*,; Vol. 30 No. 4, pp. 3-40.

Litherland, K.L., Oakley, D.R., and Proctor, B.A., (1981), "The Use of Accelerated Ageing Procedures to Predict the Long Term Strength of GRF Composites", *Cement and Concrete Research*, Vol. 11, 1981, pp. 455-466.

Makowsky, Z.S., (1982), "Symbiosis of Architecture and Engineering in the Development of Structure Uses of Plastics", in *Plastics in Material and Structural Engineering*, R.A. Bares, et al., Ed. Elsevier Scientific PUBLISHING company, New York, 1982, pp.59-72.

Masmoudi, R., Benmokrane, B., and Chaalal, O. (1996), "Cracking behavior of beams reinforced with FRP rebars", *Proc. First Int. Conf. on Composites in*

Infrastructures, Ed. by H. Saadatmanesh and M. Ehsani, Tucson, AR, Jan. 15 – 17th, 1996, pp. 374 – 388.

Mayo, R., Nanni, A., Gold, W. and Barker, M., (1999), "Strengthening of Bridge G270 with Externally-Bonded CFRP Reinforcement," *SP-188, American Concrete Institute, Proc., 4th International Symposium on FRP for Reinforcement of Concrete Structures* (FRPRCS4), Baltimore, MD, Nov. 1999, pp.429-440.

Menges, G. and Lutterbeck, K., (1984), "Stress Corrosion in Fibre-Reinforced Plastics in Aqueous Media," in *Developments in Reinforced Plastics*, Vol. 3, G. Pritchard Ed., Elsevier Applied Science.

Michaluk, C. Rizkalla, S., Tadros, G., and Benmokrane, B. (1998), "Flexural behaviour of one-way slabs reinforced by fibre plastic reinforcement", *ACI Struct J.*, Vol. 95, No. 3, pp. 353 - 365.

Morri, T., Tanimoto, T., Maekawa, Z., Hamada, H., and Kiyosumi, K. (1991), "Effect of Surface Treatment on Degradation Behavior of GFRP in Hot Water," in *Durability of Polymer Based Composite Systems for Structural Applications*, A. H. Cardon and G. Verchery Eds., Elsevier Applied Science, 1991.

Mufti, A. A., Jaeger, L. G., Bakht, B., and Wegner, L. D. (1993), "Experimental Investigation of Fibre Reinforced Concrete Deck Slabs Without Internal Steel Reinforcement " *Canadian Journal of Civil Engineering*, Vol. 20, No. 3, pp. 398-406.

Nanni A. (1993), "Fiber-Reinforced-Plastics (FRP) Reinforcement for Concrete Structures: Properties and Applications", Ed. by A. Nanni, Elsevier Science Publishers, Amsterdam, 1993, pp.3-12.

Nanni A., Bakis C.E., and Mathew J.A., (1998) "Acceleration of FRP bond Degradation", *Proc. 1st Conference on Durability of FRP Composites for Construction (CDCC'98)*, Sherbrooke (Canada), August 5-7th 1998, pp.45-56.

Nanni, A. (1997), "Grouted Anchors for FRP Tendons", *Technical Report*, The Pennsylvania State University, July 18th, 1997.

Nanni, A., (1995), "Grouted anchors for FRP tendons", *Final Report* August 12, 1995, Penn State University (Pennsylvania) pp.1-6.

Nanni, A., Bakis, C.E., O'Neil, E.F., and Dixton, T.O., (1996), "Short-Term Sustained Loading of FRP Tendon-Anchor Systems", *Technical Report*, The Pennsylvania State University.

Noritake, K., Mukae, K., Kumagai, S, and Mizutani, J., (1993), "Practical Applications of Aramid FRP Rods to Prestressed Concrete Structures" *Proceedings of the International Symposium on Fiber-Reinforced-Plastic Reinforcement for Concrete Structures*, Ed. by Antonio Nanni and Charles W. Dolan, Vancouver, Canada, Mar 28-31, 1993, American Concrete Institute, Detroit, MI, 1993, pp. 853-873. (ACI SP-138)

Pecce M., Manfredi G., and Cosenza E., (2000), "Experimental Response and Code Modelsof GFRP RC Beams in Bending", *J. Comp.Constr*, ASCE, Vol. 4, No. 4, pp. 182-190.

Phillips, M. G. (1983), "Prediction of Long-Term Stress-Rupture Life for Glass Fiber-Reinforced Polyester Composites in Air and in Aqueous Environment," *Composites*, July 1983, pp. 271-275.

Porter, L., Mehus, J., Young, A.K., O'Neil, E.F., and Barnes B.A. (1997), "Aging of Fiber Reinforcement in Concrete", *Proc. 3rd Non-Metallic (FRP) Reinforcement for Concrete Structures, International Symposium*, Sapporo, Japan, October 14-16th 1997, Sapporo Japan, Vol.2, pp.59-66.

Rahman, A.H., Taylor, D.A., and Kingsley, C.Y., (1993), "Evaluation of FRP as Reinforcement for Concrete Bridges", *Proc. FRP Reinforcement for Concrete Structures, Int. Sympos., ACI SP-138*, A. Nanni and C.W. Dolan, Eds., ACI, Farmington Hills, Michigan, pp. 71-82.

Roberts, R. C., (1982), " Environmental Stress Cracking of GRP: Implications for Reinforced Plastics Process Equipment," *Composites*, October, 1982, pp. 389-392.

Rostasy, F. S. (1993) "FRP Tensile Elements For Prestressed Concrete -- State of the art, Potentials and limits" *Proceedings of the International Symposium on Fiber-Reinforced-Plastic Reinforcement for Concrete Structures*, Ed. by Antonio Nanni and Charles W. Dolan, Vancouver, Canada, Mar 28-31, 1993, American Concrete Institute, Detroit, MI, 1993, pp. 347-366. (ACI SP-138)

Santoh, N., Kimura, H., Enomoto, T., Kiuchi, T., and Kuzuba, Y., (1993), "Report on the Use of CFCC in Prestressed Concrete Bridges in Japan" *Proceedings of the International Symposium on Fiber-Reinforced-Plastic Reinforcement for Concrete Structures*, Ed. by Antonio Nanni and Charles W. Dolan, Vancouver, Canada, Mar 28-31, 1993, American Concrete Institute, Detroit, MI, 1993, pp. 895-911. (ACI SP-138)

Schutte, C.L. (1994), "Environmental Durability of Glass-Fiber Composites", *Mat. Sci. Eng.*, R13, No. 7, November 15th, 1994.

Shih, G.C., and Ebert, L.J., (1987), "The effect of the Fiber/Matrix Interface on the Flexural Fatigue Performance of Unidirectional Fiber Composites", *Composites Science and Technology*, Vol. 28, pp. 147-161.

Tannous F.E., and Saddatmanesh H., (1999), "Durability of AR Glass Fiber Reinforced Plastic Bars", *J. Comp. Constr.*, Vol. 3 No. 1, pp.12-19.

Tinazzi, D., C. Modena, and A. Nanni, "Strengthening of Masonry Assemblages with FRP Rods and Laminates," *Proc. International Meeting on Composite Materials, PLAST 2000, Proceedings, Advancing with Composites 2000*, Ed. I. Crivelli-Visconti, Milan, Italy, May 9-11, 2000, pp. 411-418.

Uppuluri, V. S., Bakis, C. E., Al-Dulaijan, S. U., Nanni, A., and Boothby, T. E., (1996), "Analysis of the Bond Mechanism in FRP Reinforcement Rods: The Effect of Rod Design and Properties." *Proc. ACMBS-II, 2nd International Conf. on Advanced Composite Materials in Bridges and Structures*, M. M. El-Badry, ed., Canadian Soc. for Civil Engineering, Montreal, Quebec, Canada, 1996, pp. 893-900.

Van Den Ende, C. A. M., and Ven Den Dolder, A., (1991), " Comparison of Environmental Stress Corrosion Cracking in Different Glass Fiber Reinforced Thermoset Composites," in *Durability of Polymer Based Composite Systems for Structural Applications*, A. H. Cardon and G. Verchery Eds., Elsevier Applied Science.

Vijay, P.V., and Ganga Rao H.V.S., (1999), "Accelerated and Natural Weathering of Glass Fiber Reinforced Plastic Bars", *Proc. FRPRCS-4*, November 1-4th, 1999, Baltimore, USA, pp. 605-614.

Weitsman, Y.J. (1995), “Effects of Fluids on Polymeric Composites, A Review”, *Contract Report for Office of Naval Research*, No. N00014-90-J-1556, July, 1996.

Zhang S., and Karbhari V.M., (1999), “Effects of Alkaline Environment on the Durability of E-glass Fiber Composites for Use in Civil Infrastructure”, *14th Technical Conference, September 27-29th 1999*, Dayton, USA.

APPENDIX A
Environmental Cycles

1. Freeze- Thaw Cycles

   Each cycle = 120 minutes

   a. Thawing : 40 minutes, (40º F)
   b. Transition to freezing: 20 minutes
   c. Freezing state: 40 minutes, (0º F)
   d. Transition to Thawing: 20 minutes

   No. of Cycles: 50

2. High Temperatures and Relative Humidity + UV exposure

   a. No. of Cycles: 150 (50 x 3)
   b. Temperature Range: 120 ºF - 60 º F
   c. Time at high Temperature: 20 minutes
   d. Time at low temperature: 10 minutes
   e. Transition: 20 minutes
   f. After 1st 40 cycles, RH 60% - 100% at 60 º F (40 cycles)
   g. After 2nd 40 cycles, RH 60% - 100% at 80 º F (40 cycles)
   h. After 3rd 40 cycles, RH 60% - 100% at 100 º F (40 cycles)
   i. Finally before testing, time at 120 º F (at 0% RH): 60 minutes
   j. 100% RH : 15 minutes
   k. 60% RH : 10 minutes
   l. Transition : 10 minutes

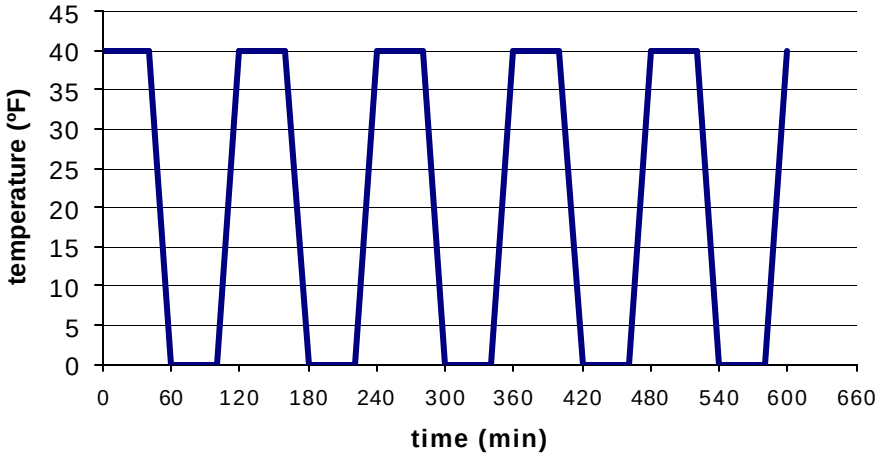

Figure A1: Freeze-thaw cycles

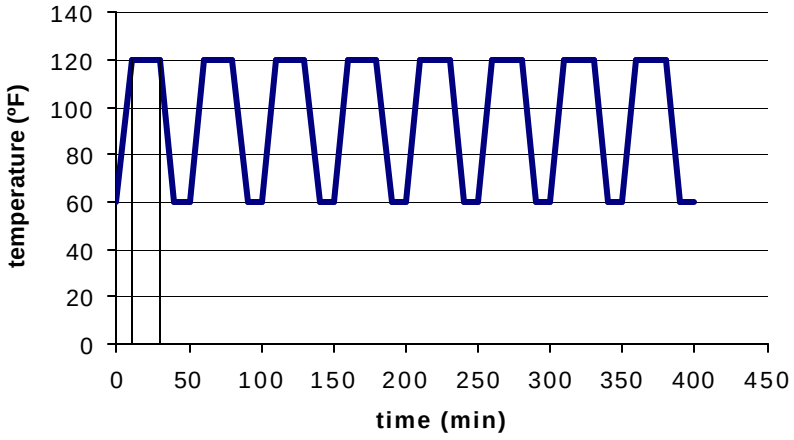

Figure A2: High temperature cycles

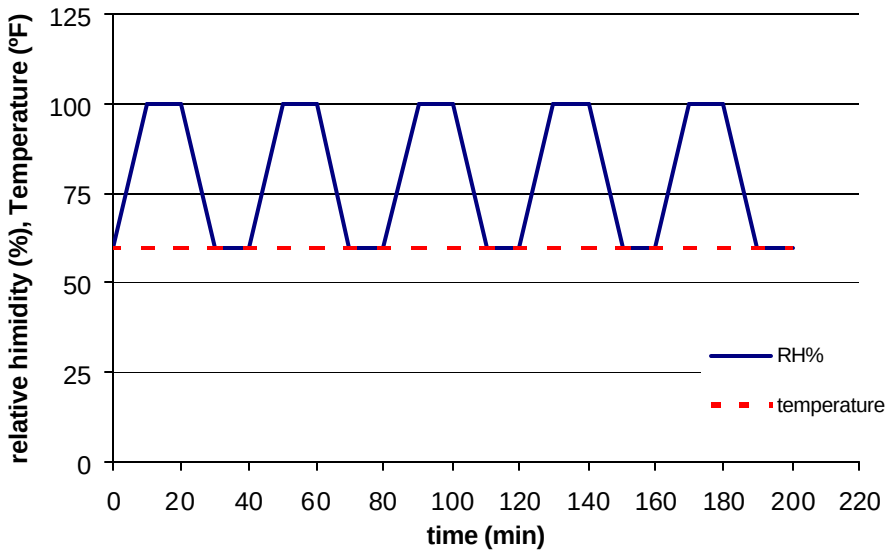

Figure A3: High RH cycles @ 60º F

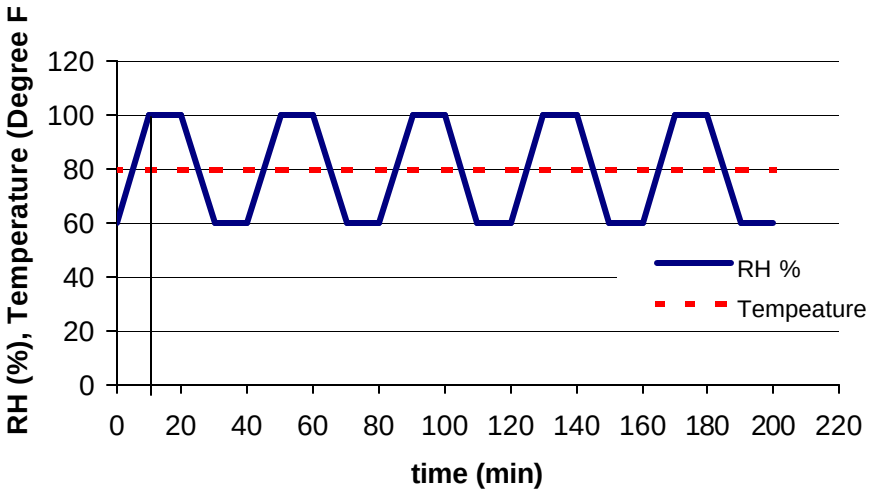

Figure A4: High RH cycles @ 80º F

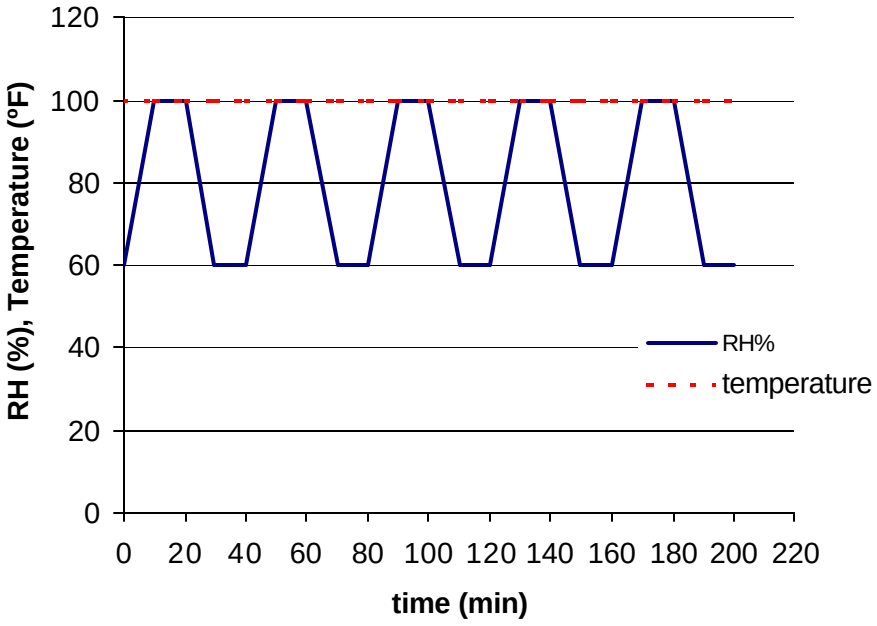

Figure A5: High RH cycles @ 100º F

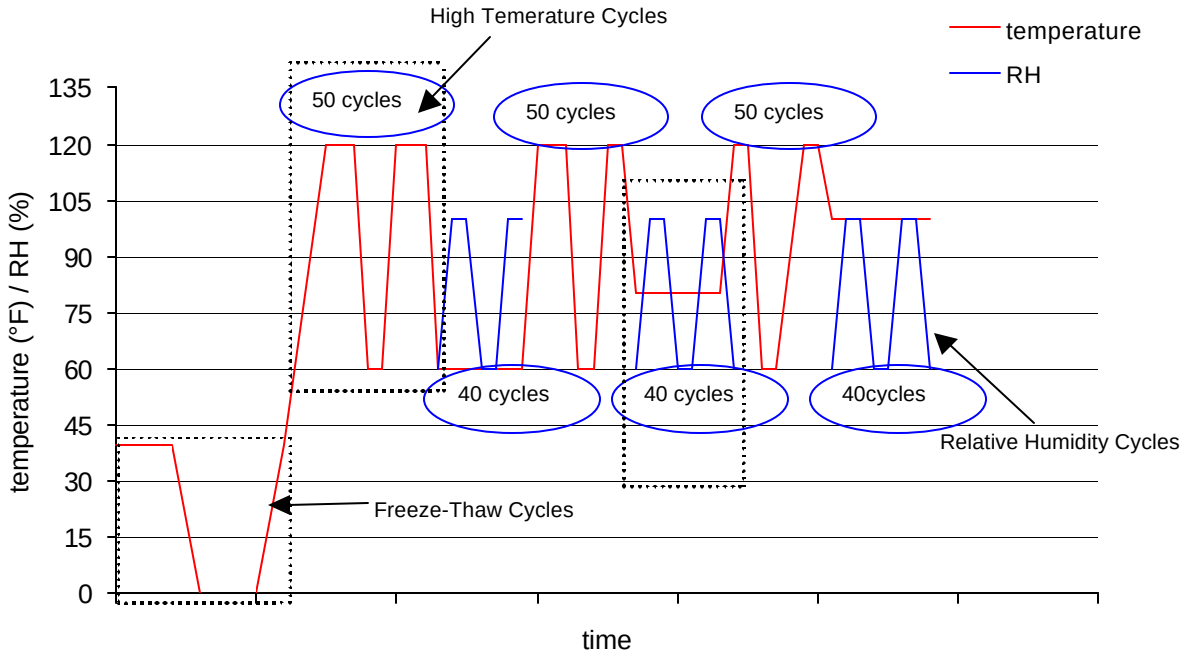

Figure A6: Combined cycles

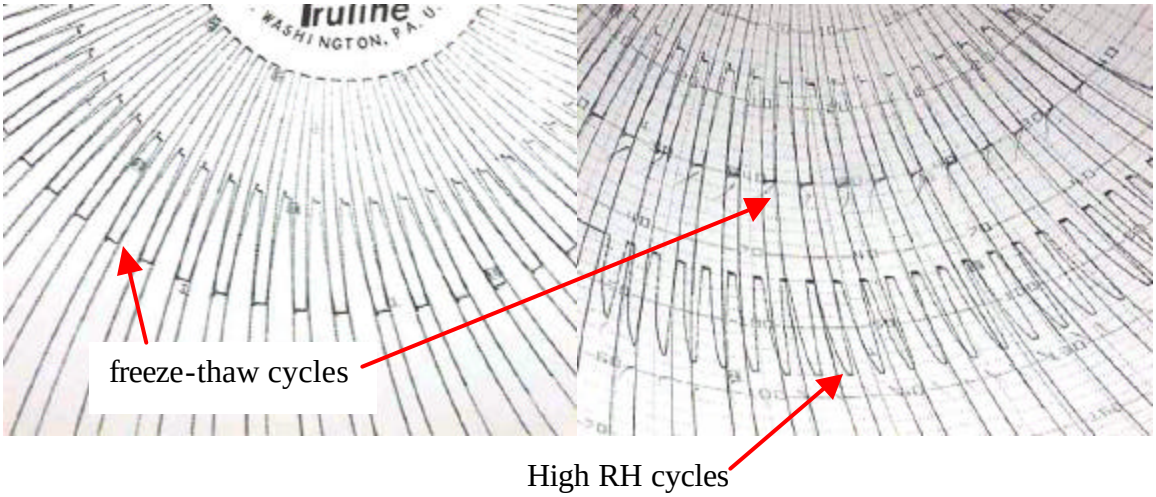

Figure A7: Thermal and RH diagrams

APPENDIX B

Table B1: Tensile test unconditioned rods - US units

rod	*d (inches)*	*ultimate stress (ksi)*	*Modulus (ksi)*	*ultimate strain*
G1 test 1	0.472	136	6094	0.0224
G1 test 2		138	6222	0.0222
G1 test 3		138	6461	0.0213
G1 test 4		128	6018	0.0213
G1 test 5		130	6080	0.0213
Mean Values		**134**	**6175**	**0.0217**
standard deviation		5	176	0.0006
G2 test 1	0.250	53	3300	0.0161
G2 test 2		51	4900	0.0104
G2 test 3		57	5000	0.0114
G2 test 4		59	5330	0.0111
G2 test 5		43	3200	0.0134
Mean Values		**53**	**4346**	**0.0125**
standard deviation		6	1014	0.0023
G3 test 1	0.375	129	5358	0.0241
G3 test 2		124	5442	0.0229
Mean Values		**127**	**5400**	**0.0235**
standard deviation		3	59	0.0008
G4 test 1	0.500	114	5167	0.0222
G4 test 2		114	5311	0.0216
Mean Values		**114**	**5239**	**0.0219**
standard deviation		0	102	0.0004
G5 test 1	0.250	162	5127	0.0316
G5 test 2		144	5430	0.0266
Mean Values		**153**	**5279**	**0.0291**
standard deviation		13	214	0.0036

C1 test 1	0.325	372	18154	0.0205
C1 test 2		350	18463	0.0189
C1 test 3		321	18747	0.0171
C1 test 4		**350**	**19398**	**0.0181**
Mean Values		348	18690	0.0187
standard deviation		21	530	0.0014

C2 test 1	0.315	276	15487	0.0178
C2 test 2		272	16015	0.0170
C2 test 3		327	15529	0.0209
C2 test 4		282	14560	0.0194
Mean Values		**289**	**15398**	**0.0188**
standard deviation		25	608	0.0017
C3 test 1	0.312	146	16080	0.0091
C3 test 2		147	15102	0.0097
C3 test 3		147	15102	0.0097
C3 test 4		147	16100	0.0091
Mean Values		**147**	**15596**	**0.0094**
standard deviation		0	570	0.0004
C4 test 1	0.250	295	18869	0.0156
C4 test 2		269	18560	0.0145
Mean Values		**282**	**18715**	**0.0151**
standard deviation		19	218	0.0008

C5 test 1	0.375	308	308	0.0195
C5 test 2		317	317	0.0182
C5 test 3		312	312	0.0192
Mean Values		**312**	**312**	**0.0190**
standard deviation		6	6	0.0009

C6 test 1	0.38 x 0.25	241	18000	0.0134
C6 test 2		262	17000	0.0154
Mean Values		**251**	**17500**	**0.0144**
standard deviation		15	707	0.0014

C7 test 1	0.38 x 0.25	272	19000	0.0143
C7 test 2		293	18000	0.0163
Mean Values		**282**	**18500**	**0.0153**
standard deviation		15	707	0.0014

Table B2: Tensile test after alkali exposure (21 days @ T = 140 °F) -US Units

rod	*d (inches)*	*ultimate stress (ksi)*	*Modulus (ksi)*	*ultimate strain*
G1 test 1	0.472	134	6030	0.0223
G1 test 2		136	5540	0.0246
G1 test 3		132	6050	0.0218
Mean Values		**134**	**5873**	**0.0229**
standard deviation		2	289	0.0015
G2 test 1	0.250	32	3800	0.0084
G2 test 2		40	4890	0.0082
G2 test 3		38	4875	0.0077
Mean Values		**37**	**4522**	**0.0081**
standard deviation		4	625	0.0004
C1 test 1	0.325	361	17677	0.0204
C1 test 2		320	18532	0.0172
C1 test 3		356	18669	0.0191
Mean Values		**346**	**18293**	**0.0189**
standard deviation		23	538	0.0016
C3 test 1	0.312	152	17370	0.0087
C3 test 2		143	15670	0.0091
C3 test 3		147	15800	0.0093
Mean Values		**147**	**16280**	**0.0091**
standard deviation		4	946	0.0003

Table B3: Tensile test after alkali exposure (42 days @ T = 140 °F) – US Units

rod	***d (inches)***	***ultimate stress (ksi)***	***Modulus (ksi)***	***ultimate strain***
G1 test 1	0.472	131	5760	0.0228
G1 test 2		136	6330	0.0216
G1 test 3		137	5730	0.0238
Mean Values		**135**	**5940**	**0.0227**
standard deviation		3	338	0.0011
G2 test 1	0.250	25	3740	0.0066
G2 test 2		36	4800	0.0076
G2 test 3		33	4700	0.0069
Mean Values		31	4413	0.0070
standard deviation		**6**	**585**	**0.0005**
C1 test 1	0.325	317	18520	0.0171
C1 test 2		298	18740	0.0159
C1 test 3		346	18136	0.0191
Mean Values		**320**	**18465**	**0.0174**
standard deviation		24	306	0.0016
C3 test 1	0.312	149	17900	0.0075
C3 test 2		145	16160	0.0090
C3 test 3		147	16540	0.0089
Mean Values		**147**	**16867**	**0.0085**
standard deviation		2	915	0.0008

Table B4: Tensile test after environmental exposure – US Units

rod	*d (inches)*	*Ultimate stress (ksi)*	*Modulus (ksi)*	*Ultimate strain*
G1 test 1	0.472	130	5800	0.0224
G1 test 2		130	6050	0.0215
G1 test 3		142	5790	0.0246
G1 test 4		124	5700	0.0218
Mean Values		**132**	**5835**	**0.0226**
standard deviation		8	150	0.0014
G2 test 1	0.250	45	3590	0.0125
G2 test 2		61	4000	0.0153
G2 test 3		45	4000	0.0112
G2 test 4		46	4330	0.0106
Mean Values		**49**	**3980**	**0.0124**
standard deviation		8	303	0.0021
C1 test 1	0.325	361	18136	0.0199
C1 test 2		361	18324	0.0197
C1 test 3		354	17943	0.0197
C1 test 4		333	18588	0.0179
Mean Values		**352**	**18248**	**0.0193**
standard deviation		13	275	0.0009
C2 test 1	0.315	302	17013	0.0178
C2 test 2		274	16100	0.0170
C2 test 3		256	15280	0.0167
C2 test 4		270	15577	0.0174
Mean Values		**276**	**15993**	**0.0172**
standard deviation		20	760	0.0004
C3 test 1	0.312	145	15300	0.0952
C3 test 2		150	14600	0.1034
C3 test 3		142	14600	0.0980
C3 test 4		150	15600	0.0968
Mean Values		**145**	**14833**	**0.0989**
standard deviation		4	404	0.0042
C4 test 1	0.250	295	17271	0.0171
C4 test 2		326	15868	0.0205
C4 test 3		285	17100	0.0167
C4 test 4		290	17500	0.0166
Mean Values		**302**	**16746**	**0.0181**
standard deviation		21	765	0.0021

FRP Specimens After Tensile Failure

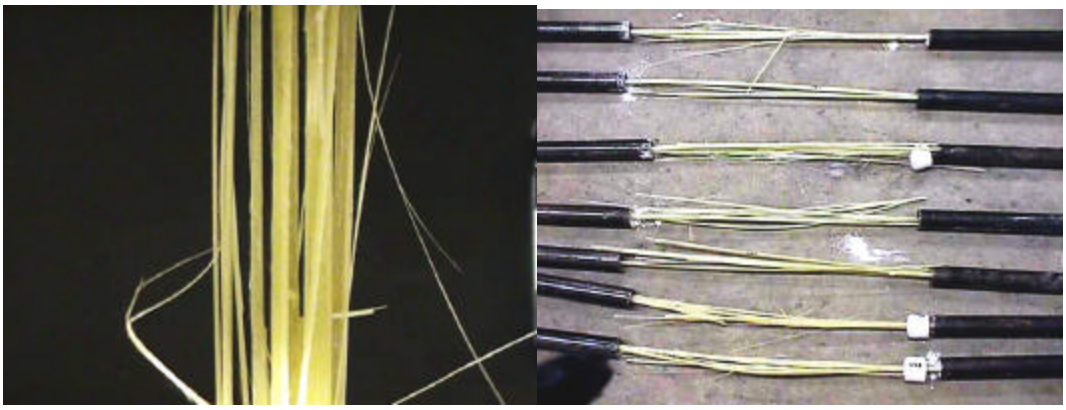

Figure B1: G1 rods

Figure B2: G2 rods

Figure B3: G3 rods

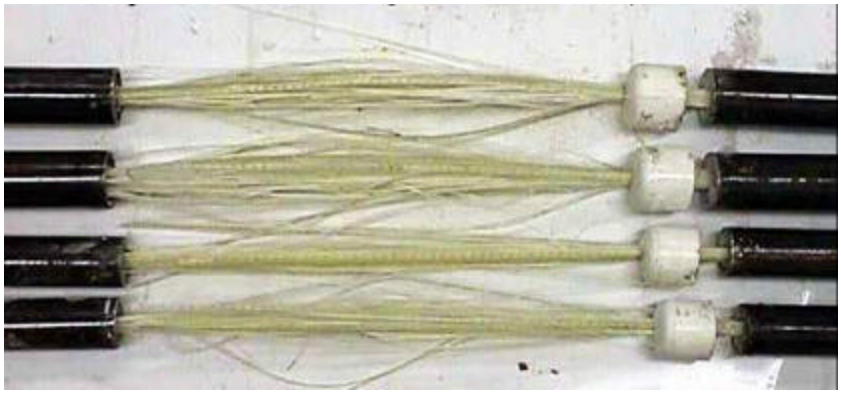

Figure B4: G4 rods

Figure B5: G5 rods

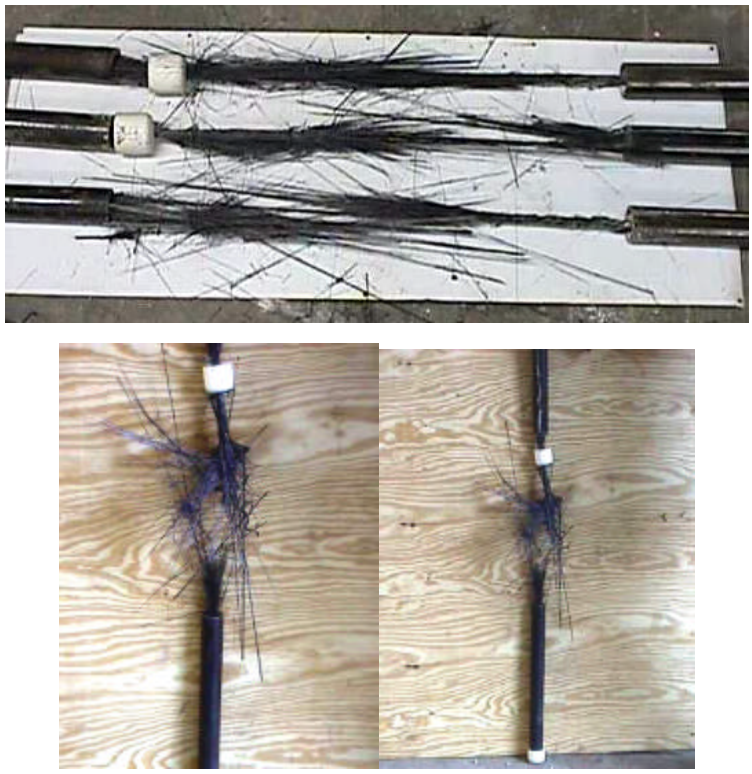

Figure B6: C1 rods

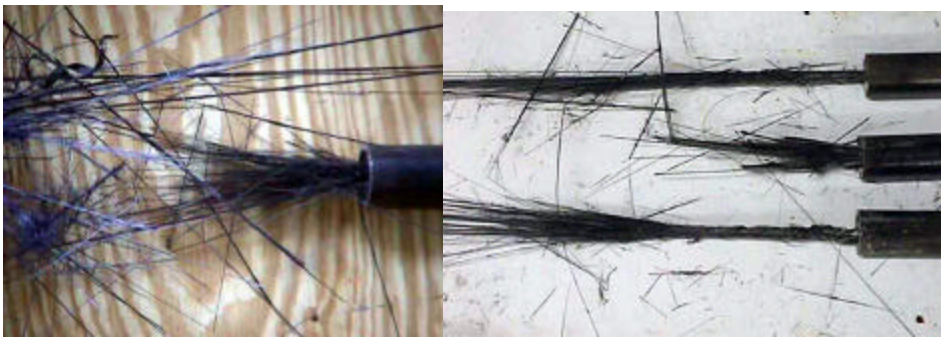

Figure B7: C2 rods

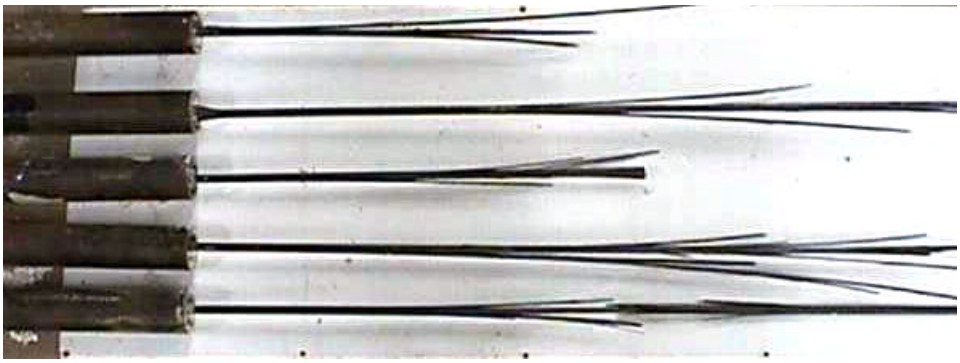

Figure B8: C3 rods

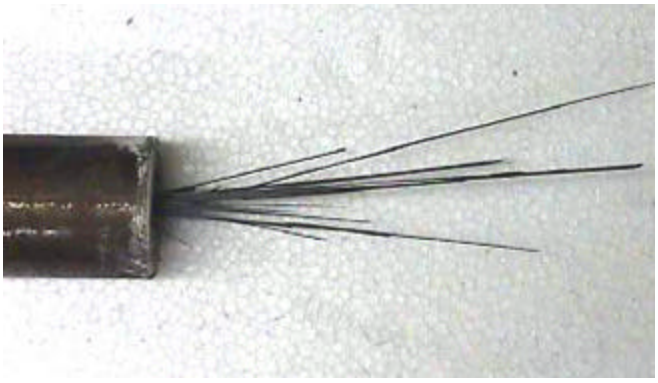

Figure B9: C4 rods

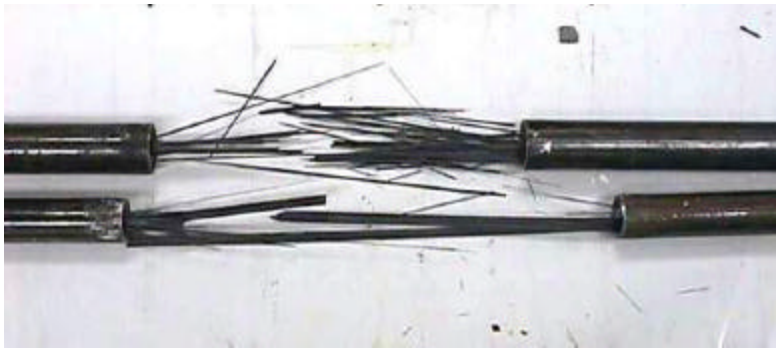

Figure B10: C5 rods

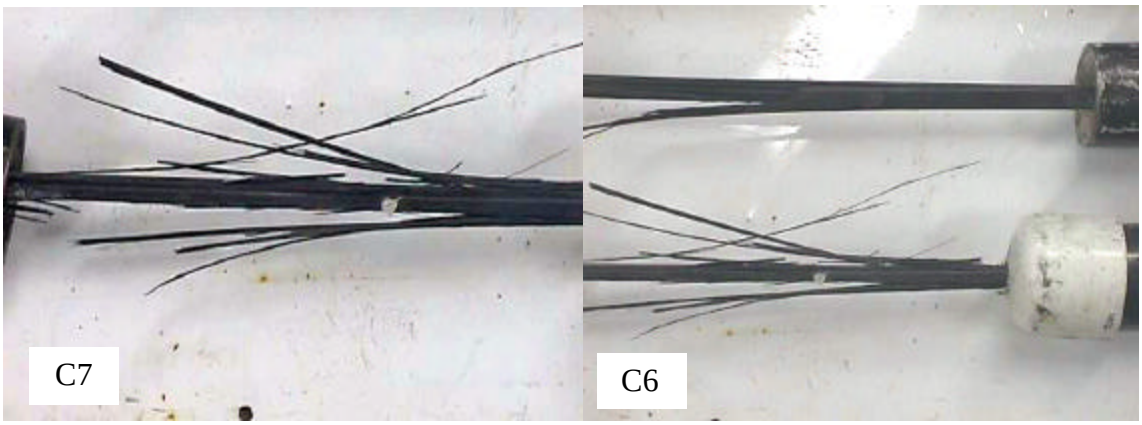

Figure B11: C6 & C7 rods

APPENDIX C

Table C1: Short shear span test unconditioned rods - Customary Units

G1	***Load (kips)***	***ISS (ksi)***	***Span (in)***	***Span/D***	***Plane of failure***
TEST 1	3.802	14.672	1.025	2.2	Vertical / Horizontal
TEST 2	3.272	12.627			
TEST 3	3.906	15.074			
TEST 4	4.214	16.262			
TEST 5	3.724	14.371			
TEST 6	4.020	15.514			
Mean values	**3.823**	**14.753**			
Standard deviation	0.320	1.235			
G2	***Load (kips)***	***ISS (ksi)***	***Span (in)***	***Span/D***	***Plane of failure***
TEST 1	0.519	7.050	0.750	3.0	Vertical
TEST 2	0.516	7.009			
TEST 3	0.430	5.841			
TEST 4	0.524	7.118			
TEST 5	0.445	6.045			
Mean values	**0.487**	**6.613**			
Standard deviation	0.045	0.617			
C1	***Load (kips)***	***ISS (ksi)***	***Span (in)***	***Span/D***	***Plane of failure***
TEST 1	0.193	1.549	1.125	3.0	Vertical
TEST 2	0.210	1.691			
TEST 3	0.279	2.243			
TEST 4	0.188	1.510			
TEST 5	0.222	1.782			
Mean values	**0.218**	**1.755**			
Standard deviation	0.037	0.294			
C2	***Load (kips)***	***ISS (ksi)***	***Span (in)***	***Span/D***	***Plane of failure***
TEST 1	0.259	2.216	1.125	3.6	Vertical
TEST 2	0.295	2.524			
TEST 3	0.321	2.747			
TEST 4	0.440	3.765			
TEST 5	0.342	2.926			
Mean values	**0.331**	**2.836**			
Standard deviation	0.068	0.583			

C3	***Load (kips)***	***ISS (ksi)***	***Span (in)***	***Span/D***	***Plane of failure***
TEST 1	0.718	6.246	0.938	3.0	Vertical
TEST 2	0.956	8.312			
TEST 3	0.932	8.103			
TEST 4	0.910	7.912			
TEST 5	0.993	8.633			
Mean values	**0.902**	**7.841**			
Standard deviation	0.107	0.931			
C4	***Load (kips)***	***ISS (ksi)***	***Span (in)***	***Span/D***	***Plane of failure***
TEST 1	0.508	6.901	0.750	3.0	Vertical
TEST 2	0.524	7.118			
TEST 3	0.506	6.874			
TEST 4	0.599	8.137			
TEST 5	0.571	7.756			
Mean values	**0.542**	**7.357**			
Standard deviation	0.041	0.563			

Table C2: Short shear span test after alkali exposure (42 days @ T = 72 °F) – US Units

G1	***Load (kips)***	***ISS (ksi)***	***Span (in)***	***Span/D***	***Plane of failure***
TEST 1	3.891	15.016	1.025	2.2	Vertical / Horizontal
TEST 2	3.508	13.538			
TEST 3	3.828	14.773			
TEST 4	3.999	15.433			
TEST 5	3.751	14.475			
TEST 6	3.986	15.382			
Mean values	**3.827**	**14.769**			
Standard deviation	0.182	0.704			
G2	***Load (kips)***	***ISS (ksi)***	***Span (in)***	***Span/D***	***Plane of failure***
TEST 1	0.455	6.181	0.75	3	Vertical
TEST 2	0.512	6.955			
TEST 3	0.510	6.928			
TEST 4	0.360	4.890			
TEST 5	0.410	5.569			
TEST 6	0.508	6.901			
Mean values	**0.459**	**6.237**			
Standard deviation	0.063	0.860			

C1	***Load (kips)***	***ISS (ksi)***	***Span (in)***	***Span/D***	***Plane of failure***
TEST 1	0.230	1.849	1.125	3.6	Vertical
TEST 2	0.251	2.018			
TEST 3	0.231	1.857			
TEST 4	0.326	2.620			
TEST 5	0.339	2.725			
TEST 6	0.245	1.969			
Mean values	**0.270**	**2.173**			
Standard deviation	0.049	0.394			

C2	***Load (kips)***	***ISS (ksi)***	***Span (in)***	***Span/D***	***Plane of failure***
TEST 1	0.315	2.695	1.125	3	Vertical
TEST 2	0.318	2.721			
TEST 3	0.360	3.080			
TEST 4	0.353	3.020			
TEST 5	0.352	3.012			
TEST 6	0.349	2.986			
Mean values	**0.341**	**2.919**			
Standard deviation	0.019	0.167			

C3	*Load (kips)*	*ISS (ksi)*	*Span (in)*	*Span/D*	*Plane of failure*
TEST 1	0.999	8.686	0.9375	3	Vertical
TEST 2	1.043	9.068			
TEST 3	0.952	8.277			
TEST 4	1.078	9.372			
TEST 5	0.993	8.633			
TEST 6	0.970	8.433			
Mean values	**1.006**	**8.745**			
Standard deviation	0.047	0.407			

Table C3: Short shear span test after alkali exposure (21 days @ T = 140 °F) – US Units

G1	***Load (kips)***	***ISS (ksi)***	***Span (in)***	***Span/D***	***Plane of failure***
TEST 1	3.262	12.588	1.025	2.2	Vertical / Horizontal
TEST 2	3.132	12.087			
TEST 3	3.000	11.577			
TEST 4	2.685	10.362			
TEST 5	2.844	10.975			
TEST 6	2.932	11.315			
Mean values	**2.976**	**11.484**			
Standard deviation	0.205	0.792			
G2	***Load (kips)***	***ISS (ksi)***	***Span (in)***	***Span/D***	***Plane of failure***
TEST 1	0.094	1.277	0.75	3	Verical
TEST 2	0.096	1.304			
TEST 3	0.054	0.734			
TEST 4	0.084	1.141			
TEST 5	0.088	1.195			
TEST 6	0.075	1.019			
Mean values	**0.082**	**1.112**			
Standard deviation	0.016	0.212			

C1	***Load (kips)***	***ISS (ksi)***	***Span (in)***	***Span/D***	***Plane of failure***
TEST 1	0.258	2.074	1.125	3.6	Vertical
TEST 2	0.166	1.334			
TEST 3	0.161	1.294			
TEST 4	0.150	1.206			
TEST 5	0.124	0.997			
TEST 6	0.151	1.214			
Mean values	**0.168**	**1.353**			
Standard deviation	0.046	0.372			

C2	***Load (kips)***	***ISS (ksi)***	***Span (in)***	***Span/D***	***Plane of failure***
TEST 1	0.345	2.952	1.125	3	Vertical
TEST 2	0.262	2.242			
TEST 3	0.261	2.233			
TEST 4	0.272	2.327			
TEST 5	0.256	2.190			
TEST 6	0.210	1.797			
Mean values	**0.268**	**2.290**			
Standard deviation	0.044	0.374			

C3	*Load (kips)*	*ISS (ksi)*	*Span (in)*	*Span/D*	*Plane of failure*
TEST 1	0.926	6.999	0.9375	3	Vertical
TEST 2	0.805	9.355			
TEST 3	1.076	8.512			
TEST 4	0.979	7.564			
TEST 5	0.870	6.999			
TEST 6	0.805	6.999			
Mean values	**0.756**	**7.738**			
Standard deviation	0.106	0.988			

Table C4: Short shear span test after alkali exposure (42 days @ T = 140 °F) – US Units

G1	***Load (kips)***	***ISS (ksi)***	***Span (in)***	***Span/D***	***Plane of failure***
TEST 1	2.702	10.427	1.025	2.2	Vertical / Horizontal
TEST 2	2.302	8.884			
TEST 3	2.749	10.609			
TEST 4	2.499	9.644			
TEST 5	2.553	9.852			
TEST 6	2.560	9.879			
Mean values	2.561	**9.883**			
Standard deviation	0.159	0.613			
G2	***Load (kips)***	***ISS (ksi)***	***Span (in)***	***Span/D***	***Plane of failure***
TEST 1	0.040	0.543	0.75	3	Vertical
TEST 2	0.066	0.897			
TEST 3	0.037	0.503			
TEST 4	0.048	0.652			
TEST 5	0.036	0.489			
Mean values	**0.045**	**0.617**			
Standard deviation	0.012	0.169			

C1	***Load (kips)***	***ISS (ksi)***	***Span (in)***	***Span/D***	***Plane of failure***
TEST 1	0.148	1.190	1.125	3.6	Vertical
TEST 2	0.155	1.246			
TEST 3	0.160	1.286			
TEST 4	0.130	1.045			
TEST 5	0.120	0.965			
TEST 6	0.118	0.948			
Mean values	**0.139**	**1.113**			
Standard deviation	0.018	0.146			

C2	***Load (kips)***	***ISS (ksi)***	***Span (in)***	***Span/D***	***Plane of failure***
TEST 1	0.173	1.480	1.125	3	Vertical
TEST 2	0.221	1.891			
TEST 3	0.224	1.917			
TEST 4	0.226	1.934			
TEST 5	0.219	1.874			
TEST 6	0.222	1.900			
Mean values	**0.214**	**1.832**			
Standard deviation	0.020	0.174			

C3	*Load (kips)*	*ISS (ksi)*	*Span (in)*	*Span/D*	*Plane of failure*
TEST 1	1.039	6.686	0.9375	3	Vertical
TEST 2	0.769	7.329			
TEST 3	0.843	6.112			
TEST 4	0.703	5.930			
TEST 5	0.682	8.520			
TEST 6	0.980	5.763			
Mean values	**0.663**	**6.723**			
Standard deviation	0.147	1.051			

Table C5: Short shear span test after environmental exposure – US Units

G1	*Load (kips)*	*ISS(ksi)*	*Span (in)*	*Span/D*	*Plane of failure*
TEST 1	4.260	16.440	1.025	2.2	Horizontal / Vertical
TEST 2	3.905	15.070			
TEST 3	3.725	14.375			
TEST 4	3.632	14.016			
TEST 5	3.903	15.062			
TEST 6	3.832	14.788			
Mean values	**3.876**	**14.958**			
Standard deviation	0.216	0.834			

G2	*Load (kips)*	*ISS(ksi)*	*Span (in)*	*Span/D*	*Plane of failure*
TEST 1	0.482	6.547	0.750	3	Vertical
TEST 2	0.501	6.806			
TEST 3	0.500	6.792			
TEST 4	0.460	6.249			
TEST 5	0.524	7.118			
TEST 6	0.480	6.520			
Mean values	**0.491**	**6.672**			
Standard deviation	0.022	0.300			

C1	*Load (kips)*	*ISS(ksi)*	*Span (in)*	*Span/D*	*Plane of failure*
TEST 1	0.211	1.696	1.125	3.6	Vertical
TEST 2	0.190	1.527			
TEST 3	0.266	2.138			
TEST 4	0.230	1.849			
TEST 5	0.236	1.897			
TEST 6	0.234	1.881			
Mean values	**0.228**	**1.831**			
Standard deviation	0.026	0.206			

C2	*Load (kips)*	*ISS(ksi)*	*Span (in)*	*Span/D*	*Plane of failure*
TEST 1	0.347	2.969	1.125	3	Vertical
TEST 2	0.375	3.209			
TEST 3	0.299	2.558			
TEST 4	0.284	2.430			
TEST 5	0.285	2.439			
TEST 6	0.382	3.269			
Mean values	**0.329**	**2.812**			
Standard deviation	0.045	0.385			

C3	*Load (kips)*	*ISS(ksi)*	*Span (in)*	*Span/D*	*Plane of failure*
TEST 1	0.736	6.399	0.938	3	Vertical
TEST 2	0.911	7.921			
TEST 3	0.889	7.729			
TEST 4	0.901	7.834			
TEST 5	0.940	8.173			
Mean values	**0.875**	**7.611**			
Standard deviation	0.080	0.697			

C4	*Load (kips)*	*ISS(ksi)*	*Span (in)*	*Span/D*	*Plane of failure*
TEST 1	0.490	6.656	0.750	3	Vertical
TEST 2	0.574	7.797			
TEST 3	0.562	7.634			
TEST 4	0.502	6.819			
TEST 5	0.547	7.430			
Mean values	**0.535**	**7.267**			
Standard deviation	0.037	0.504			

APPENDIX D

D1. Japan Society of Civil Engineering (JSCE)

The Japan design guidelines are published in "Recommendation for Design and Construction of Concrete Structures Using Fiber Reinforcing Materials". The document is the result of the work of two committees: one investigated FRP aspects, the second used those results to draw design guidelines. The guidelines were printed in Japanese in 1996 and were translated in English in 1997, in order to spread the use of FRP in civil engineering all over the world.

To calculate the design strength of FRP reinforcement a material factor γ_m is used; the value assumed is 1.15 for CFRP and AFRP, while it is equal to 1.3 for GFRP.

A test method for evaluation of alkali resistance of FRP is also provided.

Pieces of FRP rods sealed at the free ends are immersed in an alkali solution at 60°C. The recommended immersion period is one month, even if a period from 7 days to one year could be used for specific needs.

No tension is applied to the rods, although rebars are stressed during their service life. Tensile test, weight measurements and visual observation are used to detect the residual properties of the rods.

Prescriptions about a possible maximum tolerable damage status are not provided.

D2. Canadian Highway Bridge Design Code (CHBDC)

The Canadian design recommendations for bridges and structures were produced by a technical committee created by The Canadian Society of Civil Engineers in 1989. A State-of-the-Art Report in printed in 1991 and design recommendations for FRP printed in 1998 reinforcement were the most important documents produced.

The following guideline principles are given to take into account the long-term behavior of FRP in RC structures.

To consider the fact that FRP may lose strength under sustained loads, the maximum stress in non prestressed reinforcement is limited to $\phi_{FRP} \cdot F \cdot f_{pu}$. Here, f_{pu} is the "specified tensile strength" (which is the 5% percentile) of the FRP rod; ϕ_{FRP} is the resistance factor

that is set to 0.75, 0.85, and 0.85 for GFRP, AFRP and CFRP respectively, even if nothing is mentioned about what is taken into account by the use of this factor. The factor F is the stress limiting factor related to the ratio of the stresses R due to factored dead loads to the stresses due to factored live loads in the FRP rods. The value of R are reported in Table D1

Table D1: Stress limiting factor for FRP reinforcement

R =	*0.5*	*1.0*	*2.0 or more*
F for GFRP	1.0	0.9	0.8
F for AFRP	1.0	0.6	0.5
F for CFRP	1.0	0.9	0.9

The values of strength reduction as well as of stress limits are in the ranges of 0.60-0.75, 0.42-0.85 and 0.76-0.85 for GFRP, AFRP and CFRP respectively. Values depend on the ratio between dead and live load.

The maximum permissible stresses in FRP tendons for prestressed members are reported in TableD2

Table D2: Stress limiting factor for FRP prestressed rods

Prestressing Rod	***Pre-tensioning***	***Post-tensioning***
GFRP	NA	0.48 f_{pu}
AFRP	0. 38 f_{pu}	0.35 f_{pu}
CFRP	0.60 f_{pu}	0.60 f_{pu}

Environmentally caused deterioration is not explicitly treated in these design guidelines, but there are some requirements that constitute an acceptance criteria for the use of FRP in concrete. Thermoplastics are not allowed, since they may be less stable under high temperatures and aggressive environments. To avoid improper use of FRP, a table is given showing where FRP bars, grids and tendons are permissible. (See Table D3)

Table D3: Condition of use for primary FRP reinforcement and tendons

	Applications							
	Prestressed concrete beams and slabs							
	Pre-tensioned	*Post-tensioned*				*Deck Slabs*	*Stressed Wood Decks*	*Barrier Walls*
		Grouted		*Ungrouted internal*	*Ungrouted internal*			
		Alkaline	*Cement-based*					
GFRP	I	P	I	P	P	I	P	P
CFRP	P	P	P	P	P	P	I	P
AFRP	P	P	P	P	P	P	P	P

I = Inadmissible
P = Permissible

Furthermore, a concrete beam or slab with FRP tendons shall also contain supplementary reinforcement capable of sustaining the unfactored dead loads. Such reinforcement can be steel or FRP reinforcement or even FRP tendons having minimal prestressing force at the time of installation.

For FRP as secondary reinforcement, thermoplastic resin can be used, provided that the matrix is not susceptible to degradation from alkali.

D3. American Concrete Institute (ACI)

The American Concrete Institute (ACI) Committee 440 Fiber Reinforced Polymer Reinforcement was formed in 1991. In 1996 it published a State-of-the-Art Report (ACI 440R '96) addressing FRP for concrete reinforcement. A "Guide for the Design and Construction of Concrete Reinforcement with FRP Bars" was drafted in January 2000. In February 2001 provisions for FRP testing were provided in the "Recommended Test Methods For FRP Rods and sheets" ACI 440K document, that will be revisited in the next months before the final draft. The results of this work contributed to suggest provisions for mechanical test and acceptance criteria of FRP rods for concrete structures.

ACI introduced an environmental reduction factor in order to consider the deterioration of tensile-strength due to long-term environment influence. This factor should be multiplied by the characteristic strength, given by the manufacturer (mean strength minus three times the standard deviation), to obtain the design ultimate tensile strength for FRP reinforcement : $f_{fu} = C_E \cdot f_{fu}^*$. In this equation f_{fu} is the design ultimate tensile strength, C_E is the environmental factor and f_{fu}^* is the guaranteed ultimate design tensile strength as reported by the manufacturer. The environmental reduction factor to use depends on fiber type and exposure conditions. Two environmental classes were introduced: "Enclosed Conditioned Space" and "Unenclosed Conditioned Space". The reduction factors suggested are shown in Table D4:

Table D4: Environmental reduction factor

Exposure Conditions	***Rods***	C_E
Enclosed Conditioned Space	CFRP	1.00
	GFRP	0.80
	AFRP	0.90
Unenclosed Conditioned Space	CFRP	0.90
	GFRP	0.70
	AFRP	0.80

ACI provided also creep rupture stress limits, to avoid the risk of creep phenomena that could affect structural safety, as reported in Table D5. The reduction factors are the same of that used for fatigue stress limit.

Table D5: Creep/Fatigue reduction factors

Rods	*Creep rupture stress limit*
GFRP	0.20 f_{fu}
AFRP	0.30 f_{fu}
CFRP	0.55 f_{fu}

D3. British Institution of Structural Engineers (BISE) and EUROCRETE

EUROCRETE is a pan-European project started in 1993 with the purpose to provide also design guidelines for FRP reinforcement in concrete. As a result the document "Modification of Design Rules to Incorporate Non-ferrous Reinforcement" was produced and finished in 1996. Much of this work is included in "Interim Guidance on the Design of Reinforced Concrete Structures Using Fibre Composite Reinforcement" which is a guidance published by the BISE in 1999.

In these recommendations a characteristic strength is suggested to be the mean values minus 1.67 standard deviations for non-prestressed reinforcement and the mean value minus 3 standard deviations for prestressed reinforcement.

A material factor γ_m is introduced that includes effective strength reduction due to construction defects and long-term behavior.

A safety factor for environmental influence was also introduced to take into account the possible attacking agents that could affect the effective strength of FRP reinforcement. In Table D6 material factors and environmental factors are reported:

Table D6: Materials and environmental factors (EUROCRETE – BISE)

Rods	***Material factor***	***Environmental factor***
GFRP (E-glass)	3.60	3.30
AFRP	2.20	2.00
CFRP	1.80	1.67

Hot wet environment are considered the most aggressive conditions for CFRP, while moisture is considered for AFRP. Alkaline and water solutions are considered the most dangerous environments for GFRP.

The reduction factors and upper tensile strength recommendations are summarized in Table D7 for all the mentioned Institutions.

Table D7: Materials and environmental factors (Summary)

Factor	***Code***	***ACI***	***CHBDC***	***JSCE***	***BISE***
Environmental		GFRP: 0.70-0.80 AFRP: 0.80 –0.90 CFRP: 0.90-1.00	GFRP*: 0.75 AFRP*: 0.85 CFRP*: 0.85	GFRP: 0.77 AFRP: 0.87 CFRP: 0.87	GFRP: 0.30 AFRP: 0.50 CFRP: 0.60
Sustained stress		Not Specified	GFRP: 0.80-1.00 AFRP: 0.50 –1.00 CFRP: 0.90-1.00	Not Specified	
Total strength reduction due to environmental agents and sustained stress		GFRP: 0.70-0.80 AFRP: 0.80 –0.90 CFRP: 0.90-1.00	GFRP: 0.60-0.75 AFRP: 0.42 –0.85 CFRP: 0.76-0.85	GFRP: 0.77 AFRP: 0.87 CFRP: 0.87	GFRP: 0.30 AFRP: 0.50 CFRP: 0.60
Specified upper tensile stress limits due to permanent load		GFRP: 0.14-0.16 AFRP: 0.16 –0.18 CFRP: 0.44-0.50	GFRP: 0.60-0.75 AFRP: 0.42 –0.85 CFRP: 0.76-0.85	GFRP: ≤0.7 AFRP: ≤0.70 CFRP: ≤0.70.	Not Specified

* CHBDC resistance factor reported as environmental reduction factor is not well specified in the guidelines, therefore environmental effects are one of the aspects affecting the size of this factor